NTNU – Trondheim
Norwegian University of
Science and Technology

Heat exchanger network self-optimising control

Application to the crude unit at Mongstad refinery

Alexandre Leruth

Chemical Engineering
Submission date: June 2012
Supervisor: Sigurd Skogestad, IKP
Co-supervisor: Johannes Jäschke, IKP

Norwegian University of Science and Technology
Department of Chemical Engineering

Heat exchanger network self-optimising control

Application to the crude unit at Mongstad refinery

Alexandre Leruth
MSc. in Chemical Engineering

June 2012

Abstract

The master thesis is about operation of the heat exchanger network of a crude unit at Mongstad refinery (Statoil). The network is such that the crude oil feed stream is splitted in parallel branches made of shell and tube heat exchangers recovering heat from distilled products. Optimal operation of the given network is defined as the maximum achievable temperature of the crude oil outlet stream. In other words, it means to maximise the overall heat transfer in the network.

This work applies the concept of self-optimising control for the operation of the given network. The steady-state performances of the self-optimising variables derived by Jäschke (Jäschke, 2012) are assessed and two main control configurations are examined: a simple decentralised control configuration (PIDs Control) and an advanced multivariable control configuration (Model Predictive Control). The steady-state performances appears to be moderate but need to be re-assessed using a proper steady-state model. The decentralised control configuration is found to present acceptable dynamic performances while the advanced multivariable configuration only enhances them a bit.

Table of Contents

Nomenclature

A : $Exchange\ area\ [m^2]$

$c_A, c_B, c_C, c_D, c_E, c_{F*}$: $Controlled\ variable\ [K]$

$c_v, c_p, c_{p,w}, c_{p,X}$: $Heat\ capacity\ [J/kgK]$

H : $Enthalpy\ [J]$

h : $Heat\ transfer\ coefficient\ [W/m^2K]$

JT_i: $Self-optimising\ variable\ (Jäschke\ Temperature)\ [K]$

$k_1, k_2, k_{1,X}, k_{2,X}$: $Heat\ capacity\ constant\ [k_1: J/(kgK^2), k_2: J/(kgK)]$]

m_i, m_{tot} : $Mass\ flowrate\ [kg/s]$

N : $Model\ order-number\ of\ cells\ [-]$

Q : $Heat\ transfer\ [J]$

$T, T_X, T_{X,Y}, T_X^Y$: $Temperature\ [°C]$

t : $Time\ [s]$

U : $Internal\ energy\ [J]$

$\boldsymbol{U}$: $Overall\ heat\ transfer\ coefficient\ [W/m^2K]$

V, V_w : $Volume\ [m^3]$

z_i : $Valve\ position\ [-]$

z_{ic} : $Valve\ position\ setpoint\ [-]$

ρ, ρ_w : $Density\ [kg/m^3]$

Chapter 1

Introduction

This work is about operation of the heat exchanger network for pre-heat of crude oil at Mongstad Refinery (operated by our industrial partner, Statoil). The network is such that the crude oil is splitted in several branches where it is heated by heat recovery of several hot distilled products leaving the fractionation column and which needs to be cooled. The crude oil is then introduced in a fractionation column where additional heat is provided by a gas fired heater (Fig.1.1.).

Actually, energy costs represent a substantial part of the operating costs in a refinery. Optimal operation of this network has been defined as the maximum achievable temperature of the crude oil outlet stream. In other words, it means to maximise the overall heat transfer between hot and cold streams in order to save energy at the gas fired heater unit.

The central objective of our control structure will thus be to reach as near as possible this optimum. The manipulated inputs are assumed to be the valve positions (or the split fractions) distributing the crude oil in the several branches. Disturbances are given as the mass flowrates and temperatures of the feed and of hot product streams.

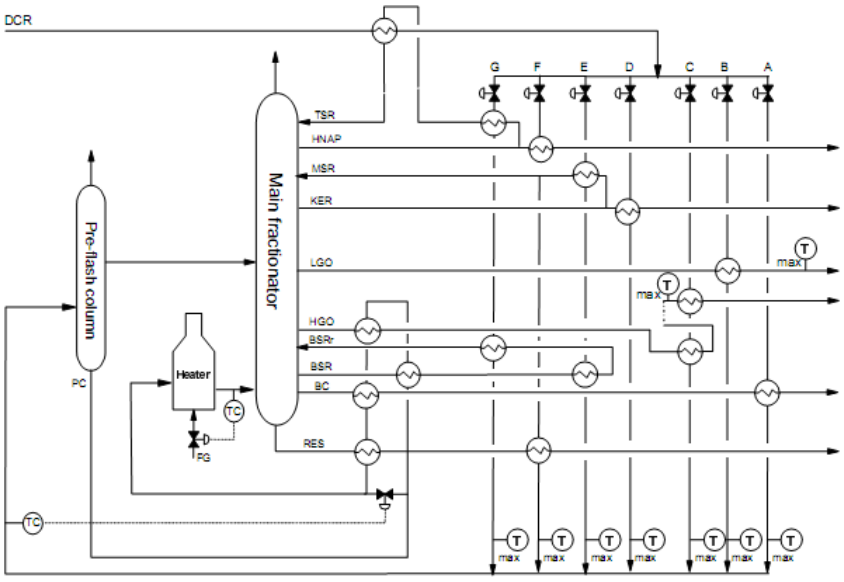

Fig.1.1. Simplified crude unit overview

Operation of heat exchanger networks is much less studied compared to their design (Glemmestad et al., 1999). Bypass selection for control of heat exchanger networks has been investigated (Mathisen et al., 1992). More considerations on utility consumption then suggested a method that minimises it (Mathisen et al., 1994a). A method based on repeated steady state optimization was presented (Boyaci et al., 1996) and then a method for on-line optimisation and control of heat exchanger networks has been also introduced (Aguilera and Marchetti, 1998).

In the Mongstad case, on-line optimisation has been implemented for the operation (Lid, Strand and Skogestad, 2002). Steady-state mass and energy balance of the whole network (20 heat exchangers) yields the process model. The model is fitted by data reconciliation and optimal split fractions are computed. When implemented, this system led to a 2% reduction in energy consumption. However, this method requires many efforts from the operators.

Indeed, using real-time optimisation brings difficulties in building and adapting accurate models for complex processes (Chachuat et al., 2009) and the combination of steady state detection, parameter estimation, data reconcilation and solving of a nonlinear optimisation problem online (White, 1997) is not very practical for operations.

In this work, the idea of self-optimising control will be applied to the given network. Self-optimising control offers to pursue economical objectives J without the need of re-optimise the system when disturbances **d** occur. Actually, self-optimising control (Skogestad, 2000) is achieved if a constant setpoint policy results in an acceptable loss L. On the Figure 1.2., we see that a loss generally results when we keep a constant setpoint rather than reoptimising when a disturbance occurs.

$$L = J(\boldsymbol{u}, \boldsymbol{d}) - J_{opt}(\boldsymbol{d}) \text{ where } \quad \boldsymbol{u} = \boldsymbol{f}(\boldsymbol{c}, \boldsymbol{d}) \qquad (1.1)$$

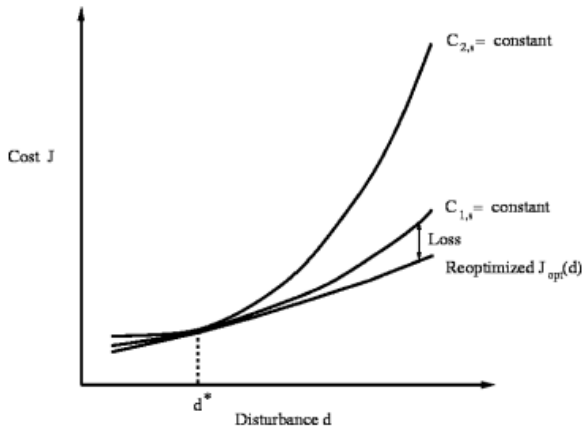

Fig.1.2. Loss as a result of a constant setpoint policy

Jäschke (Jäschke, 2011) introduced invariants for optimal operation of process systems which led to a patent application in the case of parallel heat exchangers (Jäschke, 2012). This work follows the master thesis of Daniel Greiner Edvardsen (Edvardsen, 2011) where a steady-state study using these invariants as self-optimising variables showed very promising results.

Chapter 2

Heat exchanger network dynamic model

2.1. Shell and tube heat exchangers

The Mongstad preheat train is composed of shell and tube heat exchangers made of steel. This is the more common type of heat exchanger in the petrochemical industry. They handle large flowrates due to their high hydraulic diameter. One set of tubes called the tube bundle contains the first fluid while the second fluid runs over the tubes on the shell side so that heat can be transferred between them.

Shell and tube heat exchangers are typically used for high pressure applications due to their shape which insure a strong mechanical resistance. We distinguish many types of shell and tubes heat exchanger due to the diversity of internal flow configurations. The most common are made of one, two or four passes on the tube side and only one on the shell side.

Sinnott and Towler (Sinnott and Towler, 2009) presented some reasons for using shell and tube exchangers:

- The configuration gives a large surface area in a small volume
- Good mechanical layout
- Well-established fabrication techniques
- Can be constructed from a wide range of materials
- Easily cleaned
- Well established design procedures

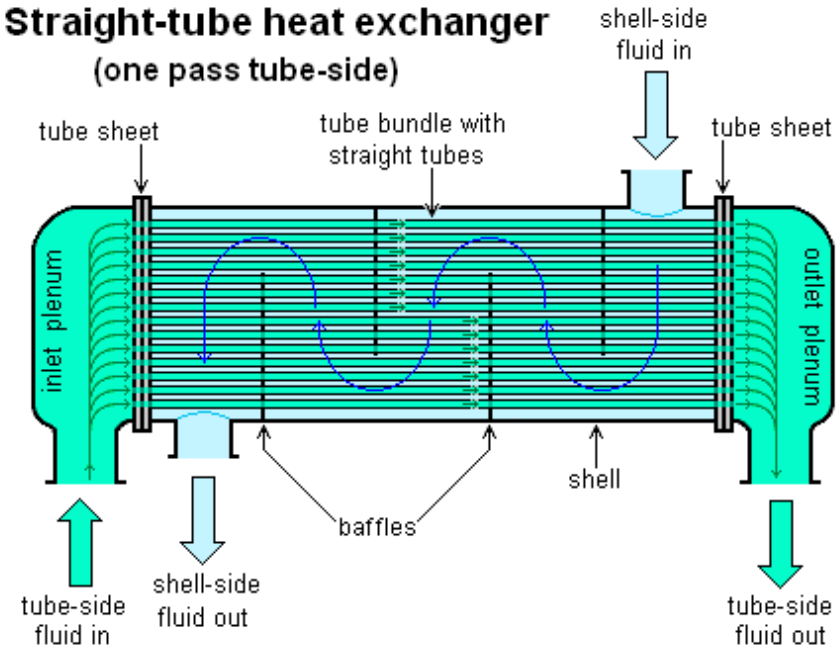

Fig. 2.1. Shell and tube Heat Exchanger (Alaquainc)

Baffles are used in shell and tube heat exchangers to lead the fluid on the shell side across the tube bundle. They are perpendicular to the shell and hold the bundle (Fig.2.1.). They also prevent the tubes from sagging and vibrating. Their influence on the flow mixing is to be considered in dynamics studies, especially in pure countercurrent heat exchangers (one pass on each side) which are the units in which the transfer is the most distributed.

With the time, the heat transfer capacity of such units in the crude oil preheat train may be reduced due to fouling. A well-known cause of fouling is asphaltene insolubility which may depose on the exchange areas.

2.2. Heat exchanger model

2.2.1. Topology and assumptions

A dynamic model of the heat exchanger network is needed in order to assess controllability. The first step is to build a general dynamic model of shell and tube heat exchanger. Following the work of Mathisen (Mathisen, 1994b), a flexible lumped multicell model has been developed in order to involve all the important features such as the number of compartments for each fluid (number of elements), fluid heat capacities, heat transfer coefficients (including convective and wall resistances) and wall capacitance.

Since flow configuration has not a major effect on the dynamics of the whole network (Mathisen, 1994b), a counter-current multi-cell topology has been introduced. As shown on the Figure 2.2., each internal fluid side is represented by a serie of N elements of fixed volume.

Hot and cold cells are interconnected by a single and independent wall element. Since the cells are assumed to be ideally mixed, all physical data are assumed to be constant in each cell.

The main assumptions are negligible heat loss, negligible pressure drop, constant wall heat capacity, constant fluid densities and equal distribution of areas and volumes over the N cells. The model is thus made of 3N states, N hot fluid temperatures, N cold fluid temperatures and N wall temperatures. By default, the number of cells has been fixed to 10 for all heat exchangers.

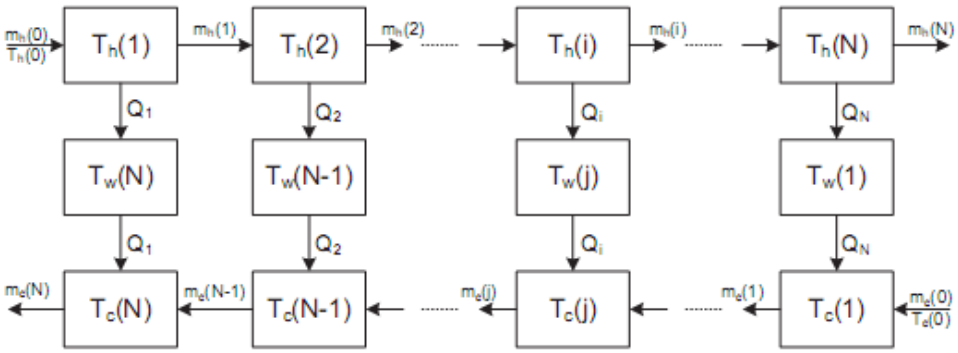

Fig. 2.2. Heat exchanger model topology

2.2.2. Derivation of the state equations

The 2N state equations for the fluid streams are derived from the energy balance on each element:

$$\dot{U}(i) = H(i-1) - H(i) \pm Q(i) \tag{2.1}$$

Assuming specific heat capacities constant in two connected elements:

$$\dot{U}(i) = c_v V(i) \frac{d(\rho(i)T(i))}{dt} = mc_p(T(i-1) - T(i)) \pm Q(i) \tag{2.2}$$

As the liquid fluids are assumed to be incompressible and $c_p \approx c_v$:

$$c_p \rho(i) V(i) \frac{dT(i)}{dt} = mc_p(T(i-1) - T(i)) \pm Q(i) \tag{2.3}$$

Introducing a simple heat transfer law where heat transfer coefficients represent convective and semi-wall resistances:

$$\frac{dT(i)}{dt} = T(i-1) - T(i) \pm \frac{hA(i)}{mc_p} \Delta T(i) \frac{m}{\rho V(i)} \tag{2.4}$$

$$= T(i-1) - T(i) \pm \frac{hA}{Nmc_p} \Delta T(i) \frac{mN}{\rho V} \tag{2.5}$$

The N state equations for the wall elements are easily obtained by energy balance :

$$\frac{dT(j)}{dt} = (h_h \Delta T_{wh}(j) - h_c \Delta T_{wc}(j)) \frac{A}{\rho_w c_{p,w} V_w} \quad (2.6)$$

2.3. Network model

The process flow diagram of the Mongstad crude oil preheat train is shown below (Fig. 2.3.). All streams are assumed to be in a complete liquid phase. The crude oil enters the network at the point ln1 and is distributed in seven branches A,B,C,D,E,F,G. The heat exchangers are represented in grey while the measurements points (temperature and/or flowrate) are indicated by a circle, white for the crude oil, colored for the hot streams.

The first part of this project was to prepare a model in order to control as best as possible the distribution of the crude oil in the network, focusing on the several branches. Since the self-optimising variables have so far been developed only for parallal branches that split from one single point and gather in another single point, the sub-network indicated by the red box has been studied in this work. This sub-network consists of 6 branches from A to F and 11 heat exchangers involved in the crude oil heating.

The rest of the network is a scheme quite similar to serie structure so the direct objective of the control strategy is different than finding an optimal distribution of the crude oil in several branches. Consequently, this second sub-network has less degree of freedom and offers less possibilities of control which could influence the final temperature. However, a study on this second sub-network or, at least, on its influences to the first sub-network will be required to implement successfully the self-optimising control method. This is left as future work.

The heat exchanger network that will be modeled in this project can be described as it is shown on the simplified process flow diagram shown in Figure 2.4.

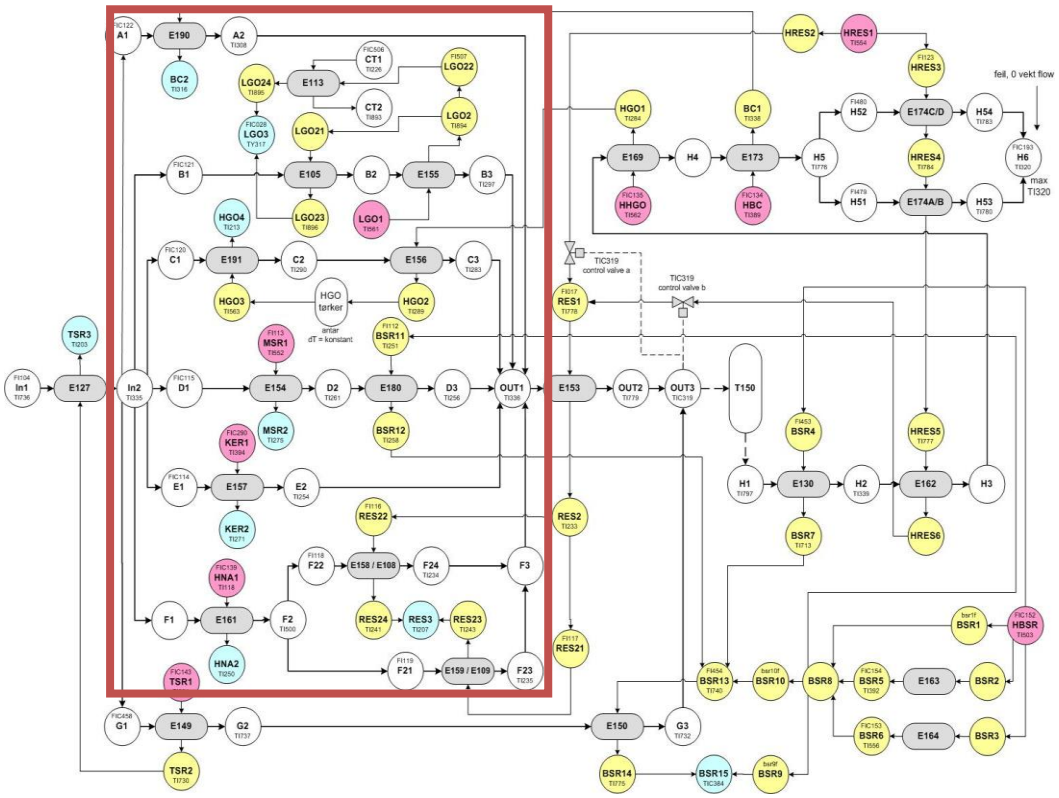

Fig. 2.3. Statoil Mongstad crude unit Heat Exchanger Network

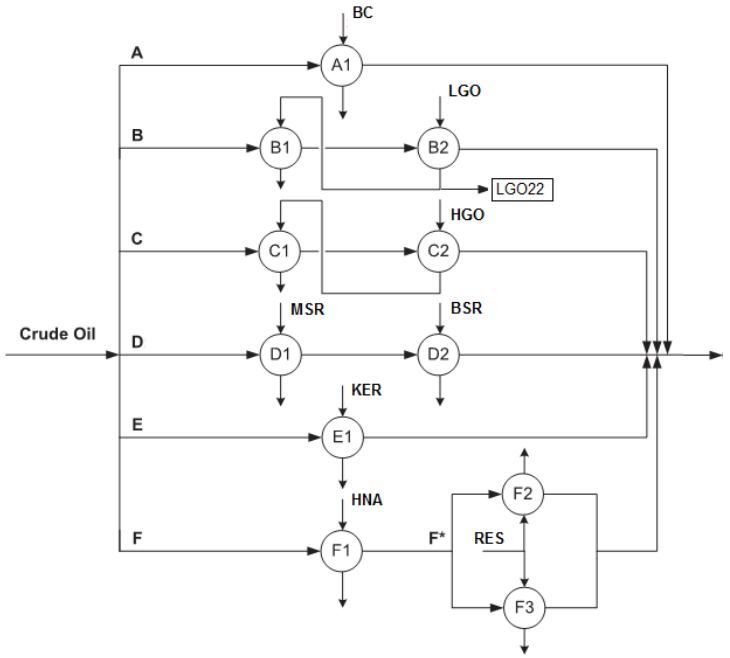

Fig.2.4. Simplified process flow diagram

2.3.1. Global energy balance

When the crude oil has been heated by the several branches of the heat exchanger network, the crude oil streams are gathered in a mixer and the outlet total temperature can be computed with the energy balance.

$$\Delta H = \sum_{streams} m_i \Delta h_i \tag{2.7}$$

$$= \sum_{streams} m_i \int_{T_{ref}}^{T_i} c_p dT \tag{2.8}$$

$$= \sum_{streams} m_i \int_{T_{ref}}^{T_i} (k_{1,crude} T + k_{2,crude}) dT \tag{2.9}$$

The formula for the heat capacities is introduced in the section 2.4.2. *Data treatment, heat capacities.*

$$\Rightarrow \Delta H = \sum_{streams} m_i \left[k_1 \frac{T^2}{2} + k_2 T \right]_{T_{ref}}^{T_i} \tag{2.10}$$

$$= \sum_{streams} m_i \, T_i \left(k_1 \frac{T_i}{2} + k_2 \right) - m_{tot} T_{ref} \left(k_1 \frac{T_{ref}}{2} + k_2 \right) \tag{2.11}$$

where $$m_{tot} = \sum_{streams} m_i \tag{2.12}$$

This amount of energy can then be expressed as a function of the unkown outlet total temperature T_{tot}:

$$\Delta H = m_{tot} \int_{T_{ref}}^{T_{tot}} c_p dT \tag{2.13}$$

$$= m_{tot} \int_{T_{ref}}^{T_{tot}} (k_1 T + k_2) dT \tag{2.14}$$

$$= m_{tot} T_{tot} \left(k_1 \frac{T_{tot}}{2} + k_2 \right) - m_{tot} T_{ref} \left(k_1 \frac{T_{ref}}{2} + k_2 \right) \tag{2.15}$$

We can then calculate T_{tot} combining the equations (2.11) and (2.15):

$$\sum_{streams} m_i \, T_i \left(k_1 \frac{T_i}{2} + k_2 \right) = m_{tot} T_{tot} \left(k_1 \frac{T_{tot}}{2} + k_2 \right) \tag{2.16}$$

This is a second order equation:

$$a T_{tot}^2 + b T_{tot} + c = 0$$

$$\text{where} \quad \begin{cases} a = \frac{m_{tot} k_1}{2} \\ b = m_{tot} k_2 \\ c = -\sum_{streams} m_i \, T_i \left(k_1 \frac{T_i}{2} + k_2 \right) \end{cases} \tag{2.17}$$

The physical solution is the temperature which will be positive, we expect the outlet temperature to be around 150-250°C.

$$T_{tot} = \frac{-b+\sqrt{b^2-4ac}}{2a} \quad (> 0) \tag{2.18}$$

$$= \frac{-m_{tot}k_2+\sqrt{{m_{tot}}^2{k_2}^2+2m_{tot}k_1\sum_{streams} m_i T_i\left(k_1\frac{T_i}{2}+k_2\right)}}{m_{tot}k_1} \tag{2.19}$$

2.3.2. Distribution valve model

The distribution of the crude oil flow in the branches is assumed to be analogous to the distribution of the electric current in a circuit of parallel resistances. Each branch of the heat exchanger network comprises a valve providing resistance to the total inlet crude oil flow (Fig. 2.5.). This resistance is assumed to be the inverse of the valve position (opening fraction). The resistance (or pressure drop) of the heat exchangers is assumed to be more or less the same in each branch and is not taken into account.

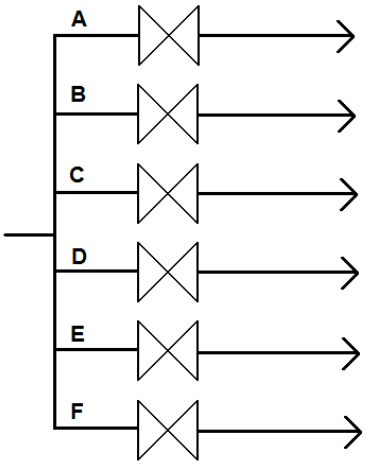

Fig. 2.5. Distribution valve model

The manipulated variables in our control problem are the valve positions:

$$z_i \in [0,1] \quad , \quad i = A, B, C, D, E, F \tag{2.20}$$

So the crude oil feed flowrate in the branch i is calculated by the formula:

$$m_i = \frac{z_i}{z_A+z_B+z_C+z_D+z_E+z_F} * m_{tot} \tag{2.21}$$

At optimal conditions, the branch having the highest feed flowrate should have its valve fully open. Otherwise, the pressure drop could be reduced in the whole network. This ascertainment will be taken into account for the design of the control structure.

2.4. Data treatment

In this project, data were provided by Statoil Mongstad and needed to be selected and treated appropriately while some unkown values had to be estimated. This section presents the steps between the data reception and the data introduction in our shell and tube heat exchanger network model.

2.4.1. Volumes and Areas

Fortunately, all heat exchanger areas were provided in the data files received from Statoil Mongstad. These values have been directly introduced in the models without any modification.

Unfortunately, some heat exchanger bundle and shell volumes were not provided in the data files received from Mongstad. Simple linear correlations based on the known heat exchangers data have been examined in order to find the best way to estimate the missing data. Similarities between the heat exchangers have been observed and we thus hope that the estimated data is reasonable.

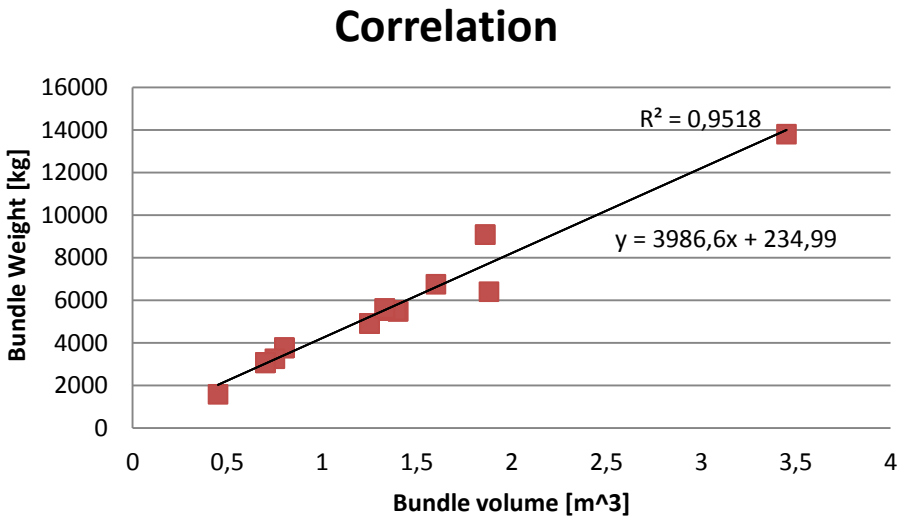

Fig. 2.6. Correlation for missing bundle volume estimations

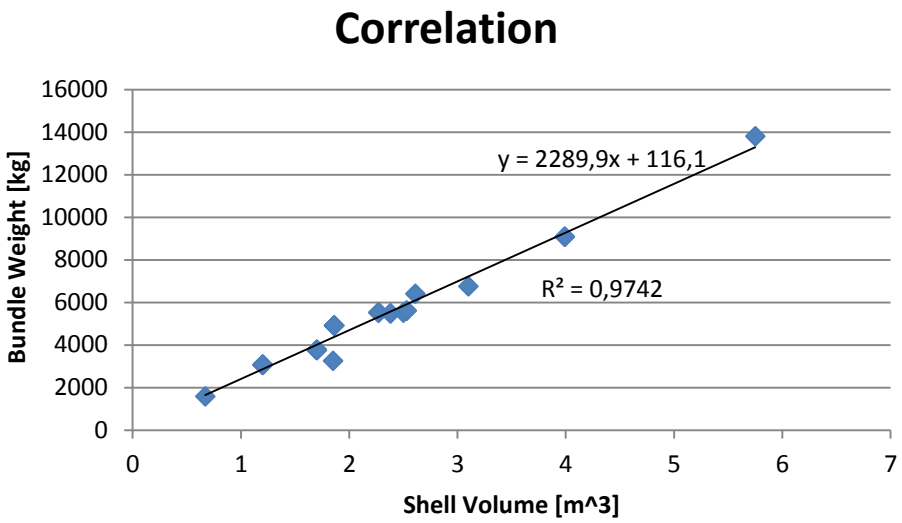

Fig. 2.7. Correlation for missing shell volume estimations

The best correlations (maximum coefficient of determination) were obtained between the bundle weight and the bundle volume (Fig. 2.6.) and between the bundle weight and the shell volume (Fig. 2.7.). So we used these two correlations in order to estimate the missing volumes *(in italic in the table 2.18.)*.

Heat exchanger	Exchange Area [m²]	Bundle Volume [m^3]	Shell Volume [m^3]	Bundle Weight [kg]	Shell Weight [kg]	Crude flow side
A1	138	0,8	1,7	3760	5450	Shell
B1	162	*0,714*	*1,287*	3080	7430	Shell
B2	203	*0,962*	*1,727*	4070	3840	Tube
C1	264	1,4	2,38	5480	7020	Tube
C2	233	*1,153*	*2,059*	4830	4890	Tube
D1	260	1,25	1,86	4910	4970	Tube
D2	313	1,88	2,61	6400	8450	Shell
E1	164	0,7	1,2	3060	3170	Tube
F1	77	0,45	0,67	1580	2420	Tube
F2	278	1,39	2,5	5520	6130	Tube
F3	278	1,33	2,53	5610	6390	Tube

Tab. 2.8. Heat exchangers data

The wall weight inside the state equations corresponds to the bundle weight (Fig.2.9.). The material of the wall is steel so the heat capacity of the wall is fixed at 460 J/kgK and the wall density to 7800 kg/m^3 (Substech).

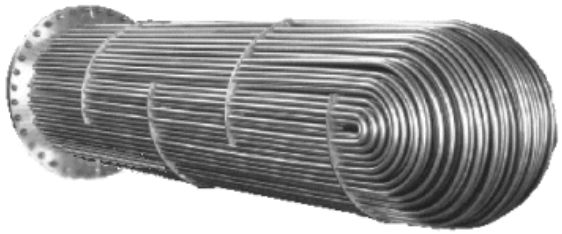

Fig. 2.9. Heat exchanger bundle (Synergycoils)

2.4.2. Fluid heat capacities

The fluid heat capacities at constant pressure were given for each fluid as a linear function of the temperature (Tab. 2.10.). So the heat capacity is adjusted in each fluid element using the current temperature (state variable) prior to calculate the temperature derivatives (state equations). On the Figure 2.11., we observe that the heat capacity of each fluid varies in its corresponding temperature range so this adjustment lead to a better accuracy of the model than the assumption of keeping them constant.

$$c_p = k_1 T + k_2 \qquad (2.22)$$

Fluid	k_1[J/kgK°C]	k_2 [J/kgK]
Crude oil	4,2594	1789,5
RES	3,6378	1779,8
BC	3,9566	1777,1
HGO	3,9802	1792,4
LGO	4,1272	1796,3
KERO	4,4296	1794,1
HNAF	4,9326	1779,1
TSR	5,0218	1779,8
MSR	4,4584	1796,7
BSR	4,0966	1787,7
FCR	3,9018	1784,7

Tab. 2.10. Heat capacities data

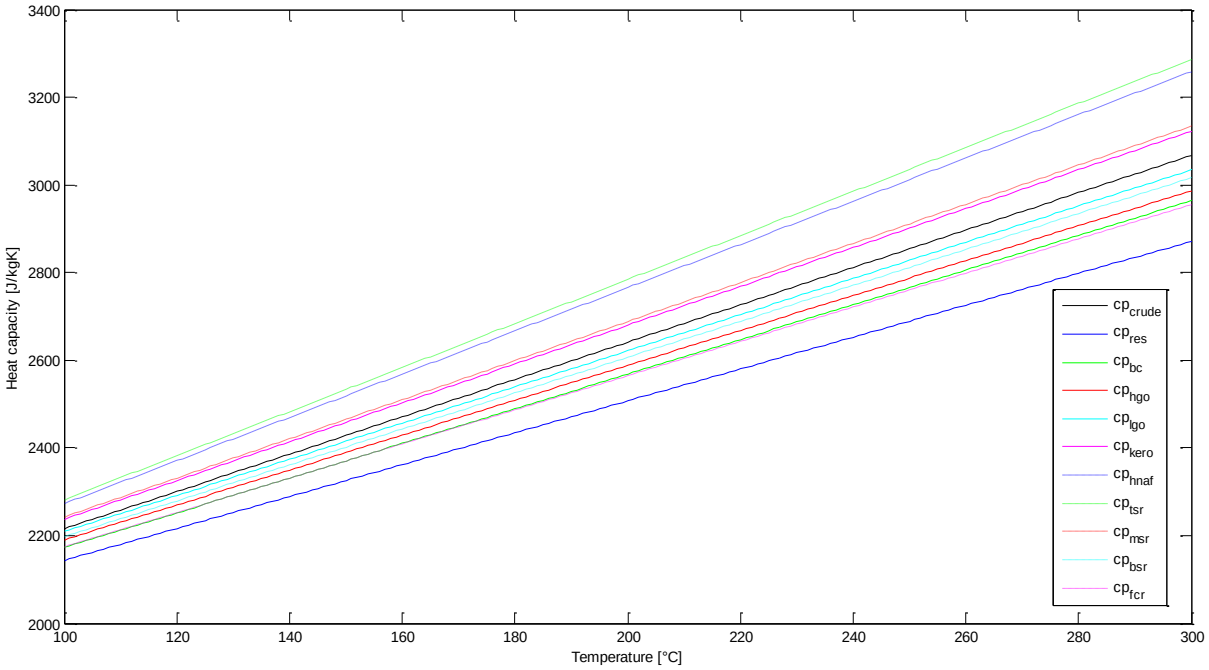

Fig.2.11. Heat capacities as a function of temperature

2.4.3. Temperatures and flowrates

The temperatures and flowrates of the network have been given by Statoil Mongstad. Production measurements between the 23 october 2011 at 13:07:25 and 24 october 2011 at 13:06:26 on a 1 minute basis have been provided. Looking at the variations on the feed temperature and other measurements, the values used for the model were collected at a point of time where the network seems to be the most stabilised, especially in a thermal perspective (Fig.2.12., red arrow): the 23 october 2011 at 18:10:36.

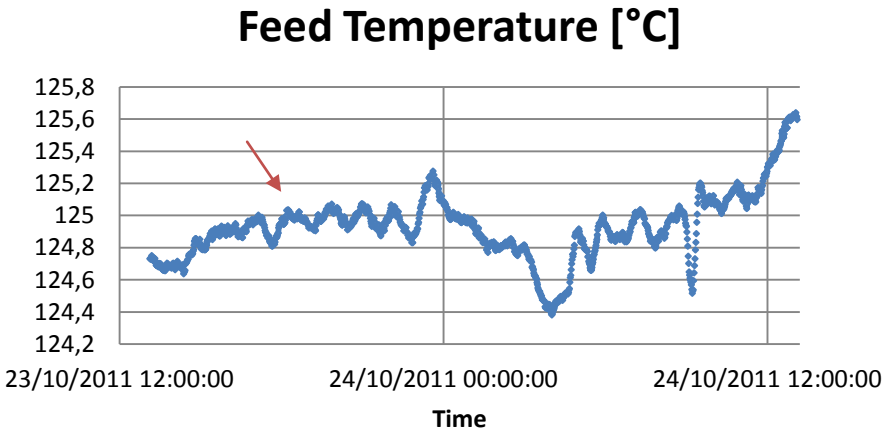

Fig. 2.12. Production feed temperature variations

Mass and energy balances have been used to estimate unkown temperatures and flowrates (some useful streams data are not present in the list provided by Statoil) and simple form of data reconciliation has been used to modify the given measurements as little as possible in order to fulfill the stationary mass and energy balances.

In order to simplify the problem, we assumed the uncertainties on the flowrates to be two times higher in percentage than the temperature uncertainties (in percentage on a Celsius temperature scale basis). Actually, we observe that flowrates vary a lot in operations and they may differ a lot compared to steady-state. For simplicity, we also assumed the crude oil feed temperature to be fixed (not subject to reconciliation) and the network crude oil outlet temperature to be not given as a data.

Actually, if the desired values for the model differs from the given data, it is probably much more due to the fact that the given data come from ongoing production with all kind of transient effects in the network (different time scales). The measurement errors are probably the main secondary source of deviations.

The data treatment for temperatures and flowrates is detailed branch per branch in the appendix. Nevertheless, we illustrate it here for branch F. Please refer to the simplified process flow diagram (Fig. 2.4.) for the notations.

- Heat exchanger F1 :

$$\Delta H_{F1,crude} = \Delta H_{HNA} \tag{2.23}$$

$$\Leftrightarrow m_F \int_{T_{in}}^{T_{F,inter}} c_{p,crude} dT = m_{MSR} \int_{T_{HNA,out}}^{T_{HNA,in}} c_{p,HNA} dT \tag{2.24}$$

$$\Leftrightarrow m_F \left[T_{F,inter} \left(k_{1,crude} \frac{T_{F,inter}}{2} + k_{2,crude} \right) - T_{in} \left(k_1 \frac{T_{in}}{2} + k_2 \right) \right]$$

$$= m_{HNA} \left[T_{HNA,in} \left(k_{1,HNA} \frac{T_{HNA,in}}{2} + k_{2,HNA} \right) - T_{HNA,out} \left(k_{1,HNA} \frac{T_{HNA,out}}{2} + k_{2,HNA} \right) \right] \tag{2.25}$$

- Heat exchanger F2 :

$$\Delta H_{F2,crude} = \Delta H_{RES,1} \tag{2.26}$$

$$\Leftrightarrow m_{F,2} \int_{T_{F,inter}}^{T_{F2,out}} c_{p,crude} dT = m_{RES,1} \int_{T_{RES,1,out}}^{T_{RES,in}} c_{p,RES} dT \tag{2.27}$$

$$\Leftrightarrow m_{F,2} \left[T_{F2,out} \left(k_{1,crude} \frac{T_{F2,out}}{2} + k_{2,crude} \right) - T_{F,inter} \left(k_{1,crude} \frac{T_{F,inter}}{2} + k_{2,crude} \right) \right]$$

$$= m_{RES,1} \left[T_{RES,in} \left(k_{1,RES} \frac{T_{RES,in}}{2} + k_{2,RES} \right) - T_{RES,1,out} \left(k_{1,RES} \frac{T_{RES,1,out}}{2} + k_{2,RES} \right) \right] \tag{2.28}$$

- Heat exchanger F3 :

$$\Delta H_{F3,crude} = \Delta H_{RES,2} \tag{2.29}$$

$$\Leftrightarrow m_{F,3} \int_{T_{F,inter}}^{T_{F3,out}} c_{p,crude} dT = m_{RES,2} \int_{T_{RES,2,out}}^{T_{RES,in}} c_{p,RES} dT \tag{2.30}$$

$$\Leftrightarrow m_{F,3} \left[T_{F2,out} \left(k_{1,crude} \frac{T_{F2,out}}{2} + k_{2,crude} \right) - T_{F,inter} \left(k_{1,crude} \frac{T_{F,inter}}{2} + k_{2,crude} \right) \right]$$

$$= m_{RES,2} \left[T_{RES,in} \left(k_{1,RES} \frac{T_{RES,in}}{2} + k_{2,RES} \right) - T_{RES,2,out} \left(k_{1,RES} \frac{T_{RES,2,out}}{2} + k_{2,RES} \right) \right] \tag{2.31}$$

In these balances, we have all the data except for m_F which is easily determined by the mass balance:

$$m_F = m_{F,2} + m_{F,3} \tag{2.32}$$

However, introducing the data (Tab 2.13.), the equations do not match perfectly so reconciliation is needed to obtain steady-state values.

$m_F\ [t/h]$	$T_{in}\ [°C]$	$T_{F,inter}\ [°C]$	$T_{HNA,in}\ [°C]$	$T_{HNA,out}\ [°C]$	$m_{HNA}\ [t/h]$
252,54	125,00	136,957	194,664	153,96	72,738

$T_{F2,out}\ [°C]$	$T_{RES,in}\ [°C]$	$T_{RES,1,out}\ [°C]$	$m_{RES,1}\ [t/h]$	$m_{F2}\ [t/h]$
205,699	244,379	172,484	113,146	119,41

$T_{F3,out}\ [°C]$	$T_{RES,2,out}\ [°C]$	$m_{RES,2}\ [t/h]$	$m_{F3}\ [t/h]$
199,086	172,207	109,10	133,13

Tab. 2.13. Branch F data

For the given values, we observe that:

$$\Delta H_{F1} = 1968{,}9\ [kJ] << \Delta H_{HNA} = 2170{,}3\ [kJ] \tag{2.33}$$

$$\Delta H_{F,2} = 5774{,}1\ [kJ] \approx \Delta H_{RES,1} = 5735{,}0\ [kJ] \tag{2.34}$$

$$\Delta H_{F,3} = 5755{,}9\ [kJ] > \Delta H_{RES,2} = 5550{,}0\ [kJ] \tag{2.35}$$

So we introduce a first reconciliation factor $\varepsilon > 0$ such that:

$$T_{r,HNA,in} = T_{HNA,in}(1 - \varepsilon) \tag{2.36}$$

$$T_{r,HNA,out} = T_{HNA,out}(1 + \varepsilon) \tag{2.37}$$

$$m_{r,HNA} = m_{HNA}(1 - 2\varepsilon) \tag{2.38}$$

$$m_{r,F} = m_F(1 + \varepsilon) \tag{2.39}$$

$$m_{r,F2} = m_{F2}(1 + \varepsilon) \tag{2.40}$$

$$m_{r,F3} = m_{r,F} - m_{r,F2} \tag{2.41}$$

$$T_{r,F,inter} = T_{F,inter}(1 + \varepsilon) \tag{2.42}$$

We optimise the sum of the energy balance absolute errors for ε (using Microsoft Excel Solver) and obtain:

$$\Delta H_{F1} = \Delta H_{HNA} = 2073{,}9\ [kJ] \tag{2.43}$$

$$\Delta H_{F,2} = 5722{,}6\ [kJ] \lesssim \Delta H_{RES,1} = 5735{,}0\ [kJ] \tag{2.44}$$

$$\Delta H_{F,3} = 5729{,}2\ [kJ] > \Delta H_{RES,2} = 5550{,}0\ [kJ] \tag{2.45}$$

So we introduce a second reconciliation factors $\gamma > 0$ such that:

$$T_{r,RES,2,out} = T_{RES,2,out}(1-\gamma) \tag{2.46}$$

$$m_{r,RES,2} = m_{RES,2}(1+2\gamma) \tag{2.47}$$

We optimise again the sum of energy balance absolute errors and obtain:

$$\Delta H_{F1} \approx \Delta H_{HNA} = 2073{,}9\ [kJ] \tag{2.48}$$

$$\Delta H_{F,2} = 5722{,}6\ [kJ] \lesssim \Delta H_{RES,1} = 5735{,}0\ [kJ] \tag{2.49}$$

$$\Delta H_{F,3} \approx \Delta H_{RES,2} = 5729{,}2\ [kJ] \tag{2.50}$$

So we finally introduce a third reconciliation variable $\delta \gtrsim 0$ such that:

$$m_{r,RES,1} = m_{RES,1}(1-2\delta) \tag{2.51}$$

$$T_{r,RES,1out} = T_{RES,1,out}(1+\delta) \tag{2.52}$$

$$T_{r,F2,out} = T_{F2,out}(1+\delta) \tag{2.53}$$

$$T_{r,F3,out} = T_{F3,out}(1-\delta) \tag{2.54}$$

And we solve the previous energy balances with the new temperatures and flowrates in order to find ε, γ and δ:

$$\Rightarrow \begin{cases} \varepsilon = 0{,}00422 \\ \gamma = 0{,}007282 \\ \delta = 0{,}000289 \end{cases} \tag{2.55}$$

The reconciled values are listed in Tab. 2.14. :

$m_{r,F}\ [t/h]$	$T_{in}\ [°C]$	$T_{r,F,inter}\ [°C]$	$T_{r,HNA,in}\ [°C]$	$T_{r,HNA,out}\ [°C]$	$m_{r,HNA}\ [t/h]$
253,60	125,00	137,535	193,843	154,610	72,125

$T_{r,F2,out}\ [°C]$	$T_{r,RES,in}\ [°C]$	$T_{r,RES,1,out}\ [°C]$	$m_{r,RES,1}\ [t/h]$	$m_{r,F2}\ [t/h]$
205,759	244,379	172,534	113,081	119,91

$T_{r,F3,out}\ [°C]$	$T_{r,RES,2,out}\ [°C]$	$m_{r,RES,2}\ [t/h]$	$m_{r,F3}\ [t/h]$
199,028	170,953	110,689	133,69

Tab. 2.14. Branch F reconciled values

2.4.4. Fluid Densities

The following table 2.15. has been provided by Statoil Mongstad. The density is given is kg/dm^3.

Temp [°C]	Crude	Residue	BPA	HGO	MPA	LGO	KERO	HNA	TPA
15	0,845	0,935	0,874	0,893	0,825	0,859	0,827	0,792	0,788
50	0,821	0,916							
100	0,788	0,89	0,823	0,844	0,768	0,805	0,77	0,73	0,7204
150	0,75	0,864							
200	0,707	0,837	0,759	0,786	0,69	0,737	0,694	0,64	0,631
250	0,657	0,81	0,724	0,754					
300	0,598	0,782	0,684	0,72	0,587	0,66	0,593	0,513	0,499
350		0,751	0,639	0,689					

Tab. 2.15. Density data

This leads to the Figure 2.16. We observe clearly the results of the crude oil fractionation separating the products according to their volatility (which is related to the density).

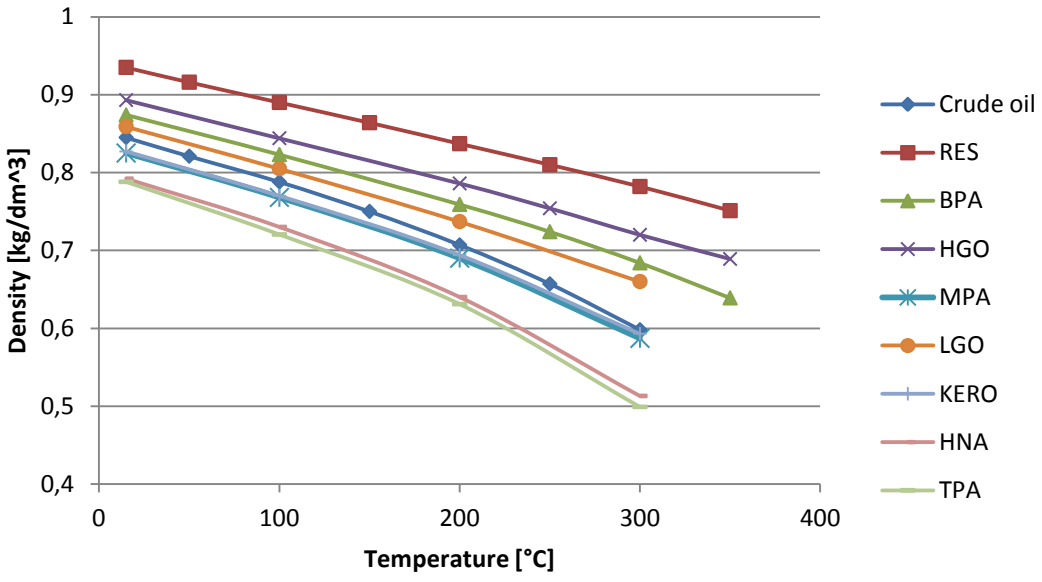

Fig. 2.16. Fluid densities as function of the temperature

Considering the range of temperature for which each fluid is concerned, we find out that the assumption of constant density required by the model is quite strong. Nevertheless, for each fluid, we fix the density value at the arithmetic mean in the temperature range using linear interpolation.

Since we do not have densities for the fluid BC, we assume this fluid to be similar to BPA (=BSR). Actually, BC is similar to BSR in respect the heat capacity values (cfr. Fig. 2.11.) and is also described as a product in the bottom of the fractionation column in Figure.1.1.

The results are shown in the table below.

Fluid	Mean temperature [°C]	Density [kg/m^3]
Crude oil	166,33	735,96
Residue (=RES)	207,6659	832,86
BPA (=BSR)	256,221	719,023
HGO	195,0137	788,892
MPA (=MSR)	199,6211	690,296
LGO	223,4688	718,929
KERO	211,1618	682,727
HNA	174,2267	663,196
BC	231,5176	736,938

Fig. 2.17. Fluid densities

2.4.5. Heat transfer coefficients

The heat transfer coefficients are the last unkown model variables and are estimated separately for each heat exchanger unit by fitting the modeled heat transfer to the reconciled heat transfer. Actually, the overall heat transfer in each heat exchanger is a single variable to be adjusted so we introduced a single variable coefficient by unit. We thus assume the heat transfer coefficient to be the same value on both streams (hot and cold).

As said previously, this simplified heat coefficient includes convective and wall resistances. That's why its value should normally be a bit higher than what can be found in the literature for physical heat coefficients (using heat transfer correlations). The global heat exchanger heat transfer coefficient **U** can be simply estimated:

$$\frac{1}{\boldsymbol{U}} = \frac{2}{h} \iff \boldsymbol{U} = \frac{h}{2} \qquad (2.56)$$

For liquid-liquid heat exchange, we can expect the **U** values in the range 150-1200 W/m²K (Lunsford, 1998) so we expect h values in the range 300-2400 W/m²K.

The heat exchanger state variables are initialised with linear temperature profiles and each branch is simulated separately and the heat transfer coefficients are easily adjusted manually to obtain the steady-state reconciled heat transfer calculated previously (Fig. 2.18.).

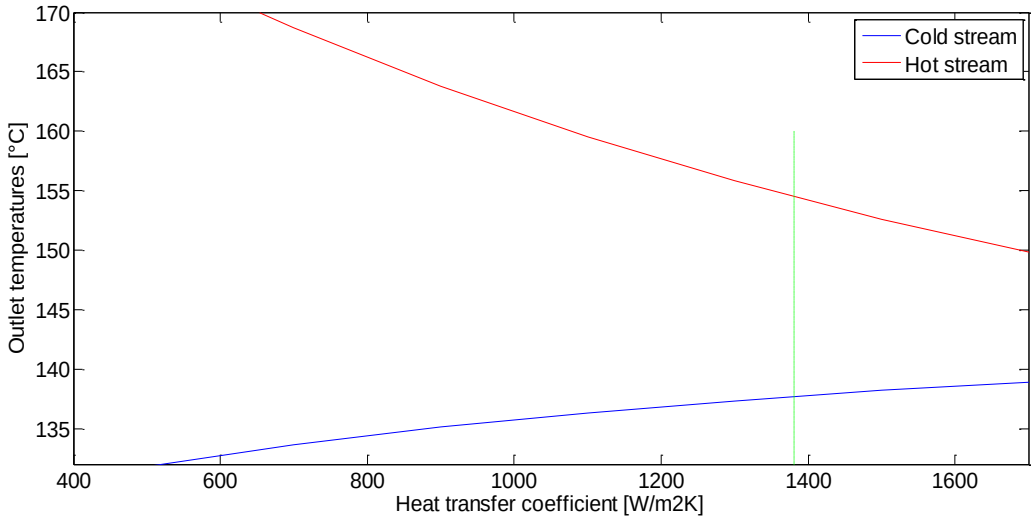

Fig. 2.18. Steady-state matching of the heat transfer, unit F1

The heat transfer coefficients values from this simulation procedure are listed in table below (Table 2.19.).

Heat exchanger	Heat transfer coefficient h [W/m²K]
A	1902
B1	1189
B2	713
C1	1565
C2	1565
D1	1250
D2	382.5
E	1976
F1	1381
F2	1462.5
F3	1257.5

Tab. 2.19. Heat transfer coefficients

Once the heat transfer coefficients are tuned, we can re-write the initialization MatLab© file for the temperature profiles by extracting them out of each heat exchanger with a sufficient simulation time for system to stabilise to its stationary point.

The temperatures profiles obtained are close to the linear profiles (Fig. 2.20 & 2.21).

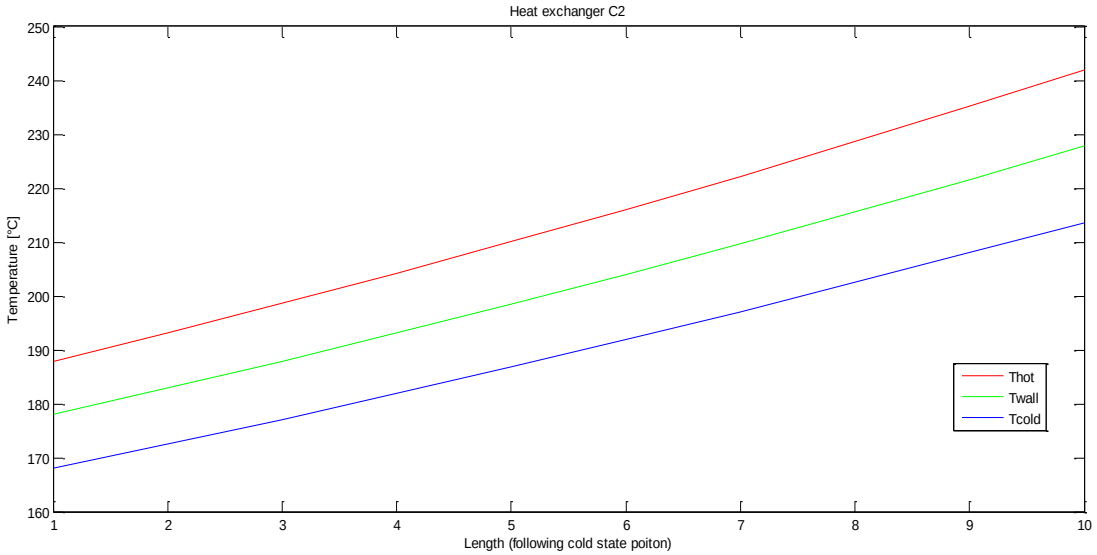

Fig. 2.20. Internal temperature profile at steady-state, unit C2

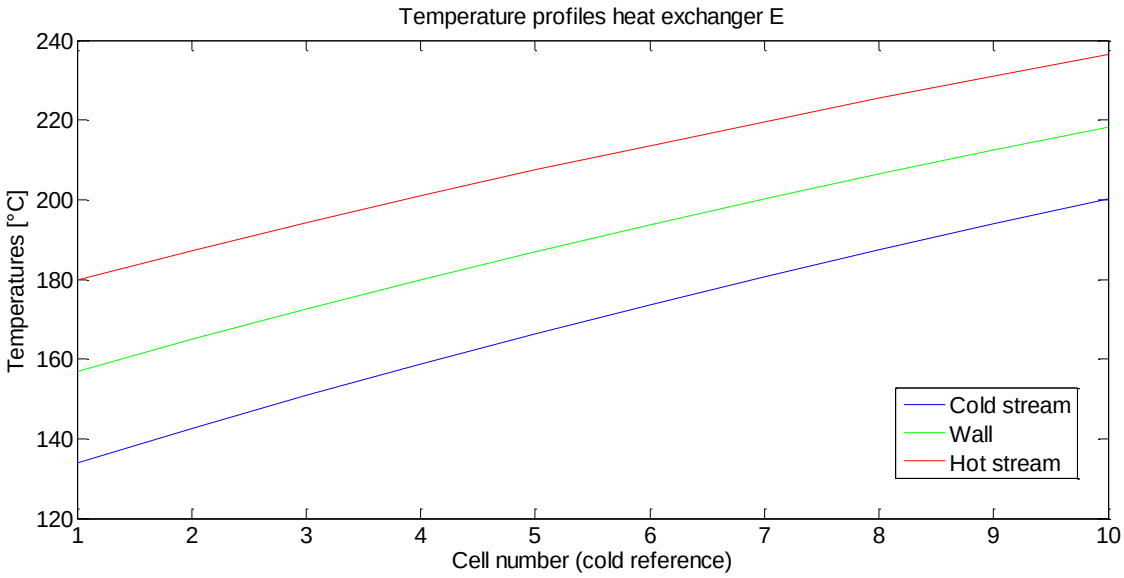

Fig. 2.21. Internal temperature profile at steady-state, unit E

2.5. Simulation tools

The software used in this project is exclusively MatLab© – Simulink which offers both flexibility in implementation and strong solving capacities. Simulink is an appropriate environment for this project. It provides an interactive graphical environment and a customizable set of blocks libraries useful for design, simulation, implementation and testing of time-varying systems including control.

2.5.1. S-function

The shell and tube heat exchanger model has been introduced in Simulink as a S-function (system-function). This mechanism offers to extend the capabilities of the Simulink environment. So an S-function is a computer language description of a Simulink block written in MatLab© or in C, C++, Fortran. S-functions are dynamically linked subroutines that the MatLab© interpreter can automatically load and execute.

Actually, S-functions use a special calling syntax called the S-function API that enables to interact with the Simulink engine. This interaction is very similar to the interaction that takes place between the engine and built-in Simulink blocks. S-functions follow a general form and can accommodate continuous, discrete, and hybrid systems. (MatLab©)

An algorithm can thus be implemented in an S-function which will be used as a block added in a Simulink model. After having written the S-function and placed its name in an S-Function block (available in the Functions block library), the user interface can be customised using masking.

The S-function is thus very convenient for creating describing a system as a set of mathematical equations. In this project, S-function were useful because they allow to custom a simple block in the user interface which will be used for all kind of heat exchanger models.

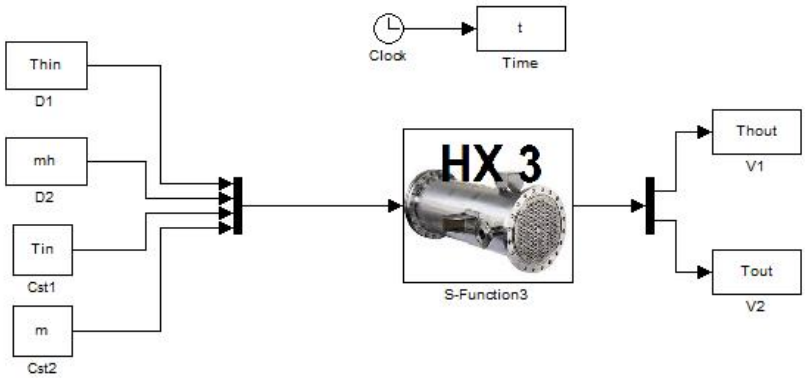

Fig. 2.22. Heat exchanger model block in the Simulink user interface

It is possible to specify parameter values to be passed to the s-functions using the S-Function block S-function parameters. The order in which the function requires them is to be respected. The parameter values can be constants, names of variables defined in the MatLab© or model workspace, or MatLab© expressions.

It is of interest to understand how S-functions work. This knowledge first requires an understanding of how the Simulink engine simulates a model, including the mathematics of blocks. So, a Simulink block consists of a set of inputs, a set of states, and a set of outputs, where the outputs are a function of the simulation time, the inputs, and the states.

$$Outputs: \quad y = f_0(t, x, u) \tag{2.57}$$

$$States: \quad \dot{x} = f_d(t, x, u) \tag{2.58}$$

$$\text{Updates}: \quad x_{d_{k-1}} = f_u(t, x_c, x_{d_k}, u) \tag{2.59}$$

$$\text{where } x = [x_c; x_d] \tag{2.60}$$

The execution of a Simulink model proceeds in stages. First comes the initialization phase. The engine then enters a simulation loop, where each pass through the loop is referred to as a simulation step. During each simulation step, the engine executes each block in the model in the order determined during initialization. For each block, the engine invokes functions that compute the block states, derivatives, and outputs for the current sample time. (MatLab©)

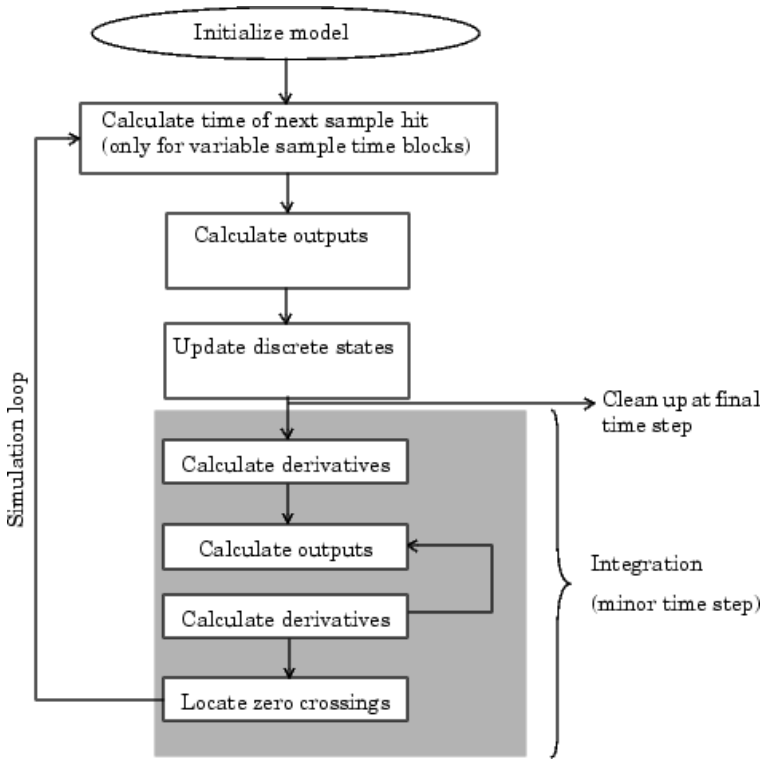

Fig 2.23. Execution of a Simulink model

The inner integration loop takes place only if the model contains continuous states. The engine executes this loop until the solver reaches the desired accuracy for the state computations. The entire simulation loop then continues until the simulation is complete. (MatLab©)

During simulation of a model, at each simulation stage, the Simulink engine calls the appropriate methods for each S-Function block in the model. Tasks performed by S-function callback methods include:

- Initialization :
  - Initializing a simulation structure that contains information about the S-function
  - Setting the number and dimensions of input and output ports
  - Setting the block sample times
  - Allocating storage areas

- Calculation of next sample hit :
  - For a variable sample time block, the next step size is calculated

- Calculation of outputs in the major time step:
  - All the block output ports are valid for the current time step

- Update of discrete states in the major time step:
  - Once-per-time-step activities such as updating discrete states

- Integration:
  - The engine calls the output and derivative or zero-crossing portions of the S-function at minor time steps and so the solvers can compute the state or locate the zero crossings. (MatLab©)

A useful concept in s-function is the presence of the flags that directs the engine to the appropriate code in the several steps of the execution. In case of direct feedthrough (the output is controlled directly by the value of an input port signal), a special flag can be used to detect algebraic loops which may force the simulation results of the S-function to not converge. (MatLab©)

2.6. Model analysis

It is of great importance to verify that the heat exchanger network dynamic model is physically coherent. We thus have to analyse how the model behaves in respect to what we would expect from the real plant, especially in the time-scale dynamics for which we want to design a new control configuration.

2.6.1. Heat Exchanger model analysis

Exchanger A is taken as an example.

Step change in a inlet temperature:

At time = 20s, the hot stream inlet temperature passes from 295.45°C to 245.45°C. The heat transfer is reduced and both outlet temperatures drops as expected. The outlet temperature of the cold stream (blue) has a fast response due to the counter-current flow configuration. The outlet temperature of the hot stream (red) has a delayed response due to the sojourn time in the heat exchanger. (Fig.2.24)

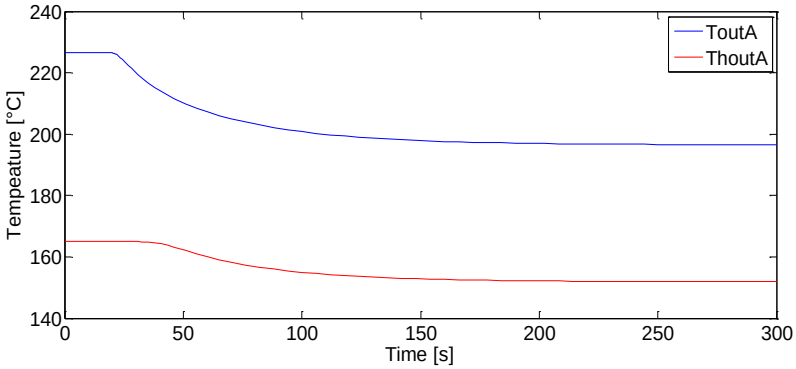

Fig.2.24. Step change in the hot stream inlet temperature

Step change in a inlet flowrate:

At time = 20s, the hot stream flowrate passes from 15.91 kg/s to 18.91 kg/s. We notice the direct change on the hot outlet temperature induced by the assumption of incompressibility. The heat transfer grows as expected. For each stream, the characteristic time of the dynamic response is very close to the sojourn time in the heat exchanger (58.9s for the crude oil; 37s for the hot fluid). (Fig. 2.25)

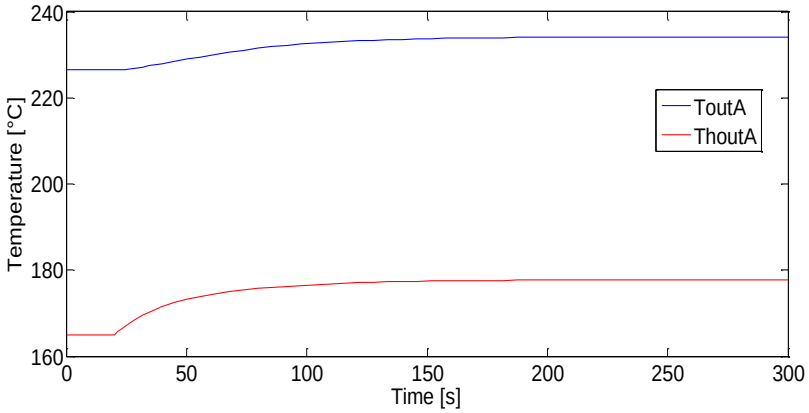

Fig. 2.25. Step change in the hot stream flowrate

2.6.2. Branch model analysis

The Branch C, constituted of two heat exchangers in serie, is taken as example.

Step change in an inlet temperature:

At time=100s, the hot stream inlet temperature passes from 248.77°C to 298.77°C. The two exchangers have together such a capacity for heat transfer that the last temperature of the hot streams (outlet of C1) has changed of 7,5°C only. The heat transfer has been reduced, in both heat exchangers with almost the same intensity. We clearly observe the slow dynamics on the heat exchanger C1 due to the capacity of the heat exchanger C2. (Fig. 2.26)

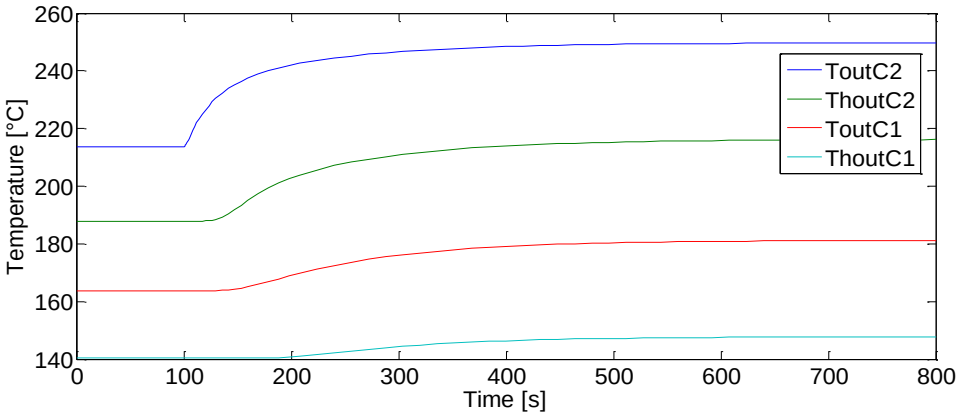

Fig. 2.26. Step change in the hot stream inlet temperature

Step change in an inlet flowrate:

At time=100s, the hot stream flowrate passes from 26.97 kg/s to 20.97 kg/s. We observe that the temperature of the hot fluids reduces very much in the heat exchanger C2 (the first to be crossed by the hot fluid) so the heat transfer on this unit tends to be conserved. The heat transfer reduces mainly on the heat exchanger C1 at lower temperatures where the temperature difference is lower. This is due to the lower driving force in the heat transfer. We observe that the temperature difference between hot and cold fluid diminishes on the first heat exchanger while it grows on the second one. (Fig 2.27)

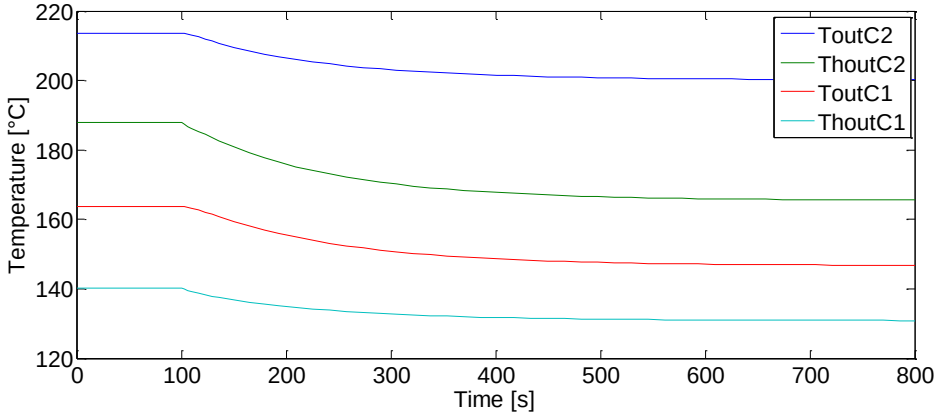

Fig.2.27 Step change in hot stream flowrate

2.6.3. Heat exchanger Network Model Analysis

The complete model is examined in Simulink.

Step change in the feed temperature:

At time=100s, the feed temperature passes from 125°C to 150°C. The fastest branch is E, then comes B, D, A and F, and finally C. The hot fluid flowrate of the branch C is very low compare to the crude oil flowrate. The temperature profiles in this branch thus are very narrow. After the step change, some heat of the crude oil is even taken by the hot fluid branch at the outlet of the first heat exchanger. This explains the observed slow dynamics. (Fig. 2.28)

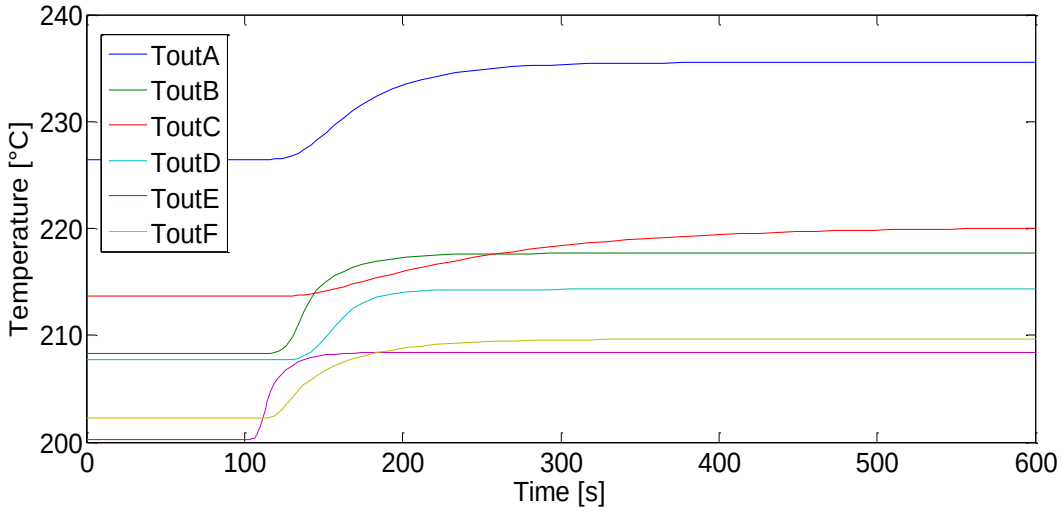

Fig. 2.28. Step change in the feed temperature – Branches dynamics

The effect on the total outlet temperature of the crude oil is plotted on Figure 2.29. The temperature grows is of 7°C only so the heat transfer has been reduced as expected (less driving force in the heat exchangers). The global dynamics of the network is observed to be quite fast but realistic. (Fig. 2.29)

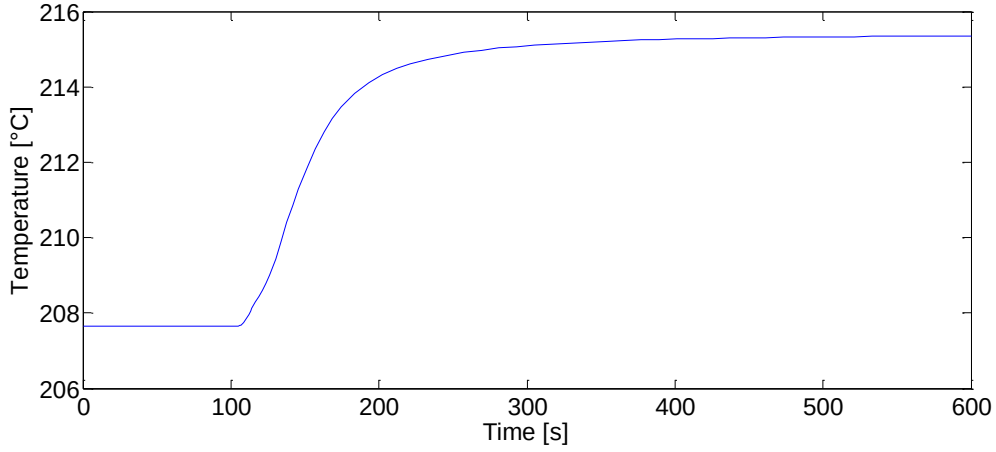

Fig. 2.29. Step change in the feed temperature – Outlet temperature dynamics

Step change in the feed flowrate:

At time=100s, the crude oil feed flowrate reduces from 254.28 kg/s to 224.28 kg/s. We observe the same relative differences between the branches in terms of fastness. The impact of the step is direct due to the incompressibility assumption. (Fig. 2.30)

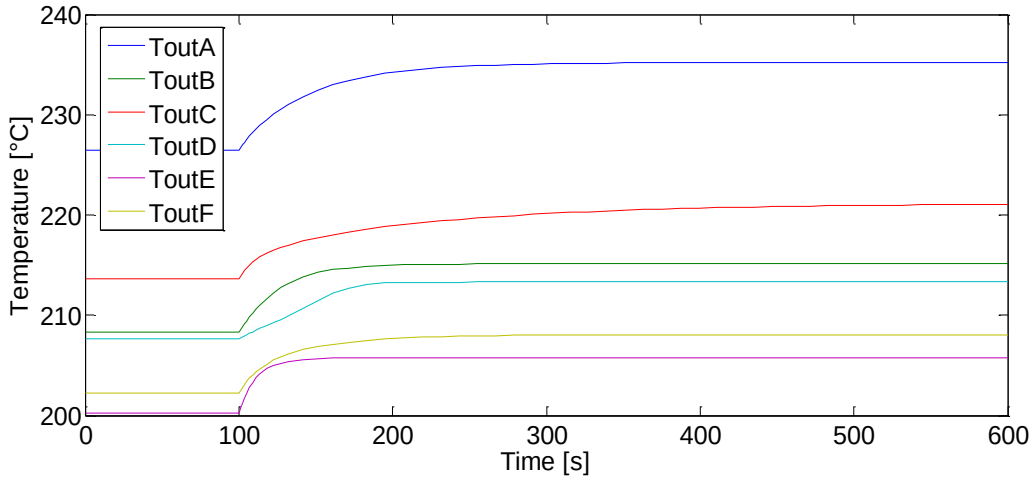

Fig. 2.30. Step change in the feed flowrate

Step change in the valve positions (manipulated variable):

The valve of the branch D is taken as example.

At time = 100s, we simulate at step change of the valve position from 0.7046 to 0.5046. This has for direct effect (algebraic relation) to reduce the mass fraction of the inlet crude oil stream going in this branch of 24,1% of its nominal value while the mass fractions of the other branches rises of 5,8% of their nominal value.

We thus observe the high gain on the branch D outlet temperature and the little reduction on all other branches. (Fig.2.31)

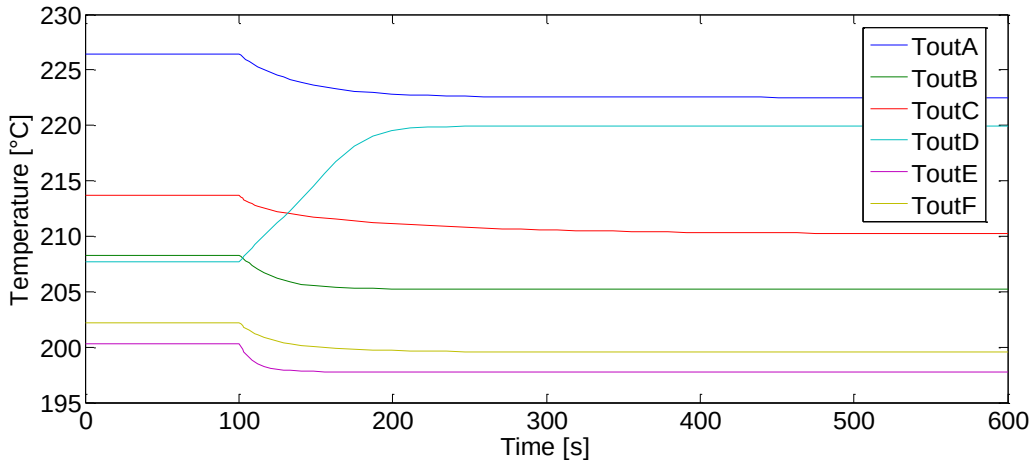

Fig. 2.31. Step change in the valve position – Branches dynamics

The response of total outlet temperature shows clearly the effect of the time-scale separation between the branches. (Fig. 2.31)

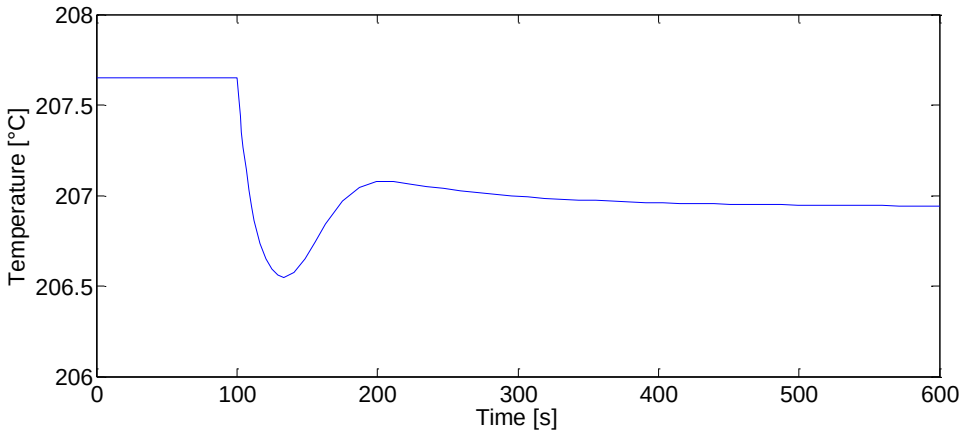

Fig. 2.31. Step change in the valve position - Outlet temperature dynamics

2.6.4. Remark

Modeling is always connected to objectives. The dynamic differences between each heat exchanger unit or branch in the network is clearly observed in our simulation results. We expect these differences to be the main physical characteristic of the system which needs to be handled by the control structure. The given model is thus believed to be accurate, robust and flexible enough for a large study of possible control configurations.

Chapter 3

Self-optimising variables

3.1. Theorical framework

In the general case, the controlled variables are selected as functions of the measurements. Experience and intuition still plays a major role in the design of controlled system. However, the controlled variables used in this work have been derived by a systematic approach. This approach associates the overall control objectives with the selection of the controlled variables. (Jäschke, 2011).

3.1.1. Self-optimising control

Self-optimising control is when near-optimal operation is achieved with constant setpoints for the controlled variables. The introduction to this concept presented here is taken from Skogestad (Skogestad, 2004). Self-optimising control offers to not re-optimise the system when disturbance occurs.

The general optimisation problem is to minimise a certain objective function subject to some constraints:

$$minimize \quad J(x, u_t, d) \tag{3.1}$$

$$subject\ to\ g(x, u_t, d) = 0, h(x, u_t, d) \leq 0 \tag{3.2}$$

Where J is the objective function, x represents the state variables, u_t the manipulated variables (available degrees of freedom) and d the disturbances. The equality constraints g include the model equations and the inequality constraint are used to respect the physics of the system (positive temperatures and mass flows for example).

Some of the inequality constraints h are often active constraints and must be equal to zero. These constraints should be controlled with a corresponding number of degrees of freedom.

Our problem is to decide what to control with the remaining degrees of freedom, u. If the states x are eliminated using the model equations g the remaining unconstrained problem is:

$$min_u \quad J(u,d) \; = J\big(u_{opt}(d), d\big) = \; J_{opt}(d) \tag{3.3}$$

where $u_{opt}(d)$ is to be found and $J_{opt}(d)$ is the optimal value of the objective function.

We want to find a subset of the measured variables named c to keep constant at the optimal values c_{opt}. Ideally, c_{opt} should be insensitive to the disturbances d to obtain optimal operation. In reality, we aim at operation close to optimal and there is a loss associated with keeping the controlled variable constant. This loss can be expressed as:

$$L(u,d) = J(u,d) - J_{opt}(d) \tag{3.4}$$

To select the controlled variables, the following guidelines presented by Skogestad (2000) can be used :

- c_{opt} should be insensitive to disturbances
- c should be easy to measure and control accurately
- c should be sensitive to change in the manipulated variable (degree of freedom)
- For cases with more than one unconstrained degrees of freedom, the selected controlled variables should be independent

These guidelines offer to reduce the effect of disturbances and reduce the implementation error.

An ideal self-optimising variable, proposed among others by Halvorsen and Skogestad (1997), is the gradient of the objective function:

$$c_{ideal} = \frac{\partial J}{\partial u} \tag{3.5}$$

which should be zero to ensure optimal operation for all disturbances. However, measurement of the gradient is usually not available, and computing it requires knowing the value of unmeasured disturbances. To find which variables are the best to keep constant (approximations of the gradient), different approaches can be used:

- Exact local method
- Direct evaluation of loss for all disturbances ("brute force")
- Maximum (scaled) gain method
- Null space method

3.2. Application to Heat exchanger network

Jäschke (Jäschke, 2012) applied his theorical work (Jäschke, 2011) on heat exchanger networks made of parallel branches for which the objective function is easily defined as the end temperature. The optimisation problem is:

$$min_u\ J = -T_{end} \tag{3.6}$$

$$subject\ to\ g = 0 \tag{3.7}$$

Where g is the steady state model of the heat exchanger network and u the available degrees of freedom. It is assumed that the hot streams are disturbances and not degrees of freedom, hence the number of degrees of freedom is equal to the number of splits in the heat exchanger network. In this work, the theory has been applied to heat exchangers where no phase change happens as it is the case in our heat exchanger network.

The work of Jäschke is subjected to a patent application while this work is subjected to be sent to an industrial partner. Consequently, we present the expression of the self-optimising variables without further development. The only major assumption made by Jäschke in its derivation has been to approximate heat transfers using the arithmetic mean temperature instead of the logarithmic mean temperature.

3.2.1. Branches composed of single heat exchangers

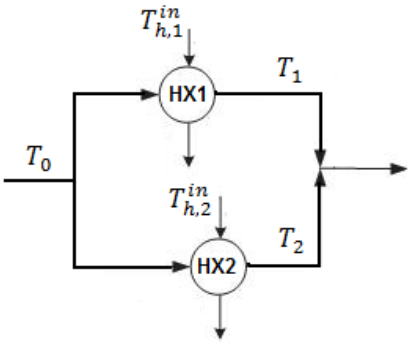

The controlled variable is:

$$c = \frac{\Delta T_1{}^2}{\Delta T_{h,1}^{in}} - \frac{\Delta T_2{}^2}{\Delta T_{h,2}^{in}} \tag{3.8}$$

where:

$$\begin{cases} \Delta T_1 = T_1 - T_0 \\ \Delta T_2 = T_2 - T_0 \\ \Delta T_{h,1}^{in} = T_{h,1}^{in} - T_0 \\ \Delta T_{h,2}^{in} = T_{h,2}^{in} - T_0 \end{cases} \tag{3.9}$$

Fig. 3.1. Branches composed of single heat exchangers

Hence, for a heat exchanger network with two heat exchangers in parallel (Fig. 3.1.) five measurements are need to achieve self-optimising control. Two measurement are needed for each heat exchanger (outlet cold temperature and inlet hot temperature) in addition to the feed temperature of the network.

3.2.2. Branches composed of two heat exchangers in series

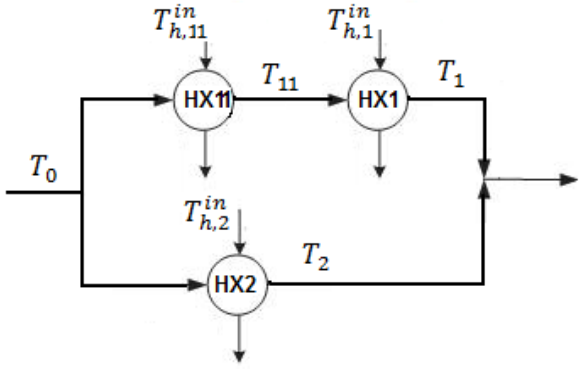

Fig. 3.2. Two heat exchangers in series on branch 1

The controlled variable is:

$$c = \left(\frac{T_{h,1}^{in} - T_1}{\Delta T_{h,11}^{in}} - 1\right)\frac{\Delta T_{11}^2}{T_{h,1}^{in} - T_1} + \frac{\Delta T_1^2}{T_{h,1}^{in} - T_{11}} - \frac{{\Delta T_2}^2}{\Delta T_{h,2}^{in}} \qquad (3.10)$$

where:

$$\begin{cases} \Delta T_{11} = T_{11} - T_0 \\ \Delta T_1 = T_1 - T_0 \\ \Delta T_2 = T_2 - T_0 \\ \Delta T_{h,11}^{in} = T_{h,11}^{in} - T_0 \\ \Delta T_{h,1}^{in} = T_{h,1}^{in} - T_0 \\ \Delta T_{h,2}^{in} = T_{h,2}^{in} - T_0 \end{cases} \qquad (3.11)$$

The ratio $\frac{\Delta T^2}{\Delta T_h^{in}}$ has been identified to be a key variable for branches made of a single heat exchanger.

In the same way, the formula $\left(\frac{T_{h,2}^{in} - T_2}{\Delta T_{h,1}^{in}} - 1\right)\frac{\Delta T_1^2}{T_{h,2}^{in} - T_1} + \frac{\Delta T_2^2}{T_{h,2}^{in} - T_1}$ is identified to be a key variable for branches made of two heat exchangers (index : $1-2$) in series.

This variables will henceforth been introduced as *self-optimising variables or Jäschke Temperatures [JT]*. Their dimension is the one of a temperature interval so their physical unit is the Kelvin [K].

We observe that the expression (3.10) reduces the the expression (3.8) if $\Delta T_{11} = 0$ (no effect of the first heat exchanger) or if $T_1 = T_{11}$ (no effect of the second heat exchanger).

3.3. Application to the studied heat exchanger network

Reproducing Fig.2.4. Simplified process flow diagram

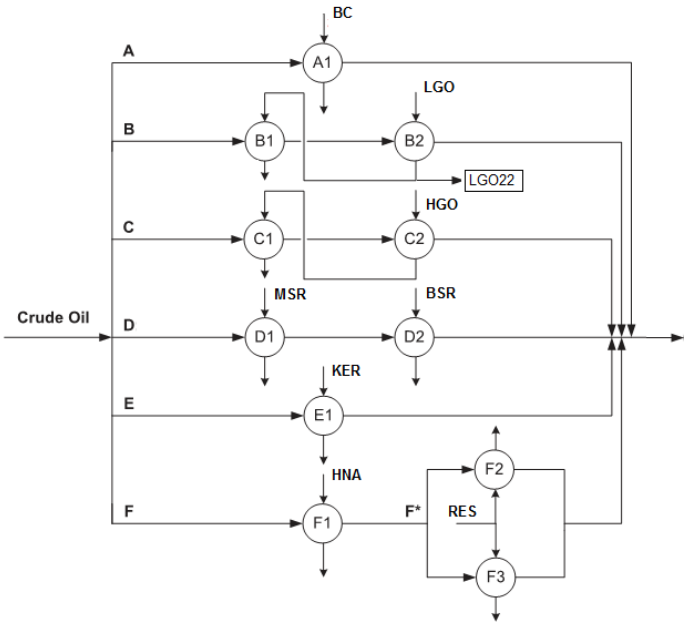

The last section led to key variables for each branch for which the equality is leading the network very close to optimal operation. Keeping the same notation introduced in the section 3.2., here are the self-optimising variables which will be used for control in this work.

$$\begin{cases} JT_A = \frac{\Delta T_A{}^2}{\Delta T_{h,A}^{in}} \\ JT_{B,2} = \frac{\Delta T_{B2}{}^2}{\Delta T_{h,B2}^{in}} \\ JT_{C,2} = \frac{\Delta T_{C2}{}^2}{\Delta T_{h,C2}^{in}} \\ JT_D = \left(\frac{T_{h,D2}^{in} - T_{D2}}{\Delta T_{h,D1}^{in}} - 1\right)\frac{\Delta T_{D1}^2}{T_{h,D1}^{in} - T_{D1}} + \frac{\Delta T_{D2}^2}{T_{h,D2}^{in} - T_{D1}} \\ JT_E = \frac{\Delta T_E{}^2}{\Delta T_{h,E}^{in}} \\ JT_F = \left(\frac{T_{h,F2}^{in} - T_{F2,tot}}{\Delta T_{h,F1}^{in}} - 1\right)\frac{\Delta T_{F1}^2}{T_{h,F1}^{in} - T_{F1}} + \frac{\Delta T_{F2,tot}^2}{T_{h,F2}^{in} - T_{F1}} \end{cases} \quad (3.12)$$

The branches B and C of our studied heat exchanger network are made of two heat exchangers in series using the same hot stream. They led us to consider also the self-optimising variables (3.13) and (3.14) and select the best one according the steady-state results.

$$JT_{B,1} = \left(\frac{T_{h,B2}^{in} - T_{B2}}{\Delta T_{h,B1}^{in}} - 1\right)\frac{\Delta T_{B1}^2}{T_{h,B1}^{in} - T_{B1}} + \frac{\Delta T_{B2}^2}{T_{h,B2}^{in} - T_{B1}} \quad (3.13)$$

$$JT_{C,1} = \left(\frac{T_{h,C2}^{in} - T_{C2}}{\Delta T_{h,C1}^{in}} - 1\right)\frac{\Delta T_{C1}^2}{T_{h,C1}^{in} - T_{C1}} + \frac{\Delta T_{C2}^2}{T_{h,C2}^{in} - T_{C1}} \quad (3.14)$$

Chapter 4

Steady-state performances

4.1. Solving the network for given self-optimising variables

The steady-state performances of given self-optimising variable are obtained by finding the split fractions of the network such that these self-optimising variables are all equal to each other.

Each split fraction has more effect on its branch-relative self-optimising variable compared to the others. Moreover, the self-optimising variable is a strictly decreasing function of its branch-relative split fraction. (Fig.4.1) Actually, only the numerator of the JT variable is function of the split fraction.

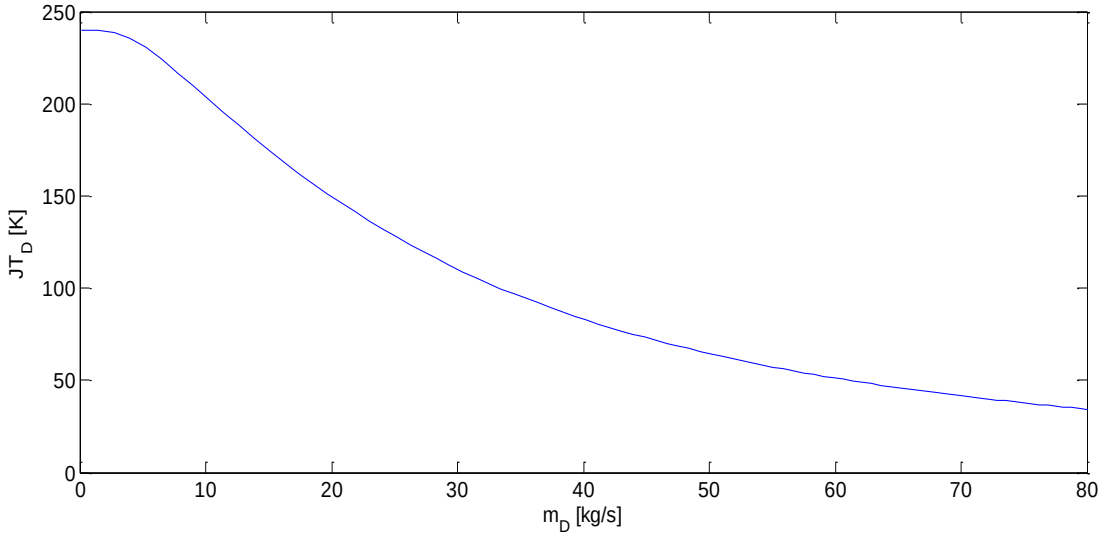

Fig. 4.1. The self-optimising variable as a function of its branch relative feed flowrate

In order to respect the constraint on the mass balance, the split fraction of branch F is defined as a result of the other split fractions. We introduce the variables:

$$c_i = JT_i - JT_F \quad ; \quad i = A, B_{1or2}, C_{1or2}, D, E \tag{4.1}$$

The algorithm process is straightforward. As long as the variables c_i are not all sufficiently close to zero (<10^{-6} K), the branch-relative split fraction of the variable c_i having the higher absolute value is adjusted. This simple algorithm converges very fast if a progressive tolerance scheme is adopted. The code can be seen in the appendix.

4.2. Selection of JT variables for branches B & C

Solving the network for each self-optimising control variables combination, the selection of $JT_{B,2}$ and $JT_{C,2}$ leads to a higher crude oil outlet temperature.

Selection for JT_B	Selection for JT_C	$JT_{A...F}$ [K]	T_{end} [°C]
$\boldsymbol{JT_{B,1}}$	$JT_{C,1}$	60,42	207,31
$\boldsymbol{JT_{B,1}}$	$JT_{C,2}$	58,60	207,58
$\boldsymbol{JT_{B,2}}$	$JT_{C,1}$	58,02	207,31
$\boldsymbol{JT_{B,2}}$	$JT_{C,2}$	56,32	207,61

Tab. 4.2. Selection of JT variables for branches B&C

4.2.1. Relative performances of $JT_{C,1}$ & $JT_{C,2}$

Focusing the analysis on several reduced networks, we observe that the steady-state performances of $JT_{C,2}$ are always higher than those of $JT_{C,1}$. In our model of branch C, the two heat exchangers in series perfectly behave as one single heat exchanger. Nothing affects the cold and hot streams between them. The two heat exchangers could even be modeled as one and we expected (according to the theory) that the self-optimizing variable $JT_{C,2}$ would lead to higher steady-state performances.

Reduced network only made of branches C and D

The simplest variable $JT_{C,2}$ relative to a branch composed of one single heat exchanger appear to be the best self-optimising variable in the case of two heat exchangers in series for both streams.

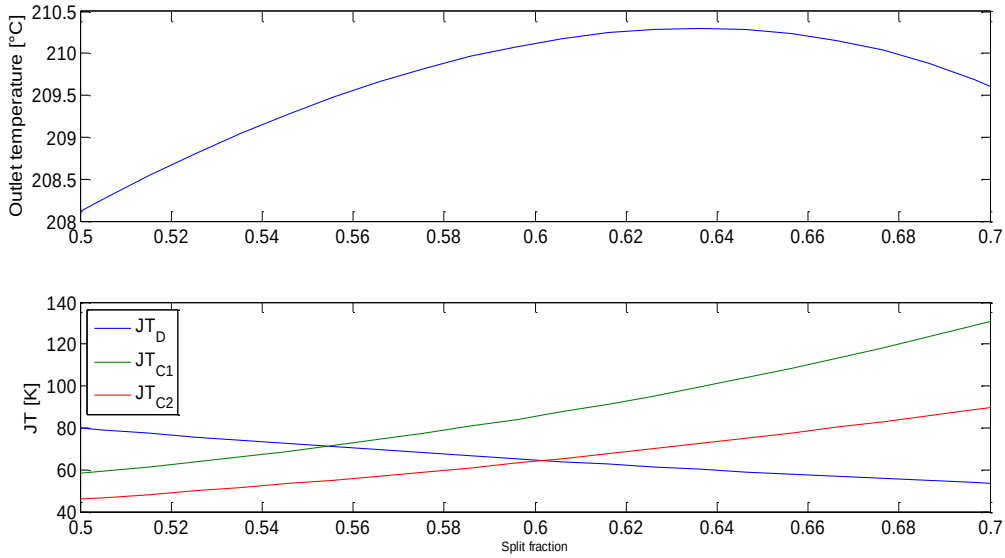

Fig. 4.3. C-D / Relative performances of $JT_{C,1}$ and $JT_{C,2}$

Reduced network only made of branches C and E

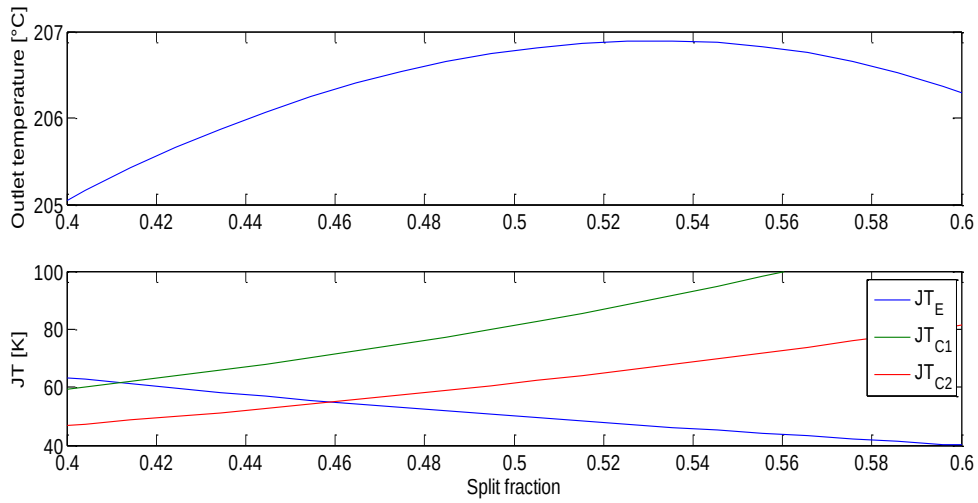

Fig. 4.4. C-E / Relative performances of $JT_{C,1}$ and $JT_{C,2}$

We observe (Fig. 4.3. & Fig.4.4.) that the variables $JT_{C,1}$ and $JT_{C,2}$ have a tendency to over-estimate very much the thermal potential of the branch C. As seen in the chapter 2, the temperature profiles of the Branch C streams are very close to each other so the overall driving force is low compared to the other branches. The high value of $JT_{C,1}$ forces too much crude oil to pass in the branch, this effect is less strong and systematic if $JT_{C,2}$ is chosen.

4.2.2. Relative performances of $JT_{B,1}$ & $JT_{B,2}$

Focusing the analysis on several reduced networks, we observe that the relative steady-state performances of $JT_{B,1}$, $JT_{B,2}$ change from network to network and cannot be presented as a general result.

Reduced network only made of branches A and B:

$$CV_1 = JT_A - JT_{B,1} \tag{4.2}$$

$$CV_2 = JT_A - JT_{B,2} \tag{4.3}$$

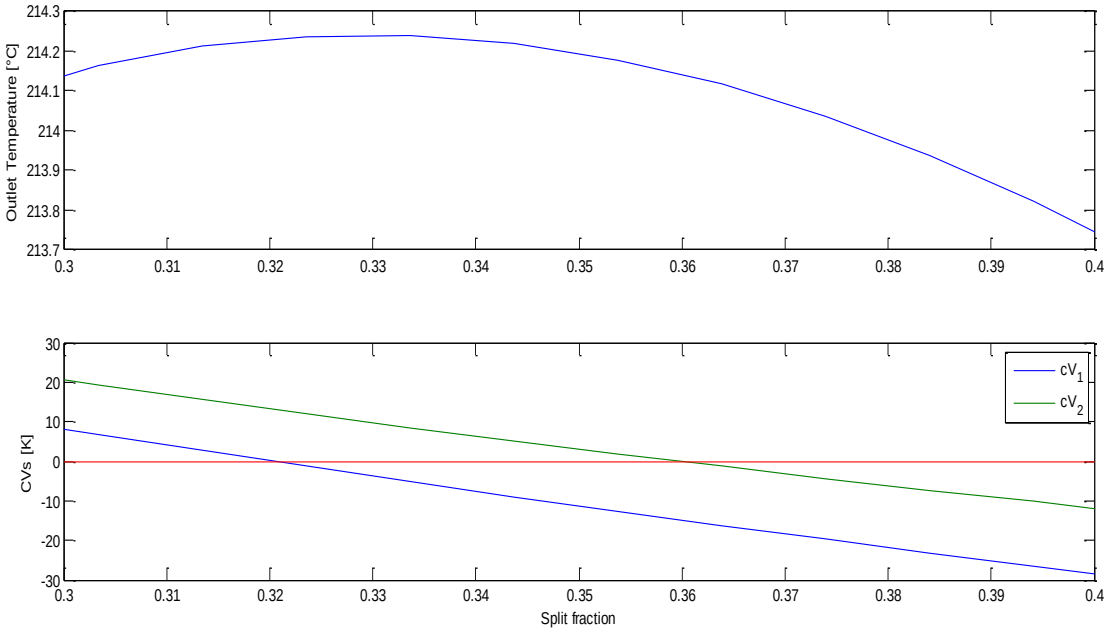

Fig. 4.5. A-B / Relative performances of $JT_{B,1}$ and $JT_{B,2}$

In this case (Fig. 4.5.), $JT_{B,1}$ lead to a slightly higher outlet temperature than $JT_{B,2}$. On the branch B, a part of the hot stream leaving the heat exchanger B2 do not enter the first heat exchanger B1. The two heat exchangers in series cannot be properly assumed to show the same physical characteristics as a single heat exchanger.

4.3. Optimal split fractions

4.3.1. Calculation procedure

The steady-state performances of the self-optimising variable are better examined by comparison to what is optimal to achieve in the network. A procedure to find the optimal split fraction is needed. As for section 4.1., an algorithm using the variables c_i and the split fractions except one (branch F) will be used.

The objective function is now to maximise the outlet temperature of the network (and not to set the variables c_i to zero. This problem appears to be convex as seen in our first and numerous simulations (Fig. 4.6, as example). The outlet temperature is a smooth continuous function and no other local optimum can be obtained than the overall optimum.

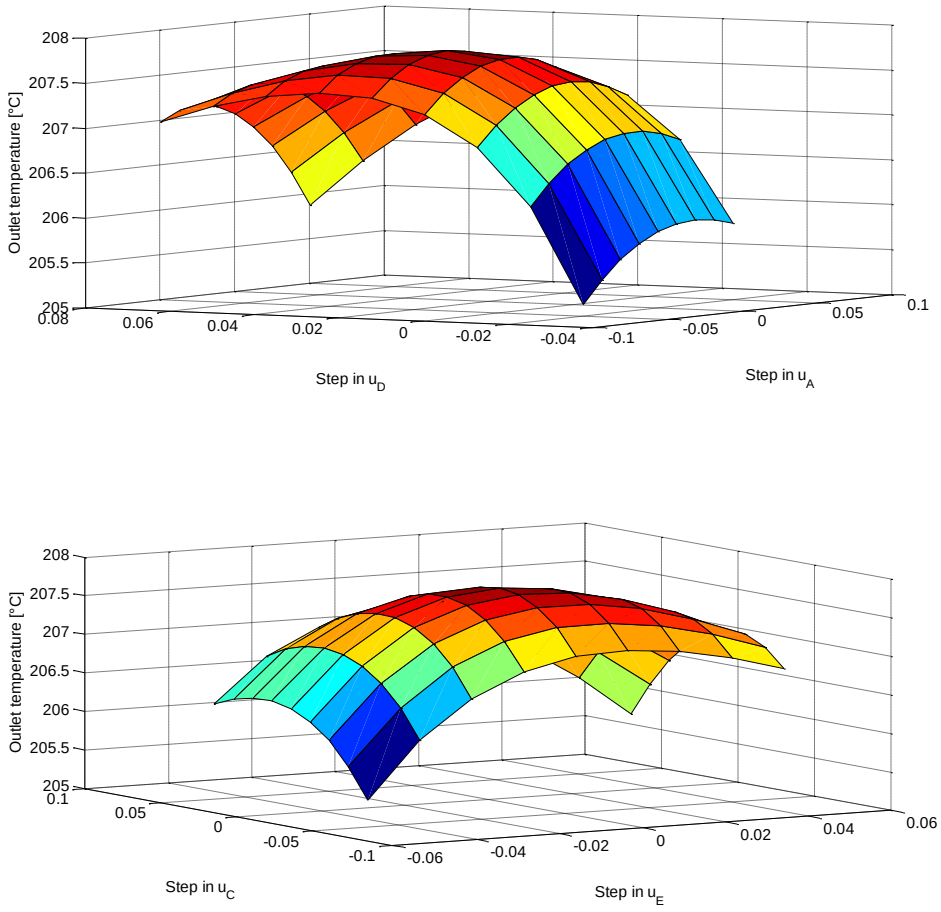

Fig. 4.6. Observed convexity of the optimisation problem

Therefore, a gradient based search algorithm can easily lead to the optimal split fractions. Again, a self-made algorithm has been made in order to keep a manual control on the solving procedure and exploit our understanding of the model.

The principle used is very simple and allow the network to converge very fast. As long as the local gradient is not close enough to zero, the algorithm looks for the optimal point in the gradient direction by adapting the searching step according the results. The code of the self-made algorithm can be found in the appendix D (MatLab© file optim.m).

4.3.2. Results

The split fractions, crude oil outlet temperatures of each branch and the values of the self-optimising variables are compared in three comparative cases: initial conditions (or initial split), optimal conditions (or optimal split) and self-optimising conditions (or self-optimising split). (Tab. 4.7) The initial conditions corresponds to the split fractions as initialised in the model based on the data received from the operation (where real-time optimisation is achieved) and their reconciliation as presented in chapter 2.

Outlet Temperatures [°C]	Initial split	Optimal split	Self-optimising split
Branch A	226,455	228,452	222,98
Branch B	208,298	211,779	214,69
Branch C	213,673	217,49	208,49
Branch D	207,679	201,44	202,41
Branch E	200,279	200,39	206,03
Branch F	202,218	203,545	202,93
Network	**207,65**	**207,79**	**207,61**

Tab. 4.7. Outlet temperatures

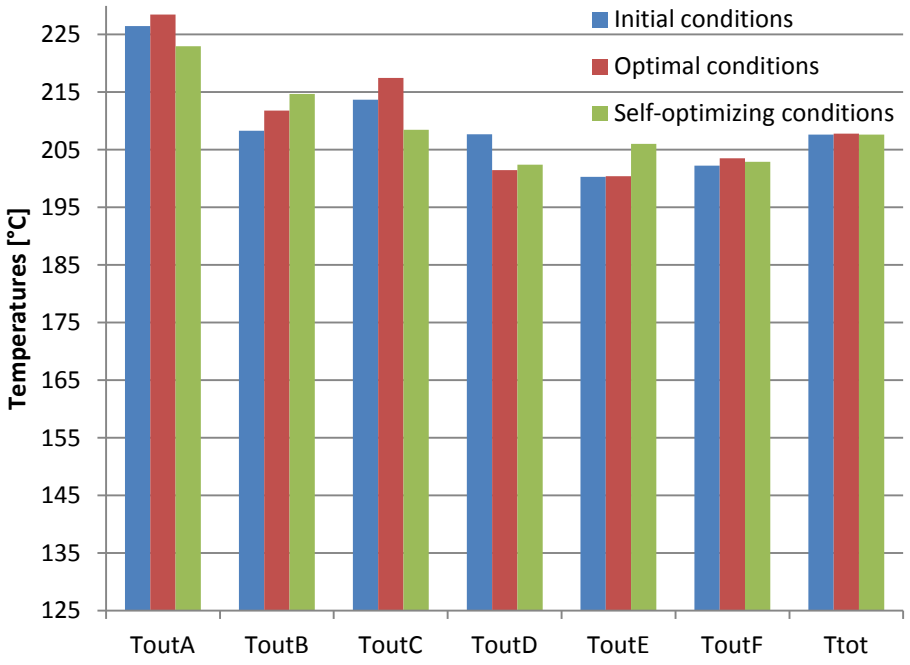

Fig. 4.8. Outlet temperatures

Although the self-optimising conditions introduce some change in the distribution of the crude oil in the network, the network outlet temperature stays at a high value and very close to the optimum. (Fig. 4.8. & 4.9.) This can be explained by the flatness of the optimum.

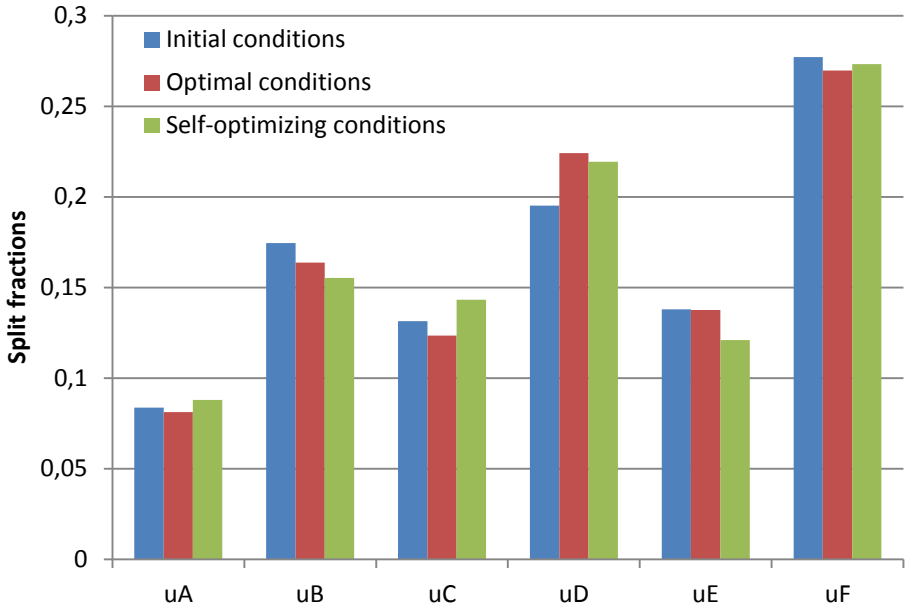

Fig. 4.9. Split fractions

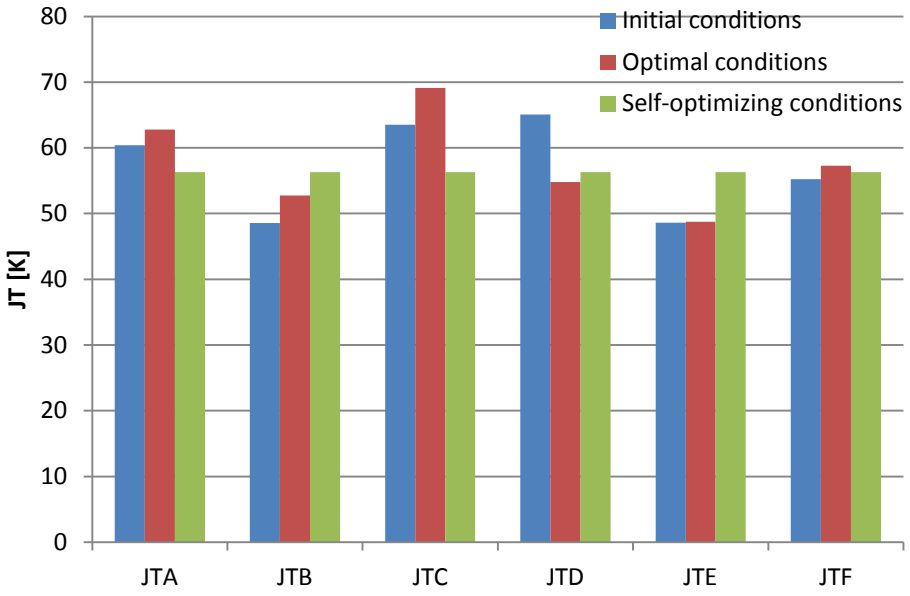

Fig. 4.10. Self-optimising variables

We observe that the self-optimising variables are not strictly equal at optimum. This may open a door for a "practical" adjustement of their expression (for example, in the form of a non-theorical additional term which could use more process information than simple temperature measurements). Such an adjustement will not be suggested here and this is left as an idea for further work in order to improve the self-optimising variables steady-state performances.

For single disturbances in the heat exchanger network (tab.4.11), there is almost no gain using self-optimising control since the constant split (computed by the real-time optimiser in the base case) still provides a higher outlet temperature in many cases. Both constant split and self-optimising split stays relatively close to the optimum.

Disturbance on hot streams	Outlet temperatures [°C]		
	Constant split	Optimal split	Self-optimising split
Base case (No disturb.)	**207,65**	**207,79**	**207,61**
-10% flowrate – Branch C	206,94	207,18	206,98
+10% flowrate – Branch C	208,25	208,37	208,21
-10% flowrate – Branch F (HX F2&F3 hot stream)	206,89	207,07	206,88
+10 flowrates – Branch D	207,87	208,05	207,87
-10°C inlet – Branch C	206,70	206,86	206,72
+10°C inlet – Branch C	208,61	208,74	208,52
-10°C inlet – Branch B	206,64	206,81	206,62
+10°C inlet – Branch E	208,53	208,67	208,51

Tab. 4.11. Steady-state performances – single disturbance

If disturbances are combined on several branches then the constant split could be far for the optimum split while the self-optimising split still stays relatively close to it. However, as seen in table 4.12, if the hot streams flowrates on branches A,C,E are reduced by 5% while the hot streams flowrates on B,D,F grow by 5%, the constant split still provide a competitive outlet temperature.

Disturbance on hot streams -5% on flowrates : A,C,E +5% on floxrates : B,D,F		Constant split	Optimal split	Self-optimising split
Split fractions	A	0,0837	0,0773	0,0847
	B	0,1745	0,1681	0,1585
	C	0,1315	0,117	0,1369
	D	0,1952	0,2265	0,222
	E	0,138	0,1331	0,1181
	F	0,2771	0,278	0,2798
Outlet temperature [°C]		**207,65**	**207,86**	**207,65**

Tab. 4.12. Steady-state performances – Combined disturbances 5% flow

Finally, if the hot streams flowrates on branches A,C,E grows this time by 10% of their nominal value while the hot streams flowrates on B,D,F are reduced by 10%, the self-optimising split is now making a small positive difference (table 4.13).

The self-optimising variables cannot provide better steady-state performances than the constant split given by the Real-Time Optimiser in the case of small disturbances.

For major combined disturbances, the steady-state performances of the self-optimising variables give a guarantee for the heat exchanger network to stay relatively close to the optimum while a constant split could differ a lot from it. If the network is subjected to such major disturbances (performance drift of the heat exchangers for example) then the use of self-optimising control could be justified. (tab. 4.13,4.14,4.15)

Disturbance on hot streams +10% on flowrates : A,C,E -10% on floxrates : B,D,F		Constant split	Optimal split	Self-optimising split
Split fractions	A	0,0837	0,0894	0,0947
	B	0,1745	0,1545	0,1485
	C	0,1315	0,1367	0,1561
	D	0,1952	0,2189	0,2145
	E	0,138	0,1472	0,1273
	F	0,2771	0,2533	0,2589
Outlet temperature [°C]		**207,25**	**207,45**	**207,27**

Tab. 4.13. Steady-state performances – Combined disturbances 10% flow

Disturbance on hot streams -5% onflowrates& +5°C : A,C,E +5% on flowrates & -5°C : B,D,F		Constant split	Optimal split	Self-optimising split
Split fractions	A	0,0837	0,0754	0,082
	B	0,1745	0,1696	0,1609
	C	0,1315	0,1144	0,1316
	D	0,1952	0,2306	0,2272
	E	0,138	0,1276	0,1117
	F	0,2771	0,2824	0,2866
Outlet temperature [°C]		**208,64**	**208,92**	**208,73**

Tab. 4.14. Steady-state performances – Combined disturbances 5% flow &5°C

Disturbance on hot streams +10% on flowrates & -10°C : A,C,E -10% on flowrates &+10°C: B,D,F		Constant split	Optimal split	Self-optimising split
Split fractions	A	0,0837	0,0939	0,1007
	B	0,1745	0,1515	0,1433
	C	0,1315	0,1429	0,1678
	D	0,1952	0,2091	0,2031
	E	0,138	0,1589	0,1404
	F	0,2771	0,2437	0,2447
Outlet temperature [°C]		**205,65**	**205,97**	**205,75**

Tab. 4.15. Steady-state performances – Combined disturbances 10%flow &10°C

Note that the steady-state performances have been evaluated using a model build for a study on dynamics. For further work, the author suggests to build an accurate steady-state model in order to validate (or not) the given results and these statements.

Chapter 5

General features of the control configuration

5.1. Objectives

The control system based on the self-optimising approach pursues an economical objective. In comparison to a control system for stabilization, control for economics is usually taken into account in the upper layers of the control system made of the most advanced controllers (multivariable, RTO). These upper layers then communicate setpoints to the stabilizing layer, usually made of more simple controllers (PID) (Skogestad and Postletwhaite, 2005).

The self-optimising control approach suggests using a single integrated layer where economic self-optimising variables do not change with disturbances and prices. In our work, we thus aim at controlling the heat exchanger network with a single control layer. We look forward to a control configuration which will smoothly operate the valve positions in order to pursue the equality of the self-optimising variables. Steep changes, inverse responses and oscillations should be limited as much as possible.

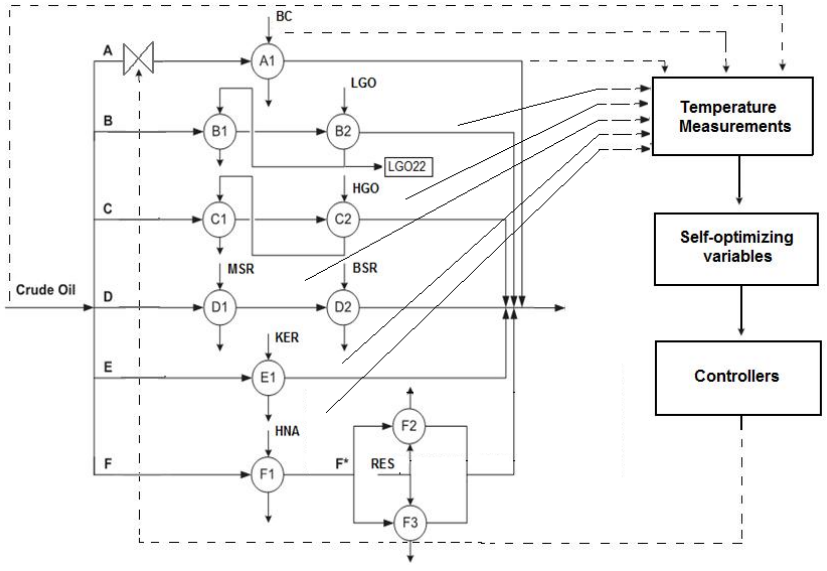

Fig. 5.1. General control configuration for a single valve position

5.2. Temperature measurements

All temperature are assumed to be measured with a sensor device for which the dynamics is approximated by a simple first-order transfer function having time constant of 5 seconds including a delay of 1 second.

$$g_{sensor}(s) = \frac{1}{(5s+1)} e^{-s} \qquad (5.1)$$

5.3. Constrained case

By default, the operation of the heat exchanger network has been seen through the single objective of heating the crude oil as much as possible (unconstrained problem). It is possible that the operation of some heat exchangers of the network is constrained by a setpoint on the hot stream side (fixed duty or temperature outlet).

In this work, this case has been considered as a trivial problem. Actually, such an active constraint could be easily handled by the valve position of the respective branch, adjusting the oil stream to fulfill the constraint. So, if there was a constraint, this would be handed as in Figure 5.2. Doing so, we would remove both a branch and a degree of freedom of our control problem. All the unconstrained branches could then form a sub-network where self-optimising control can be implemented.

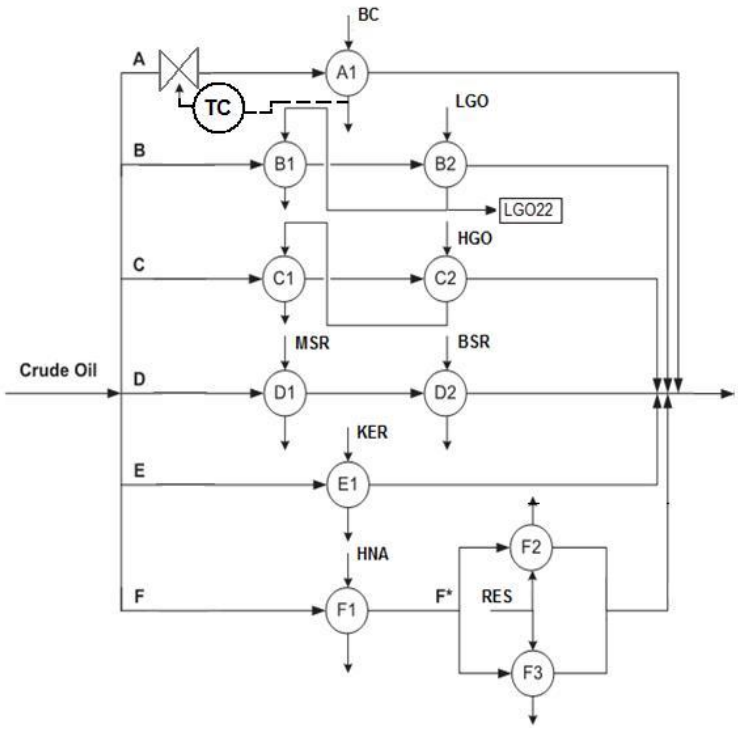

Fig. 5.2. Control configuration for handling a constraint

5.4. Secondary split on branch F

On the branch F after the first heat exchanger is there a subdivision of the crude oil stream where two heat exchangers in parallel are used to recover heat from the same hot source. Moreover, these two heat exchangers have very similar physical characteristics (volumes, areas, heat transfer coefficient).

The distribution of the crude oil between them is thus not expected to vary a lot. Whatever the disturbance on the crude oil or on the hot stream, the split fraction should stay close to 0,5. Consequently, we observe that the distribution of the crude oil would not have major effect on the branch F crude oil outlet temperature and of course even less on the network outlet crude oil temperature.

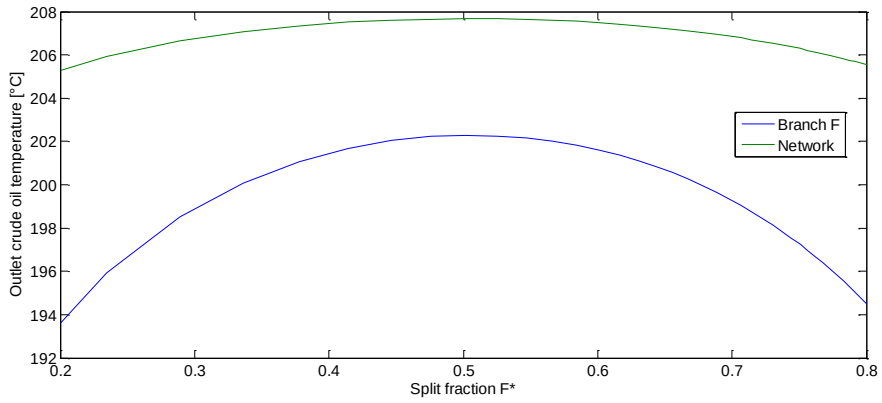

*Fig.5.3. Outlet temperatures as a function of the split fraction F**

Even though a constant split would be sufficient, the self-optimising control methodology could be implemented on this internal part of the network.

The valve positions of the crude oil on each sub-branch would be the manipulated variables and algebraically would determine the split fraction (cfr. section 2.3.2.). The valve position of the sub-branch passed by the highest flowrate would be automatically set to 1. The control structure would result in modifying the other one. A PI controller would be used to do so.

The controlled variable would be:

$$c_{F^*} = JT_{F3} - JT_{F2} \tag{5.2}$$

$$c_{F^*} = \frac{\Delta T_{F3}{}^2}{\Delta T_{h,F3}^{in}} - \frac{\Delta T_{F2}{}^2}{\Delta T_{h,F2}^{in}} \tag{5.3}$$

Obviously, $c_{F^*} = 0 \; if \; T_{F3} = T_{F2}$ so the controlled variable could simply be :

$$c_{F^*} = T_{F3} - T_{F2} \tag{5.4}$$

5.5. SIMC tuning rules for PI(D) controllers

Brief summary of the SIMC tuning (Skogestad, 2003)

The SIMC tuning rules of a PI(D) controller expressed in its series form :

$$c(s) = K_c \frac{(\tau_I s+1)}{\tau_I s} \quad [(\tau_D s + 1)] \tag{5.5}$$

The first step in the controller design procedure is to obtain from the original model an approximate first (or second) order model including time delay in the form :

$$g\,(s) = \frac{k}{(\tau_1 s+1)} e^{-\theta s} \tag{5.6}$$

The model information such as the plant gain (k), the dominant lag time constant (τ_1) and the delay (θ) can be found in two ways :

- estimation based on the open-loop step response
- identification from the original transfer function (half-rule, approximations if needed)

Then, the idea is to specify the desired close-loop response (method named direct synthesis for setpoints). We thus solve the close-loop system equation for the corresponding controller :

$$\frac{y}{y_s} = \frac{g(s)c(s)}{g(s)c(s)+1} \Leftrightarrow c(s) = \frac{1}{g(s)} \left(\frac{1}{\frac{1}{\left(\frac{y}{y_s}\right)_{desired}} - 1} \right) \tag{5.7}$$

Since we desire a simple first-order response with time constant τ_c (single parameter for our controller):

$$\left(\frac{y}{y_s}\right)_{desired} = \frac{1}{\tau_c s+1} e^{-\theta s} \tag{5.8}$$

Therefore, introducing a first-order Taylor series approximation of the delay:

$$e^{-\theta s} \approx 1 - \theta s \tag{5.9}$$

$$c(s) = \frac{(\tau_1 s+1)}{k} \frac{1}{(\tau_c+\theta)s} \tag{5.10}$$

This is a PID controller (5.5) for which :

$$\begin{cases} K_c = \frac{1}{k} \frac{\tau_1}{(\tau_c+\theta)} \quad (*) \\ \tau_I = \tau_1 \\ [\tau_D = 0] \end{cases} \tag{5.11}$$

This PID-setting was derived by considering only the setpoint response and disturbance rejection can be improved by modifying the integral time for lag dominant processes ($\tau_1 \gg \theta$).

Analysing the close-loop characteristic polynomial in the case of a PI-controller :

$$1+g(s)c(s) = \frac{\tau_I \tau_1}{kK_c} s^2 + \tau_I s + 1 \tag{5.12}$$

$$= \left(\sqrt{\frac{\tau_I \tau_1}{kK_c}}\right)^2 s^2 + 2\sqrt{\frac{\tau_I \tau_1}{kK_c}} * \frac{1}{2}\sqrt{\frac{kK_c \tau_I}{\tau_1}} * s + 1 \tag{5.13}$$

$$= \phi^2 s^2 + 2\phi * \xi * s + 1 \tag{5.14}$$

Oscillation occurs for

$$\xi < 1 \implies \frac{1}{2}\sqrt{\frac{kK_c \tau_I}{\tau_1}} < 1 \tag{5.15}$$

So a robust choice is to take

$$\frac{1}{2}\sqrt{\frac{kK_c \tau_I}{\tau_1}} = 1 \overset{(*)}{\Rightarrow} \tau_I = 4(\tau_c + \theta) \tag{5.16}$$

To summarise for all processes, we keep the tuning rule :

$$\tau_I = \min(\tau_1, 4(\tau_c + \theta)) \tag{5.17}$$

Example : PI controller tuning for the F* split

Open-loop step change in the valve position of sub-branch F3: at time t=5000s, z_{F3} passes from 0.9529 to 0.9629. The controlled variable (5.3) has been used.

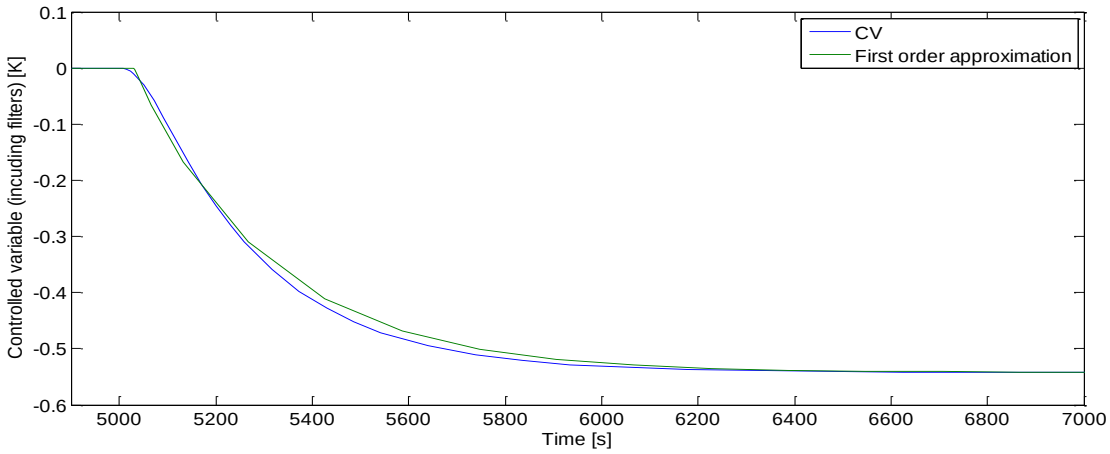

Fig. 5.5. Step change in valve position of sub-branch F3

The step response is used to approximate a first order transfer function between the manipulated variable and the controlled variable including time delay:

$$g(s) = \frac{k}{(\tau_1 s+1)} e^{-\theta s} \tag{5.18}$$

With:

$$\begin{cases} k = \frac{\Delta y}{\Delta u} = \frac{-0.54235}{0.01} = -54.235 \\ \tau_1 = 270s \\ \theta = 30s \end{cases} \tag{5.19}$$

According to the SIMC tuning rules and choosing $\tau_c = 240s$,

$$c(s)_{PI\ Controller} = K_c \frac{(\tau_I s+1)}{\tau_I s} \tag{5.20}$$

With :

$$\begin{cases} K_c = \frac{1}{k} \frac{\tau_1}{(\tau_c+\theta)} = -0.01741 \\ \tau_I = min\big(\tau_1, 4(\tau_c+\theta)\big) = \tau_1 = 270s \end{cases} \tag{5.21}$$

Close-loop simulation results

At time t=4000s, the crude oil inlet temperature passes from 125°C to 135°C.

At time t=5000s, the hot stream inlet temperature passes from 244,38°C to 234,38°C.

At time t=6000s, the crude oil flowrate passes from 70,45 kg/s to 59,88 kg/s.

At time t=7000s, the hot stream flowrate passes from 62,16 kg/s to 74,59 kg/s.

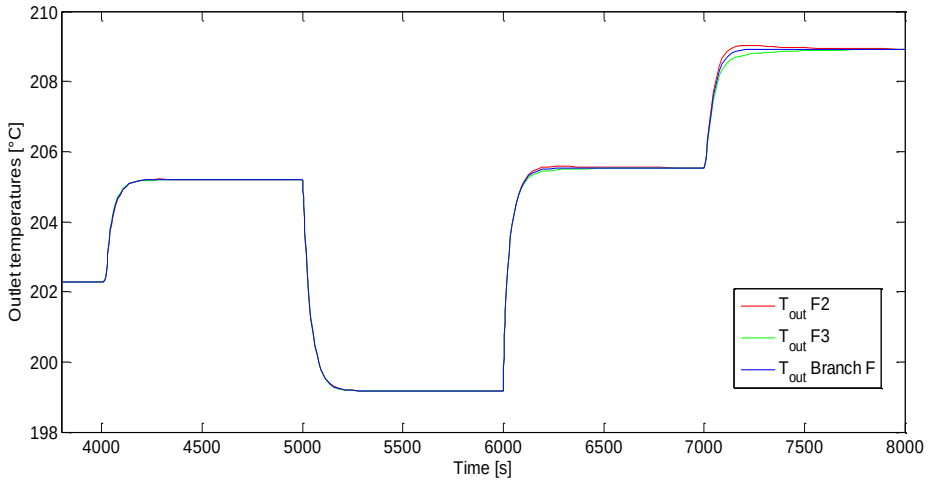

Fig. 5.6. Close –loop simultation – Outlet temperatures

The implemented control has no distinguishable effects on the branch dynamics, as desired. (Fig. 5.6) On the graph, we notice the fastest responses of the heat exchanger F2 due to its slightly larger heat transfer coefficient.

The valve position F2 stays to 1 since the sub-branch F2 keeps a higher crude oil flowrate than the sub-branch F3. The changes on the valve position F3 are smooth as desired. (Fig.5.7)

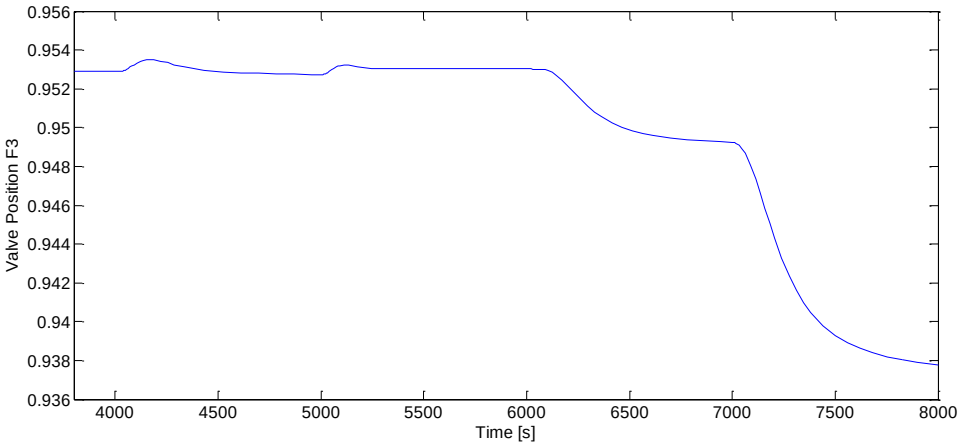

Fig. 5.7. Close-loop simulation – Valve operation F3

5.6. Controlled variables

In the section 2.3.2., the branch valve positions have been introduced as our manipulated variables. In order to reduce the pressure drop as much as possible, it has been observed that the branch having the highest crude oil flowrate should always have its valve fully open. In the nominal conditions, it is the branch F. All our control structures will thus focus on manipulating the other valve positions and set, by default, the valve on branch F fully open.

If there is such a disturbance in the system that the self-optimising variables requires lead to a higher flowrate on another branch than branch F, the corresponding valve position will saturate (being fully open) without being able to grow the crude oil flowrate anymore.

In order to avoid this saturation effect, the values given by the controllers for the valve positions $[z_{ic}]$ will be artificially allowed to pass the value 1. These values will then be algebraically treated in such a way that the highest will be set to 1 and the others proportionally adjusted in order to get back a physical sense $[z_i]$.

$$z_{Fc} = 1 \tag{5.22}$$

$$z_i = \frac{z_{ic}}{\max(z_{ic})} \quad ; \quad i = A, B, C, D, E, F \tag{5.23}$$

The control structure will have to adjust the variables $z_{Ac}, z_{Bc}, z_{Cc}, z_{Dc}$ *and* z_{Ec}. In order to do so, the following simple combinations of the self-optimising variables will be used:

$$c_i = JT_i - JT_F \quad ; \quad i = A, B, C, D, E \tag{5.24}$$

Actually, the self-optimising variable on each branch need to be taken into account. The special role played by the one of the biggest branch $[JT_F]$ is believed to provide high robustness due to the higher capacity of this branch (inertia effect) and its lowest tendency to be strongly affected by steep changes in the whole network. Good dynamic performances are thus expected to result.

Chapter 6

Decentralised control

The first control structure to be examined is the simple one where each self-optimising controlled variable c_i is given to a PI controller which gives correction values to the branch respective valve position z_{ic} $(i = A, B, C, D, E)$ (Fig.6.1.). This control structure includes thus 5 different PI controllers, one for each branch except branch F. Such a decentralised control structure could exploit the fact that the interactions between branches are not very strong.

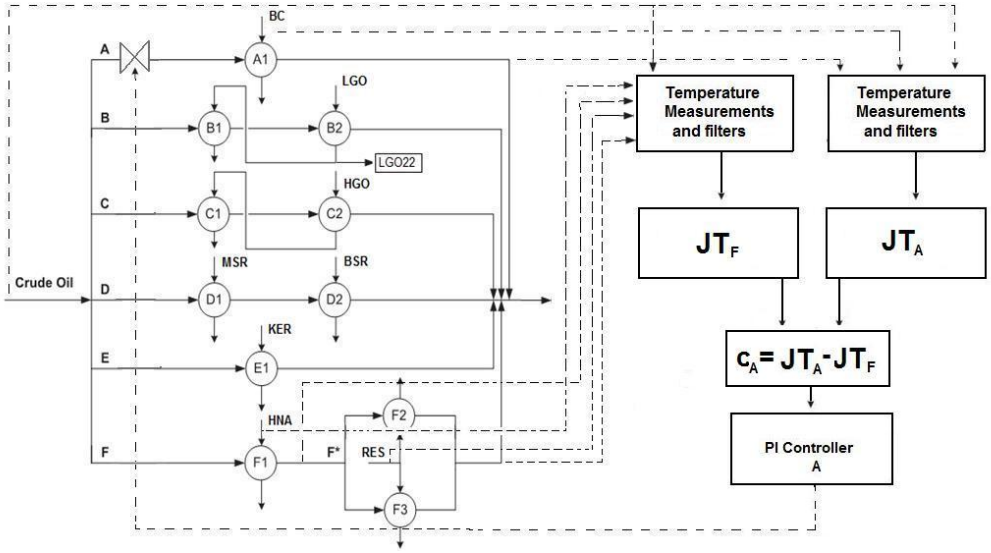

Fig. 6.1. Decentralised control configuration

6.1. Dynamics of the self-optimising variables

The open-loop dynamics of the self-optimising variables bring essential information to be taken into account prior to the design of such a simple control structure. Actually, this information allows us to infer appropriate tuning parameters and the need for additional elements like filters.

For the branches A,B,C and E, the response of the self-optimising variable is simulated for a step change in:

- the crude oil flowrate (+10% of the nominal value at time t=5000s)
- the crude oil temperature (+10°C at time t=5500s)
- the hot stream flowrate (-10% of the nominal value at time t=6000s)
- hot stream inlet temperatures (-10°C at time t=6500s)

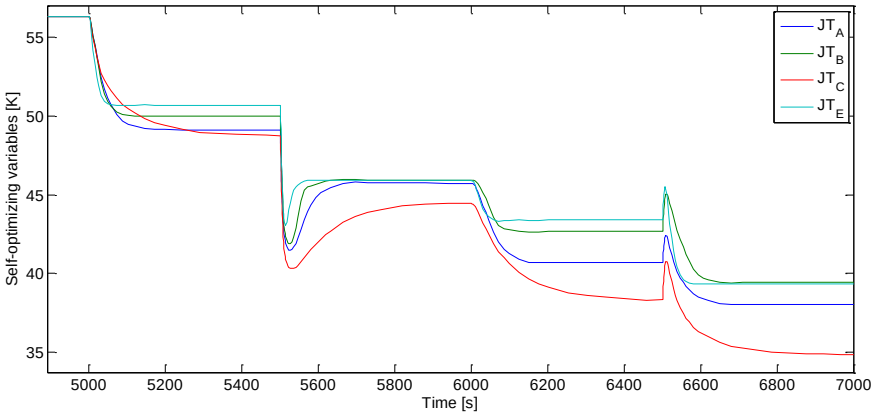

Fig. 6.2. Dynamics of the self-optimising variables A,B,C,E

For the branches D and F, the response of the self-optimising variable is simulated for step changes in:

- the crude oil flowrate (+10% of the nominal value at time t=5000s)
- the crude oil temperature (+10°C at time t=5500s)
- the hot stream flowrate of the first heat exchanger (-10% of the nominal value at time t=6000s)
- the hot stream flowrate of the second (and third) heat exchanger(s) (-10% of the nominal value at time t=6500s)
- the hot stream inlet temperature of the first heat exchanger (-10°C at time t=7000s)
- the hot stream inlet temperature of the second (and third) heat exchanger(s) (-10°C at time t=7500s)

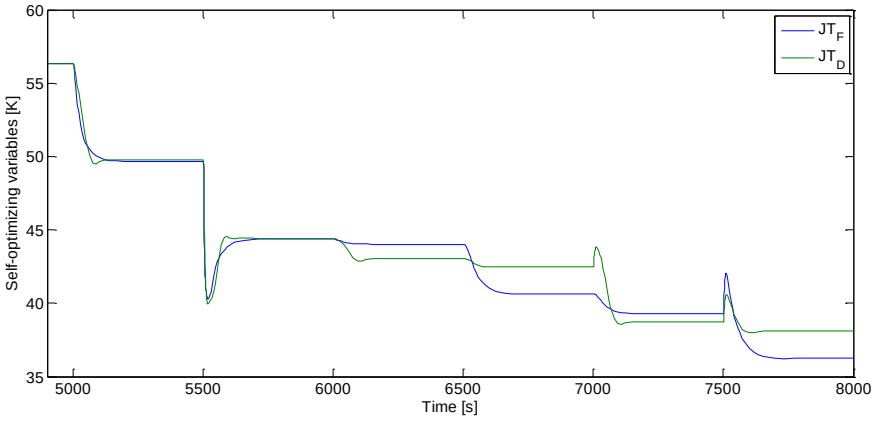

Fig. 6.3. Dynamics of the self-optimising variables D,F

The step changes in flowrates affect the self-optimising variable only by the crude oil outlet temperature measures. The thermal capacities of the heat exchangers thus determine the dynamics of the observed response. In this case, the self-optimising variables present a dynamics appropriate for being used directly as controlled variables.

For the crude oil inlet temperature step changes, direct response and overshoots of self-optimising variable response are observed. This is due to the fact that the self-optimising variables are function of the inlet temperature measure. Taking the branch A as example, the numerator of the self-optimising variable is a square function of the crude oil inlet temperature while the denominator is a linear function. The step change affects thus very much the numerator (fast time-scale) and this explains the overshoot. After that, the denominator stays at a constant value due to the fact it is a function of inlet temperatures. The numerator then grows slowly until the outlet oil temperature measure stabilises to its new higher value (slow time-scale).

$$JT_A = \frac{(T_A - T_0)^2}{T_{h,A}^{in} - T_0} \tag{6.1}$$

For the hot stream inlet temperature step changes, inverse responses are observed. Again, this is due to the fact that denominator of the self-optimising variable diminishes on a very fast time-scale (direct function) while the numerator diminishes on a slow time-scale (function of the outlet temperature).

6.2. Filters for feedforward control abatement

The direct responses of the self-optimising variables are expected to be the cause of an unwanted feedforward control by the PI controllers, even more in the case of inverse responses. Additional dynamics on the inlet temperature measurements are thus introduced using first-order function filters. Outlet temperature measurements dynamics are unchanged.

6.2.1. Inlet hot temperature measurements filters

We decide to add filters for all hot stream inlet temperature measurements with such time constant values that we reduce the impact of the inverse response of the self-optimising variable for a -10°C step change in the hot inlet temperature to 5s.

$$g_{filter}(s) = \frac{1}{(\tau_f s + 1)} \tag{6.2}$$

Measured variable	Filter time constant τ_f [s]
$T_{h,A}^{in}$	100
$T_{h,B}^{in}$	240
$T_{h,C}^{in}$	200
$T_{h,D1}^{in}$	160
$T_{h,D2}^{in}$	280
$T_{h,E}^{in}$	40
$T_{h,F1}^{in}$	20
$T_{h,F2}^{in}$	240

Tab. 6.4. Filter time constants for hot inlet temperatures

Redoing the -10°C step change at time t=5000s on the inlet hot temperatures with the filters (and at time t=6000s for the second hot stream of branches D and F), we obtain:

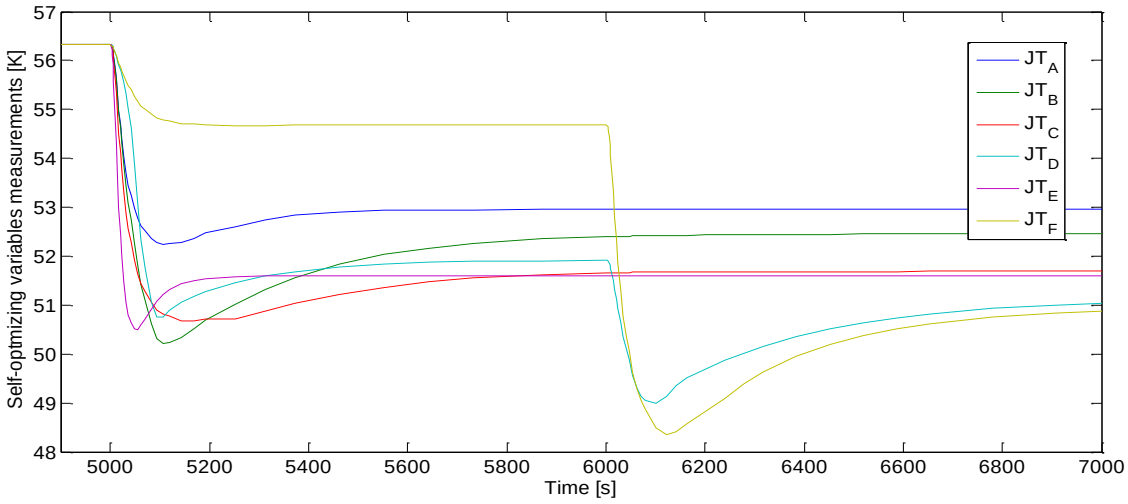

Fig. 6.5. Dynamics of the self-optimising variables after hot inlet temperature filtering

6.2.2. Crude oil inlet temperature measurement filter

A step change in the crude oil inlet temperature will affect all the self-optimising variables at the same time. Therefore, we need to consider here the dynamics of the selected controlled variables $c_i = JT_i - JT_F$ and not the one of the self-optimising variables JT_i.

Without filter, we observe (Fig. 6.6):

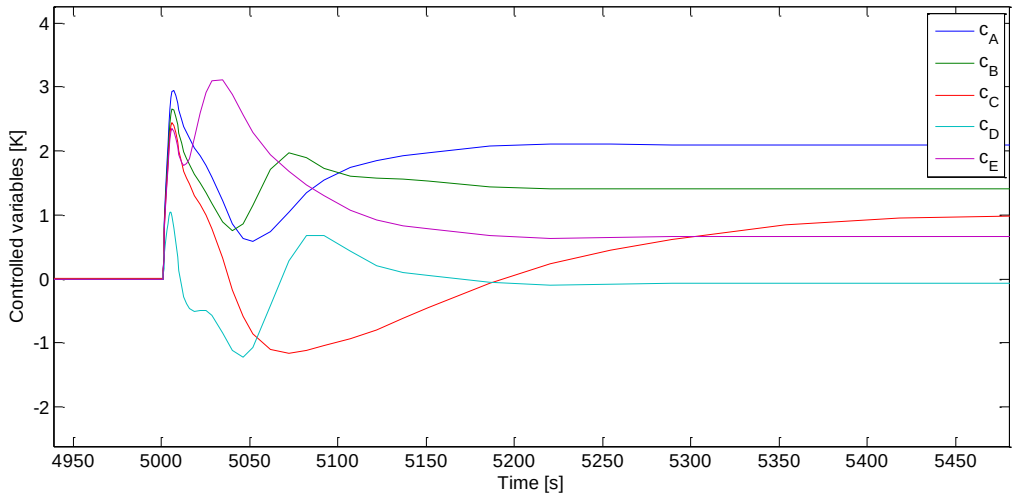

Fig. 6.6. Dynamics of the controlled variables

The responses of the controlled variables oscillate due to the overshoot responses of the self-optimising variables (previously observed in 6.1.) and the time-scale dynamics differences between the branches i and F.

The cancellation of such oscillations would require an excessive filtering system and so they will have to pass through the control structure. However, we firstly design a simple filter for the crude oil inlet temperature measurement in order to reduce the impact of the first fast oscillation.

Measured variable	Filter time constant [s]
T_0	200

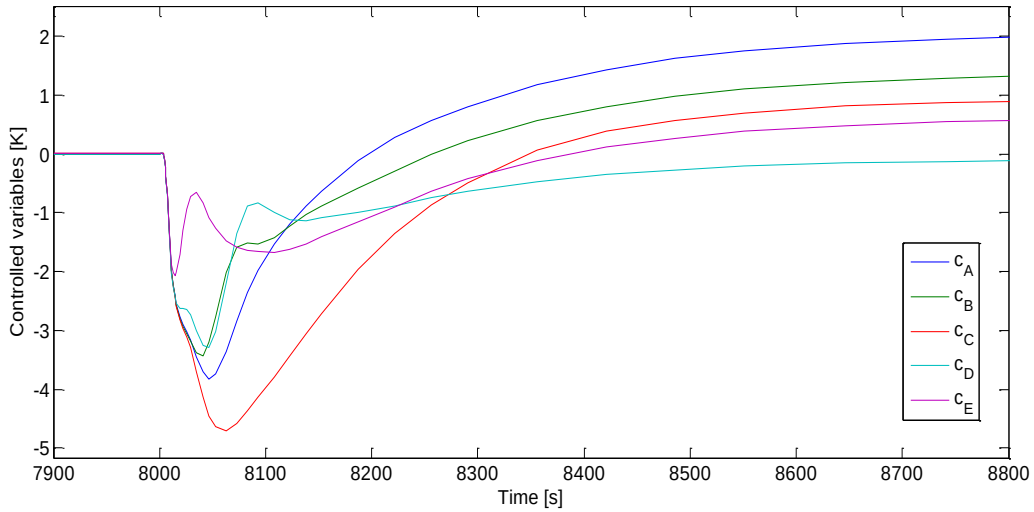

Fig. 6.7. Dynamics of the controlled variables after feed temperature filtering

The impact and the fastness of the first oscillations have been very slightly reduced (Fig.6.7.) but the improvements are very small and another kind of filter is needed.

So, we decide to filter the self-optimising variables in order to reduce the oscillations. Actually, we also want to avoid an extreme PI control tuning with very short process characteristic time τ_1 and very long control characteristic time τ_c that would not lead to a smooth disturbance rejection.

Measured variable	Filter time constant [s]
JT_A	30
JT_B	30
JT_C	10
JT_D	10
JT_E	100
JT_F	30

The dynamics of the controlled variables is then simplified for the control structure. On the following graph, we can observe their new response for a step change in the crude oil inlet temperature (+10°C at time t=5000s) and the crude oil flowrate (-10% at time t=7000s). A few oscillations remains but we now expect them to be smoothly treated by the control structure.

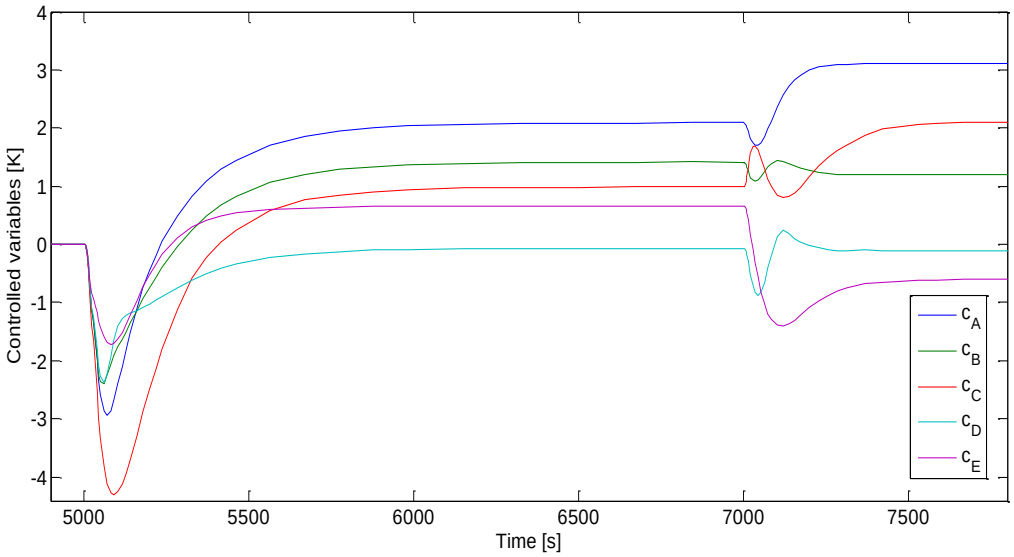

Fig. 6.8. Dynamics of the controlled variables including all filters

6.3. PI controllers tuning

Each PI controller is separately tuned according to the SIMC tuning rules (cfr. section 5.5). The whole tuning process is detailed in the appendix.

Branch		A	B	C	D	E
First-order transfer function between z and c $\frac{k}{(\tau_1 s+1)} e^{-\theta s}$	k	-237.11	-120.3	-152.17	-88.52	-137.05
	τ_1 [s]	64.83	58.33	61.64	48.1	99.2
	θ [s]	12	8	10	8	10
Controller time constant τ_c[s]		240	240	120	240	240
Controller transfer function $K_c \frac{(\tau_I s+1)}{\tau_I s}$	K_c	-0.001085	-0.001955	-0.003116	-0.002119	-0.002895
	τ_I[s]	64.83	58.33	61.64	48.1	99.2

Tab. 6.9. PI Controller tuning

6.4. Simulation results

As desired, the close-loop simulations of this first control structure made of decentralised PI controllers and filters result in a relatively smooth operation of the valve positions.

The following figures (Fig. 6.10 & 6.11) refer to a simulation (taken as example) made of four successive step changes in:

- the feed temperature (+10°C at time t=5000s)
- the feed flowrate (-10% of the nominal value at time t=6000s)
- the hot stream inlet temperature on branch C (-10°C at time t=7000s)
- the hot stream flowrate on branch E (-10% at time t=8000s)

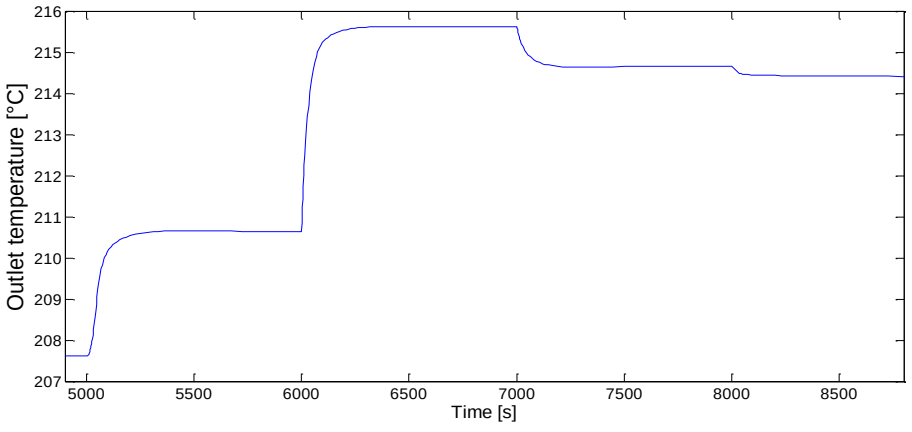

Fig.6.10. Simulation results – Outlet temperature

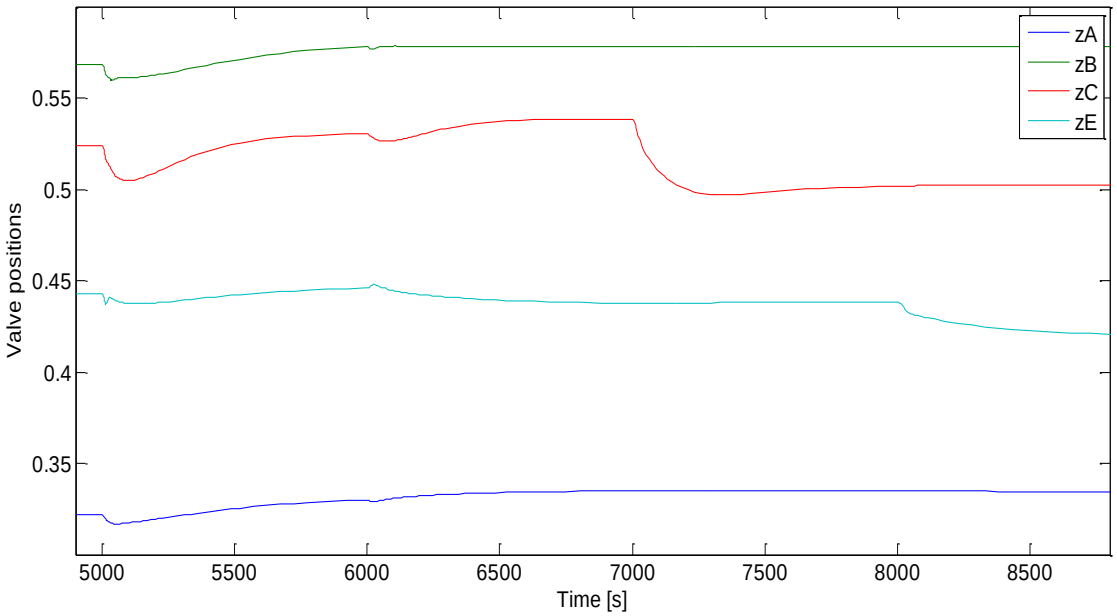

Fig.6.11. Simulation results – Valve operation

The system especially handles very well disturbances on the hot stream temperatures and flowrates due to the forced regular response of the controlled variables made by the filters.

The disturbances on the feed induces conflicting dynamics responses between each branch relative self-optimising variables as we expected from the open-loop simulation (Fig. 6.8.) even of filters were used. This explains some fast oscillations of the valve positions, especially on the branch E where the obtained close-loop dynamics is in a similar same time-scale than the branch F dynamics used by the controller. (Fig. 6.11)

In case of a major disturbance, the decentralised control structure is seen as a very robust one. The new optimum point is slowly reached by the system by a smooth operation of the valves even if the condition of one valve fully open changes from a branch to another.

The following figures (Fig. 6.12 & 6.13) are obtained in the case of a major step change in the second hot stream flowrate in branch F (-80% of the nominal value).

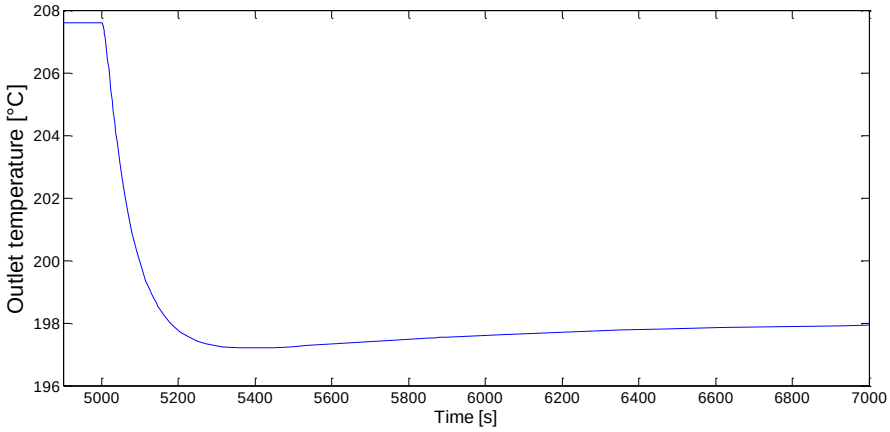

Fig.6.12. Major step change – Outlet temperature

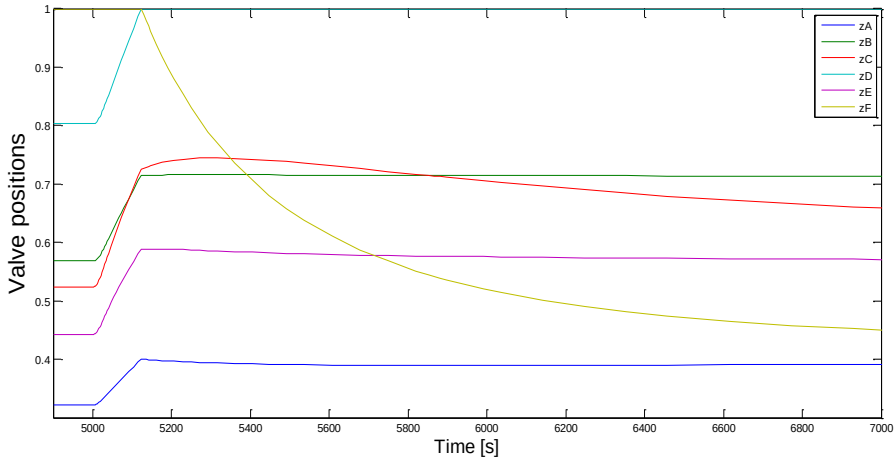

Fig.6.13. Major step change – Valve operation

When the condition of having a valve fully open changes from the branch F to another, the valves dynamics are slowing down. Actually, referring to the equations (5.22) and (5.23),

$$z_{Fc} = 1 \qquad (5.22)$$

$$z_i = \frac{z_{ic}}{\max\,(z_{ic})} \quad ; \quad i = A, B, C, D, E, F \qquad (5.23)$$

When such a major change happens, the values z_{ic} given by each controller have a lower impact on the system since they are treated proportionally to $\max\,(z_{ic})$ which has become higher than 1. This explains the observed slow answer and so the robustness of the control configuration for such major changes.

The crude unit heat exchanger network is physically not subjected to such brute step change. Introducing a more realistic oscillating feed temperature including noise in the system (Fig.6.14),we first observe that the outlet crude oil temperature is reflecting the capacity of the network (Fig. 6.15, lower amplitude and little phase shift). We observe a relatively big phase shift in the valve positions (Fig. 6.16) due to the relatively important time capacity of the filters and the PI controllers.

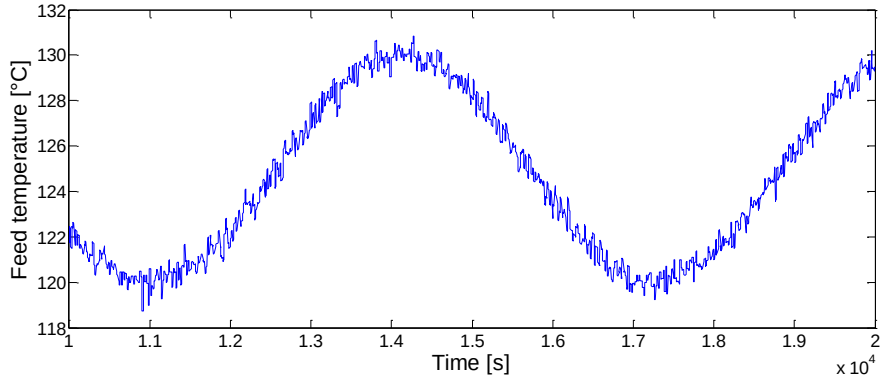

Fig.6.14. Oscillating feed temperature including noise

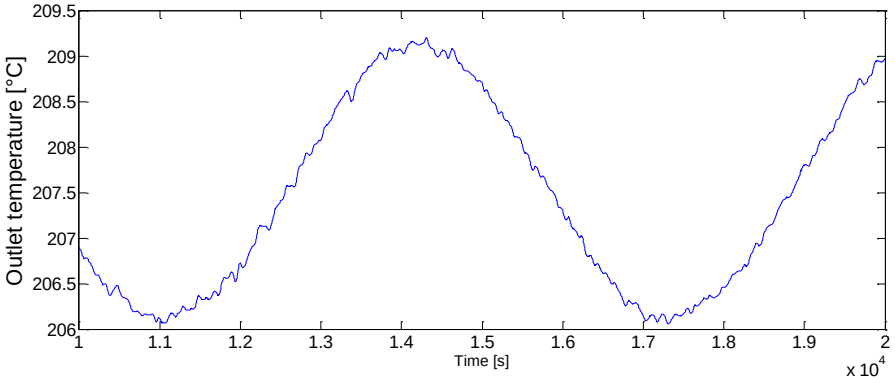

Fig.6.15. Effect on the outlet temperature

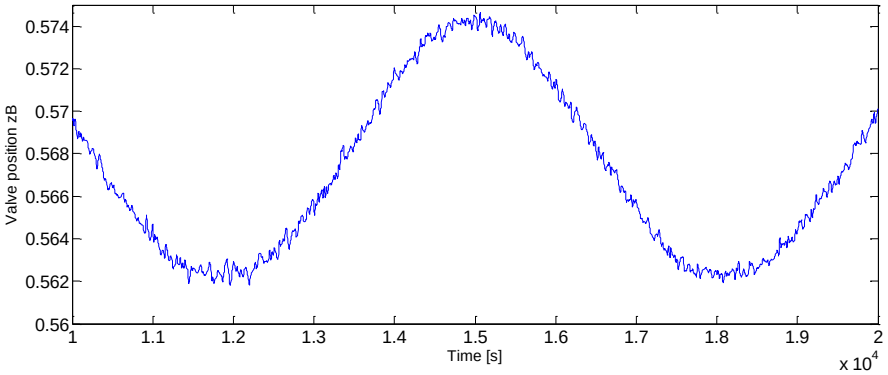

Fig.6.16. Effect on a valve position

6.5. Decentralised control configuration without filters

If the fastness of the control is seen as an important objective instead of smooth valve operations, we could be interested by removing all the filters introduced.

In such a case, the transfer function first-order approximations between each valve position and its controlled variable will be modified as such:

Branch	θ [s]	τ_1[s]
A	5	37.9
B	5	28.0
C	5	39.2
D	5	35.25
E	5	14.25

Tab.6.17. Open-loop first-order transfer functions without filter

Choosing $\tau_c = 60$ s as control time (higher residence time in the heat exchanger network), we obtain the tuning parameters following the SIMC tuning rules:

PI Controller	K_c	τ_I [s]
A	-0.002459	37.9
B	-0.003581	28.0
C	-0.003963	39.2
D	-0.001625	35.25
E	-0.001600	14.25

Tab.6.18. PI controllers tuning without filter

The simulations introduced in the section 6.4. lead now respectively to the Fig. 6.19. &6.20.

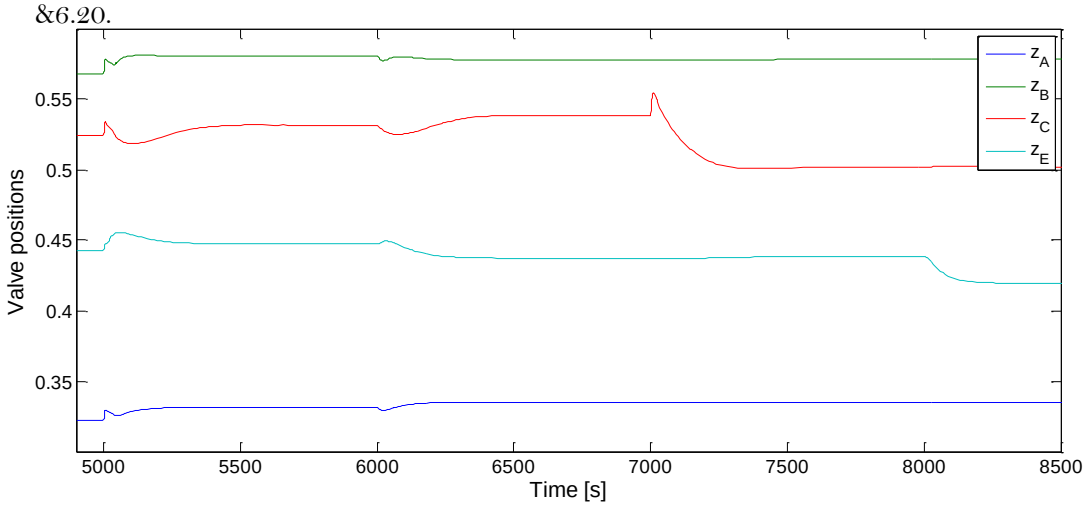

Fig.6.19. Simulation results - Valve operation without filter

The control configuration is a bit faster as desired. However, we observe many strong inverse responses and other oscillating behaviors on the fast time-scale.

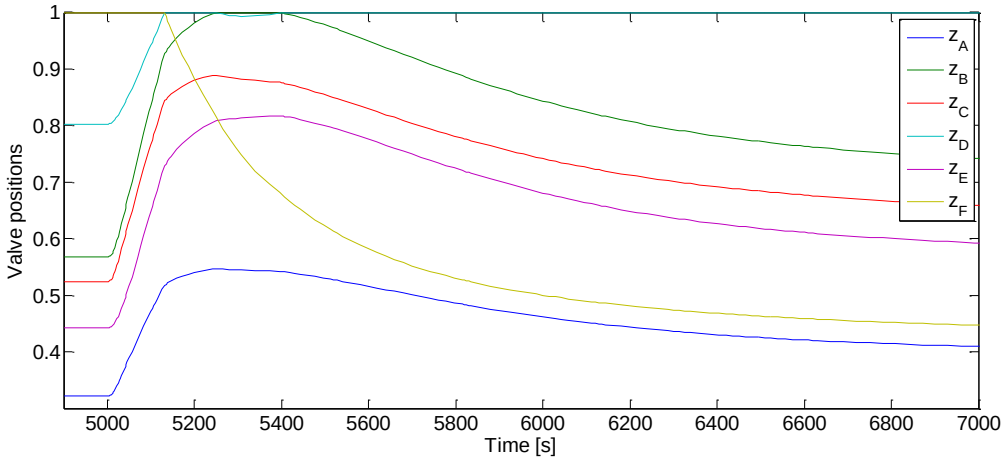

Fig.6.20. Major step change - Valve operation without filter

For major changes, we observe stronger responses during the first 100 seconds which lead the system farther than the new stationary point (general overshoot). The system needs then more time to come back and stabilise. As a consequence, the overall response of the control structure is slow. The objective of having a fastest control structure is thus not achieved for major disturbances.

Again, for an oscillating feed temperature including noise as shown on Fig. 6.21.

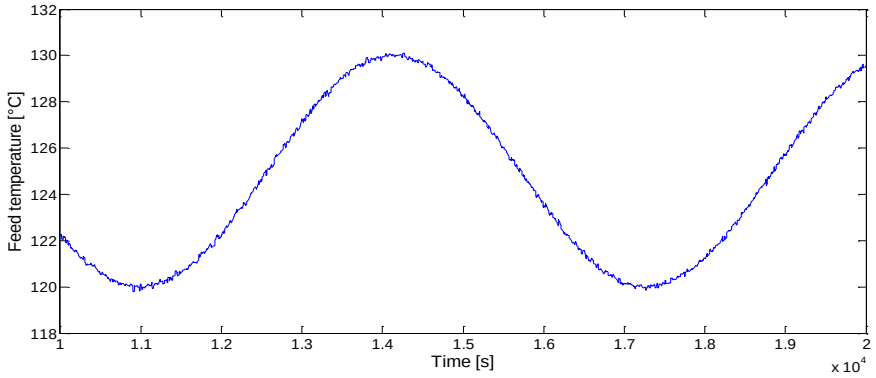

Fig.6.21. Oscillating feed temperature including noise

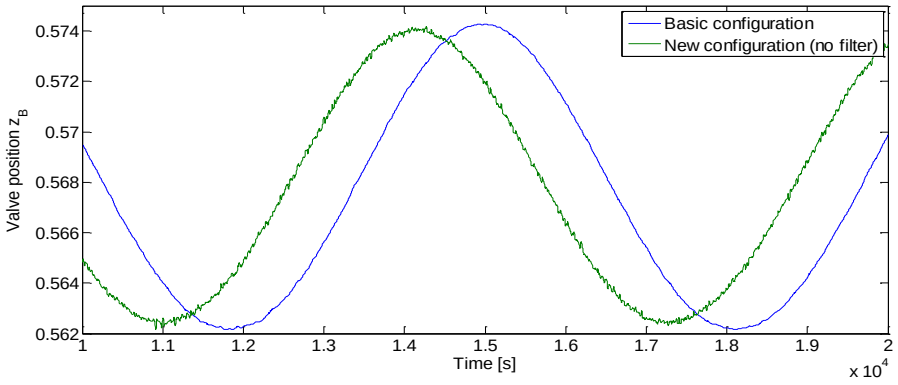

Fig.6.22. Effect on a valve position

We observe that the decentralised control structure without filter has an extremely reduced phase shift compared to the previous structure. However, the noise has strong impacts on the valve positions due to the absence of filter on the feed temperature.

Chapter 7

Advanced multivariable control

Now that the simplest control configuration has been examined, we are interested by the gain that can be obtained with an advanced multivariable feedback control configuration. As shown on the figure 7.1., a multivariable feedback control configuration will use all the controlled variables to give new setpoints to each manipulated variable. The well known advanced form of multivariable control introduced in our work is Model Predictive Control [MPC], commonly used in the chemical process industry.

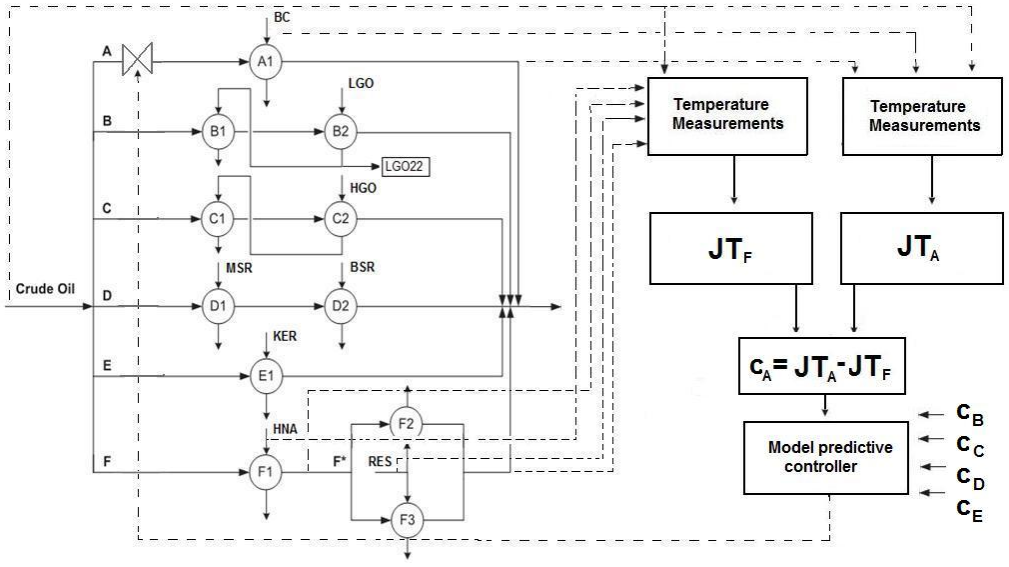

Fig. 7.1. Multivariable control configuration

MPC forecasts the process behavior over the manipulated variables. MPC uses a process model, linear or non-linear and a mathematical programming, typically quadratic programming (QP) in the case of linear process models or sequential quadratic programming (SQP) for non-linear process models. In contrast to the Linear Quadratic Gaussian control, MPC can include explicit constraints on the inputs and outputs, and optimises over a finite horizon. (Imsland, 2007)

The MatLab© MPC toolbox presents a MPC Controller block in Simulink that uses linear state-base process model for the prediction and a QP optimiser.

7.1. Model linearization

So far, the open-loop system between the manipulated variables (valve positions) and the controlled variables (combination of the self-optimising variables) has been non-linear, especially due to the complex form of the self-optimising variables. However, a linear time-invariant (LTI) model is needed to build the MPC Controller. We thus need a linear approximation of the open-loop system. The accuracy of this approximation is a key issue affecting controller predictions and so its performances.

The Simulink environment provides a convenient and useful graphical interface for model linearization (Linear Analysis Tool) at a specified operating point.

This tool successfully recognises all the state variables of our Simulink model :

- 330 state variables corresponding to the 30 cell temperatures for the 11 heat exchangers
- 38 state variables corresponding to the 38 first-order transfer functions used for the measurement dynamics and filters
- 5 state variables corresponding to the integration part of the PI Controllers

Prior the linearization, we specify the stationary operating point where both the filters and the PI Controllers are deactivated. These "states" identified by Simulink thus do not play any role and everything linked to them is set to 0. The last thing to specify in the interface is, of course, the five inputs (valve positions) and the five outputs (controlled variables).

Afterwards, the high order of the obtained LTI model can be reduced without reducing significantly the accuracy of the LTI model. Several methods for residualizing the less controllable and observable states exists such as the Hankel norm approximation (Skogestad and Postletwhaite, 2005) that can be executed in one single command in the MatLab© workspace. In this work, the LTI model has finally not been reduced since we were focusing on the best results possible and the MPC Controller was able to handle this high order model.

7.2. Model Predictive Controller tuning

At least three main parameters need to be tuned to obtain an efficient Model Predictive Controller: the control interval, the prediction horizon and the control horizon. Many others parameters can be introduced such as constrains or weights on inputs or outputs but they have not been used in this work. Actually, our model for the valve distribution is build in such a way that it is not subjected to constraints and we want to avoid weights on inputs that could lead to steady-state offsets.

The cost function used by the optimiser is thus a simple quadratic function of the controlled variables (the weights are equally distributed among the variables):

$$J = c_A^2 + c_B^2 + c_C^2 + c_D^2 + c_E^2 \qquad (7.1)$$

In order to have a smooth operation of the valves and reduce the impact of inverse responses, the control interval has been set to 60 seconds which corresponds to the highest residence time of the crude oil in the network (branch A).

The prediction horizon has to be fixed as a multiple of control intervals. Since we focus very much on the best configuration possible, it has been set to 10 which is a value beyond which we have not observed significant gain in the control quality of the MPC. The control horizon has been fixed to 1 so the MPC re-optimise its prediction and thus corrects its decision at each control interval.

7.3. Comparative simulation results

The close-loop simulation results of the MPC are shown directly in comparison with the results of our previous decentralised control configuration using PI controllers and filters.

As done previously, the following figures (Fig. 7.2, 7.3, 7.4) refer to a simulation made of four successive step changes in:

- the feed temperature (+10°C at time t=5000s)
- the feed flowrate (-10% of the nominal value at time t=6000s)
- the hot stream inlet temperature on branch C (-10°C at time t=7000s)
- the hot stream flowrate on branch E (-10% at time t=8000s)

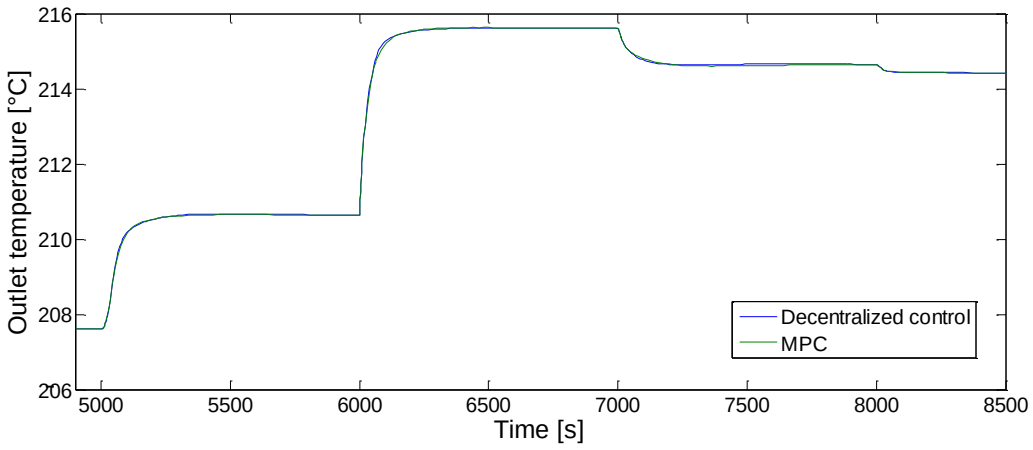

Fig. 7.2. Simulation results – Outlet temperature

The dynamics on the outlet temperature of the crude oil (overall objective) does not really differ from a control configuration to another. The dynamics is mainly a characteristic of the plant (open-loop system), the contribution of the control system is not significant. The optimum point in the system is very flat and we know that the valve position changes by self-optimising control only bring the same small (but valuable) difference at the steady-state level.

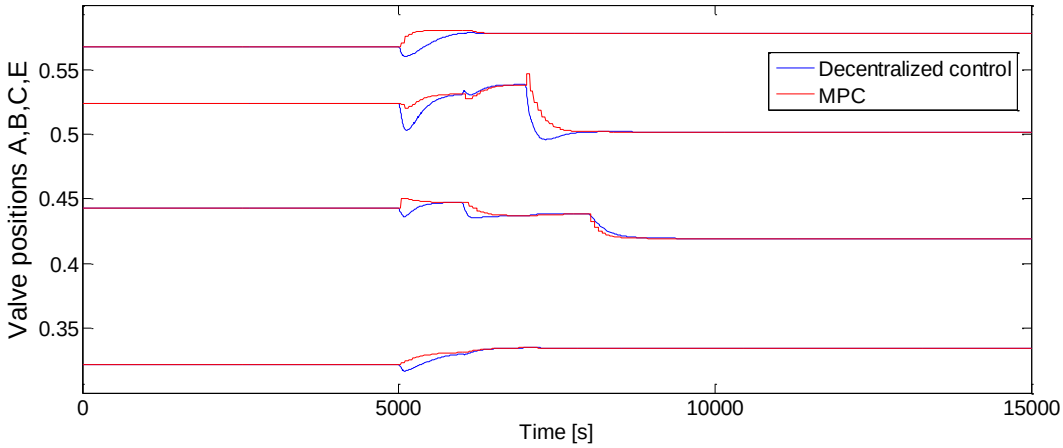

Fig. 7.3. Simulation results – Valve operation

It appears that the valve operations are generally faster and still relatively smooth using the MPC configuration. However, this is not observed in every simulation and for all valve positions. All inverse responses cannot be avoided by the MPC since we have not introduced the filters for this control configuration.

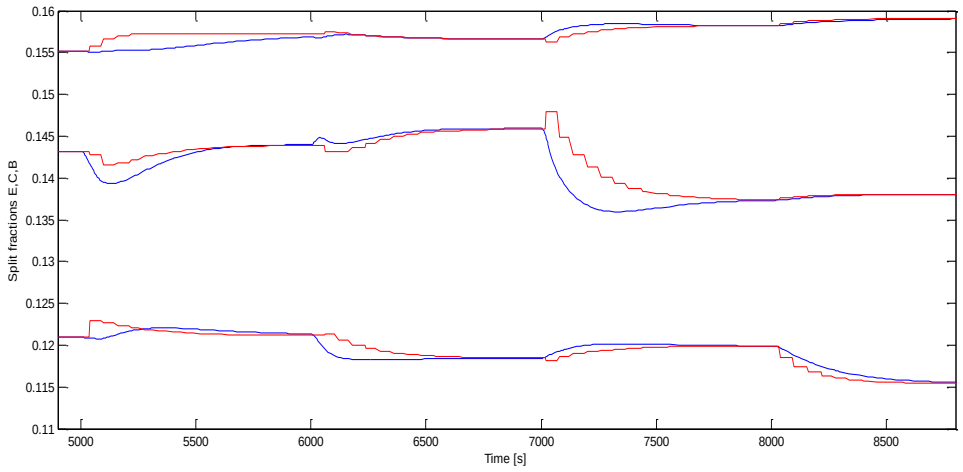

Fig. 7.4. Simulation results – Split fractions

Looking at the split fraction of the feed flowrate, we observe that faster stabilization of the valve positions does not always lead to faster stabilization of its branch relative crude oil flowrate due to the influence of other valve positions. As a central controller, the MPC tends to force the branches to react in same time-scale dynamics.

In case of major disturbance (Fig.7.5. & 7.6.), this common time-scale response of the MPC configuration is better observed. The following figures are obtained in the case of a step change in the second hot stream flowrate in branch F (-80% of the nominal value).

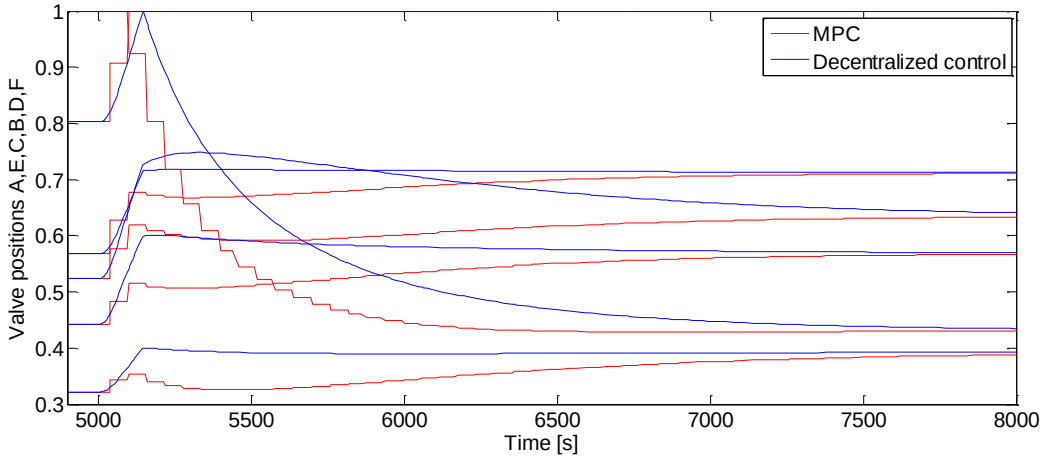

Fig. 7.5. Major step change – Valve operation

The new optimum point is smoothly reached by all the valve positions that are not fully open. We also observe that the valve subjected to a major change is clearly seen as a priority by the controller while the other valves are subjected to a long and not strictly increasing curve to reach their new steady-state value.

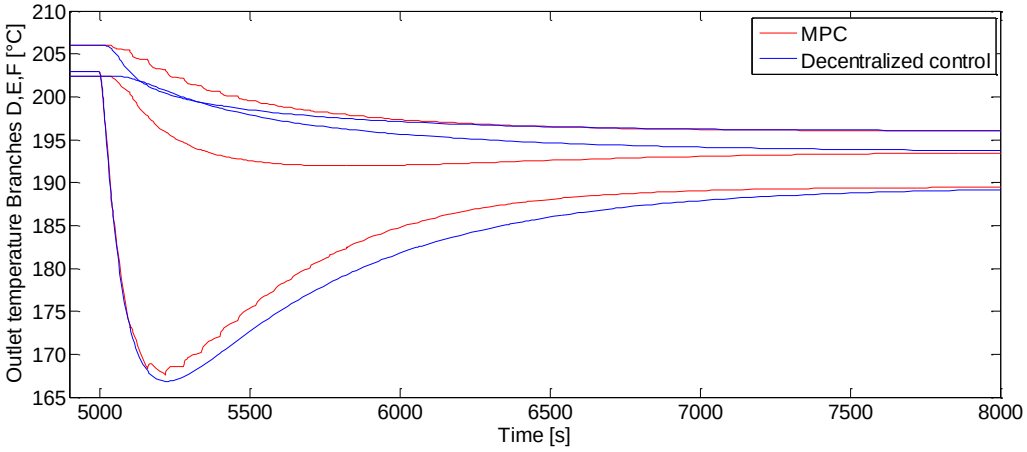

Fig. 7.6. Major step change – Branch Outlet temperatures

Note that the effect on the network outlet crude oil temperature cannot be distinguished from a control configuration to the other.

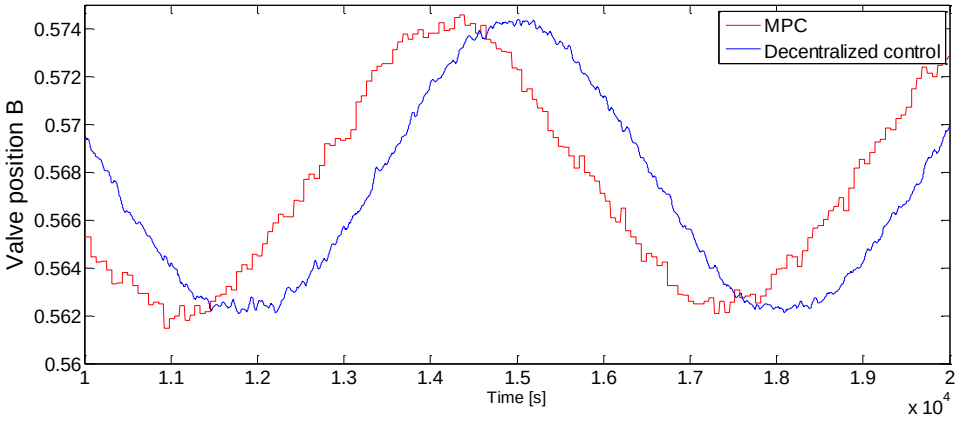

Fig. 7.7. Effect of an oscillating feed temperature on a valve position

For an oscillating feed temperature including noise, the MPC configuration does not present a significant phase shift compared to a decentralised control configuration including filters. (Fig. 7.7.) However, the noise affects much the valve operation. The MPC simulation results would be very close to a decentralised control configuration without filters (not shown on the graph).

Chapter 8

The case of flow control

8.1. Introduction

This chapter has been added here based on discussions with our industrial partner (Statoil) in the last days of this work. It appears that flow control is actually implemented for the operation of the given network. The control structure is then asked to give setpoints to the crude oil flowrates of the branches A,B,C,D,E while the crude oil flowrate of branch F results from the mass balance. Moreover, the sub-split on branch F is given as constant.

Introducing the crude oil flowrates of the branches A,B,C,D and E as our new manipulated variables, we decided to adapt our three previous control structure: decentralised control with filters, decentralised control without filters and advanced multivariable control (MPC). This chapter aims at comparing them directly and so the explanations about the tuning will not be detailed as previously.

The objective of smooth operations is still valid in the case of flow control and so the interest in the decentralised control structure with filters is justified. Since the filters were introduced looking at the self-optimising variables responses for disturbances, new manipulated variables do not lead to modifications regarding their placement and their time constants.

8.2. Controllers re-tuning

8.2.1. Decentralised control with filters

The 5 PI controllers are retuned using the SIMC tuning rules (cfr. 5.5) (Tab. 8.1).

Branch		A	B	C	D	E
First-order transfer function between z and c $\frac{k}{(\tau_1 s+1)} e^{-\theta s}$	k	-4.5573	-2.7774	-3.3026	-2.3229	-2.9914
	τ_1 [s]	68.9	58.2	67.9	50.4	87.0
	θ [s]	8	9	6	8	10
Controller time constant τ_c[s]		240	240	120	240	240
Controller transfer function $K_c \frac{(\tau_I s+1)}{\tau_I s}$	K_c	-0.0610	-0.0842	0.1632	-0.0875	-0.1163
	τ_I[s]	68.9	58.2	67.9	50.4	87.0

Tab. 8.1. PI Controllers retuning –flow decentralised control with filters

8.2.2. Decentralised control without filters

The 5 PI controllers are retuned using the SIMC tuning rules (cfr. 5.5) (Tab. 8.2).

Branch		A	B	C	D	E
First-order transfer function between z and c $\frac{k}{(\tau_1 s+1)} e^{-\theta s}$	k	-4.5573	-2.7774	-3.3026	-2.3229	-2.9914
	τ_1 [s]	37.0	29.1	46.0	34.4	16.2
	θ [s]	5	5	5	5	5
Controller time constant τ_c[s]		60	60	60	60	60
Controller transfer function $K_c \frac{(\tau_I s+1)}{\tau_I s}$	K_c	-0.1249	-0.1612	-0.2143	-0.2278	-0.0833
	τ_I[s]	37.0	29.1	46.0	34.4	16.2

Tab. 8.2. PI Controllers retuning – flow decentralised control without filters

8.2.3. Advanced multivariable control (MPC)

For the MPC, while new manipulated variables require a new linearization, the same tuning parameters (control interval, prediction horizon and control horizons) have been selected.

8.3. Comparative simulation results

The three control structures are directly compared running the same close-loop simulations for each one.

The figure 8.3 (three graphs) refer to the simulation (as introduced in chapters 6&7) made of four successive step changes:

- the feed temperature (+10°C at time t=5000s)
- the feed flowrate (-10% of the nominal value at time t=6000s)
- the hot stream inlet temperature on branch C (-10°C at time t=7000s)
- the hot stream flowrate on branch E (-10% at time t=8000s)

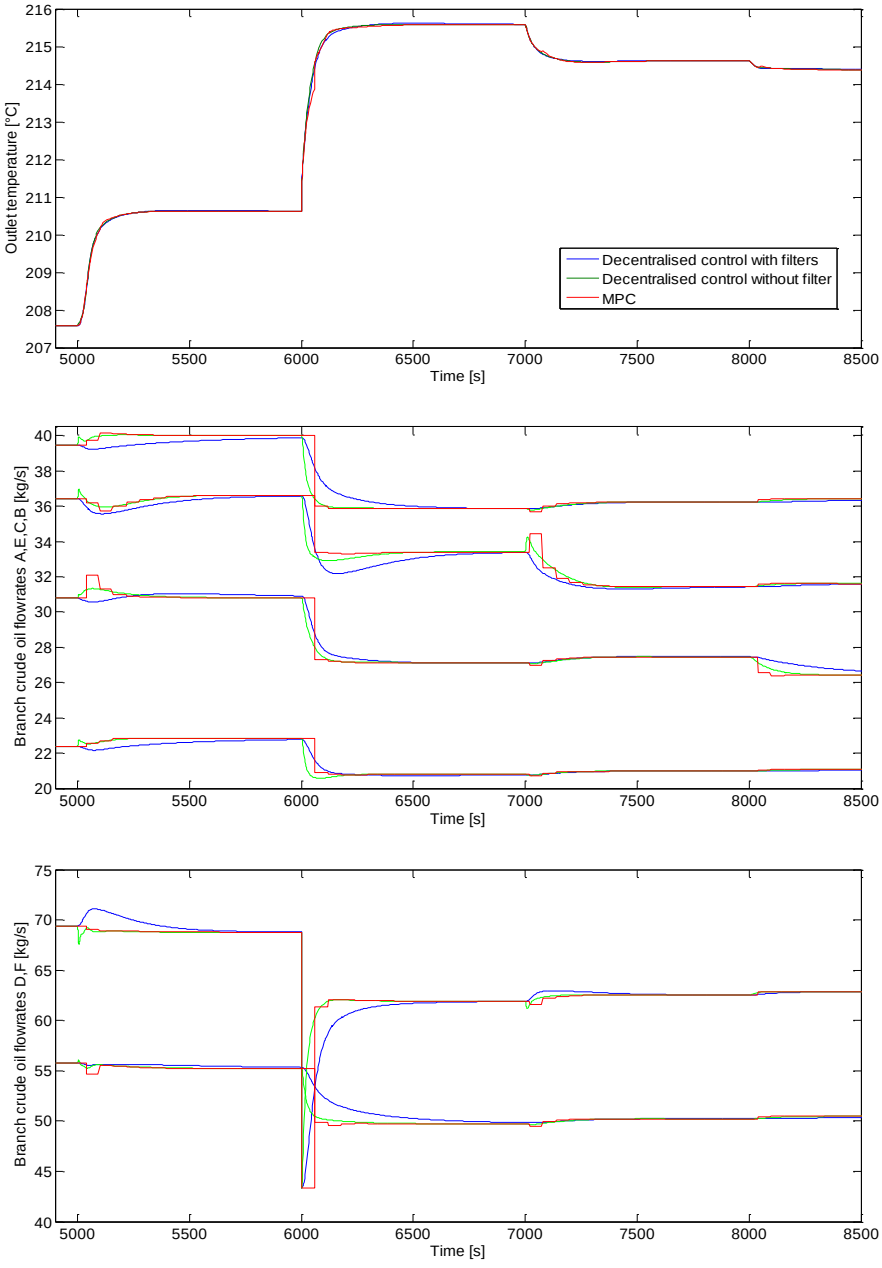

Fig.8.3. Comparative simulation results

In the case of flow control, the same general conclusions can be written. The decentralised control configuration with filters offer to get rid of fast oscillations while the MPC tuning is such that it is not canceling them completely. The fastest control configuration is seen as the decentralised control without filter and the gain using a multivariable controller is hard to see. The main difference with the previous case is the direct impact on branch F for a feed flowrate due to its setting by the mass balance. However, this is an intrinsic characteristic of the plant structure and the control configuration is powerless regarding to this issue.

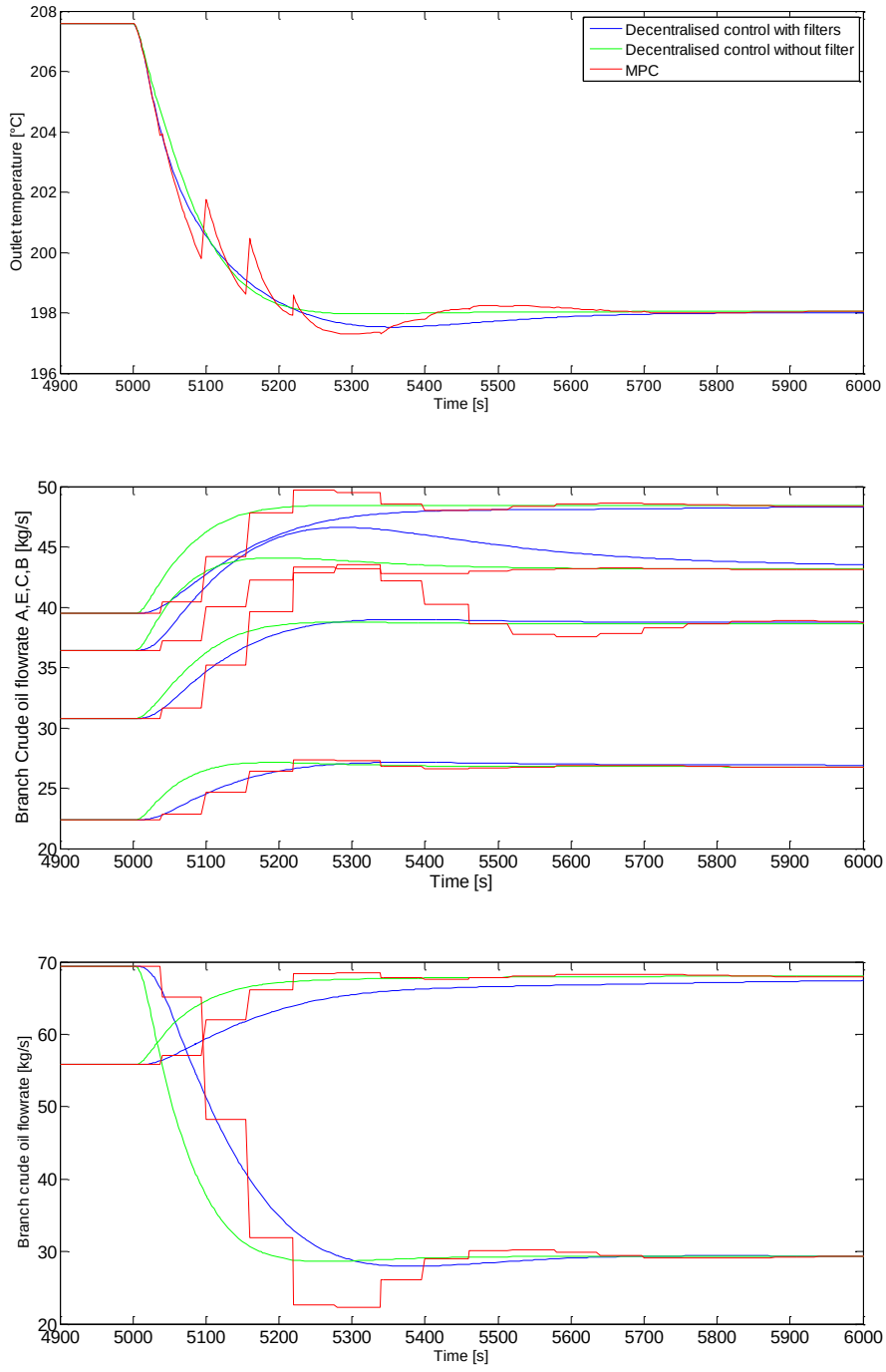

Fig.8.4. Comparative simulation results – Major step change

In the case of a major step change (Fig.8.4.), flow control configurations lead to other and new conclusions. The simplest decentralised control configuration without filter is observed to be the best option. By contrast to valve operation, flow operation leads to more inertia of the manipulated variables and we do not observe overshoots anymore even if no one single filter is used. The MPC is obviously not adapted to this case. This can be explained by the absence of weights on the inputs in the cost function and especially by the fact that the linear model differs very much of the complex model in case of such major disturbances in the system.

Finally, for an oscillating feed temperature with noise, the same conclusions can be written as seen for valve operations. The use of filters cancel the impact of the noise but induce a phase shift.(Fig. 8.5.)

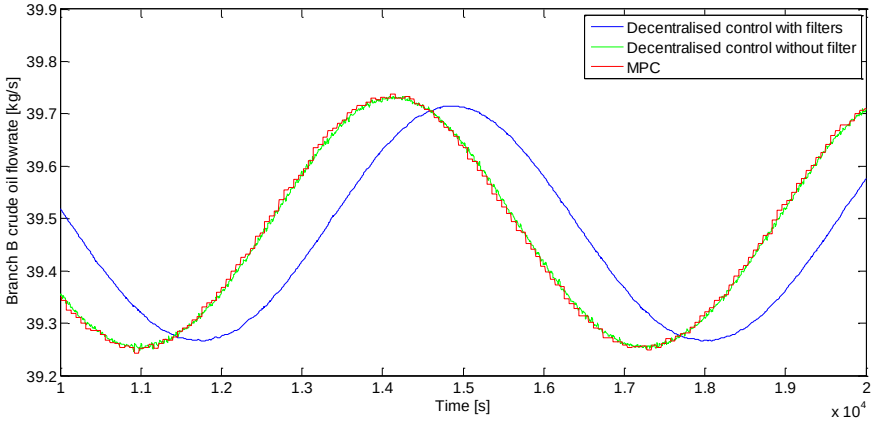

Fig.8.5. Comparative simulation results – Major step change

Chapter 9

Conclusion

The reduced crude unit heat exchanger network studied in this work presents dynamic differences between branches that have been successfully captured in our model. Our control design studies have thus been based on the knowledge of these physical characteristics of the given plant.

The simple self-optimising variables derived by Jäschke (Jäschke, 2012) present moderate steady-state performances which need to be re-assessed with an accurate steady-state model (the values in section 4.3.2. should be considered with caution). Nevertheless, these variables still offer to lead the system close to the optimal point only with a few temperature measurements.

The self-optimising variables dynamics present undesirable transient effects, especially at high frequencies (fast-time scales). Since the control pursues an economical objective, smooth operation has been sought in this work. So filtering on selective measurements (feedforward control abatement, etc.) has been suggested to limit any hard valve or flow operation in the case of a simple control configuration.

A decentralised control configuration made of 5 simple PI controllers is believed to be satisfactory for the operation of the given network. In this case, the operation smoothness is balanced with the control phase shift due to the filters. The close-loop system is observed to have a strong robustness and so can handle safely huge disturbances. This control configuration will not require any modeling effort for industrial implementation which constitutes a major advantage.

The overall results of the MPC configuration are considered to be only a bit better than those of the decentralised control configuration using filters. Actually, the MPC computes a close-loop optimal time-scale dynamics which can be approximately found in the decentralised configuration (tuning of each PI controllers separately). If relatively hard valve or flow operations were allowed, there would not be significant differences between the dynamics performances of a decentralised control configuration without filters and the MPC configuration.

However, the physical computing time of the MPC has not been taken into account and could lead to a poorer performance on the real plant compared to fast PI controllers.

A.Leruth, June 2012

Bibliography

Boyaci, C., Uzturk, D., Konukman, A. E. S., Akman, U., 1996. Dynamics and Optimal Control of Flexible Heat-Exchanger Networks. Computers and Chemical Engineering 20 (Supplement 2), 775 – 780.

Chachuat, B., Srinivasan, B., Bonvin, D., 2009. Adaptation Strategies for Real-Time Optimisation. Computers and Chemical Engineering 33 (10), 1557 – 1567.

Edvardsen, D.G., 2011, Optimal operation of Heat Exchanger Networks, master thesis, Norwegian University of Science and Technology.

Glemmestad, B., Skogestad, S., Gundersen, T., 1999. Optimal operation of heat exchanger networks. Computers and Chemical Engineering 23 (4-5), 509 – 522.

I.A. Wiehe and R.J.Kennedy, 2000, Energy and Fuels, 14, 56-63

Imsland L., 2007, An introduction to Model Predictive Control, Norwegian University of Science and Technology

Jäschke, J., 2011. Invariants for Optimal Operation of Process Systems. Doctoral thesis, Norwegian University of Science and Technology.

Jäschke J., 2012, United Kingdom Patent Application No. 1207770.7, Parallel Heat Exchanger control

Lid,T.,Strand,S.,Skogestad,S.,On-line optimisation of a crude unit heat exchanger network, 2000

Lid, T., Skogestad, S., 2001. Implementation issues for real-time optimisation of a crude unit heat exchanger network. In: Gani,R.,Jorgensen,S.B.(Eds.),European Symposium on Computer Aided Process Engineering - 11, 34th European Symposium of the Working Party on Computer Aided Process Engineering. Vol. 9 of Computer Aided Chemical Engineering. Elsevier, pp. 1041 – 1046.

Lundsford K.M., 1998, *Increasing heat exchanger performance*, Bryan research and Engineering, Inc. Texas

Mathisen, K. W., Skogestad, S., Wolff, E. A., 1992. Bypass Selection for Control of Heat Exchanger Networks. Computers and Chemical Engineering 16 (Supplement 1), 263 – 272.

Mathisen, K.W., Morari, M., Skogestad, S., Wolff, E. A., 1994a. Optimal Operation of Heat Exchanger Networks Presented at Process Systems Engineering (PSE'94), Kyongju, Korea.

Mathisen, K. W., Morari, M., Skogestad, S., 1994b. Dynamic models for heat exchangers and heat exchanger networks. Computers and Chemical Engineering 18 (1), 459–463.

Sinnott, R., Towler, G., 2009. Chemical Engineering Design, 5th Edition. Elsevier Ltd., Oxford.

Skogestad, S., 2000. Plantwide control: the search for the self-optimising control structure. Journal of Process Control 10.

Skogestad, S., 2003, Simple analytic rules for model reduction and PID controller tuning, Journal of Process Control 13, 291–309

Skogestad, S., 2004, Near-optimal operation by self-optimizing control: From process control to marathon running and business systems, Computers & Chemical Engineering 29(1), 127-137

Skogestad, S., Postelthwaite, I., 2005, Multivariable feedback control, Analysis and Design, John Wiley & Sons, Ltd, Second edition

White, D. C., 1997. Online optimisation: What, where and estimating ROI. Hydrocarbon Processing 76 (6), 4351.

Web resources:

http://www.mathworks.se/help/toolbox/simulink/

http://www.alaquainc.com/Heat_Exchangers.aspx

http://www.substech.com/dokuwiki/doku.php?id=stainless_steel_2205

http://synergycoils.com/products/tube/index.htm

Appendix

A. Data Reconciliation – Temperatures and flowrates

Branch A :

$$\Delta H_{A,crude} = \Delta H_{BC}$$

$$\Leftrightarrow m_A \int_{T_{in}}^{T_{A,out}} c_{p,crude} dT = m_{BC} \int_{T_{BC,out}}^{T_{BC,in}} c_{p,BC} dT$$

$$\Leftrightarrow m_A \left[T_{A,out} \left(k_{1,crude} \frac{T_{A,out}}{2} + k_{2,crude} \right) - T_{in} \left(k_1 \frac{T_{in}}{2} + k_2 \right) \right] = m_{BC} \left[T_{BC,in} \left(k_{1,BC} \frac{T_{BC,in}}{2} + k_{2,BC} \right) - T_{BC,out} \left(k_{1,BC} \frac{T_{BC,out}}{2} + k_{2,BC} \right) \right]$$

Since m_{BC} was missing in the asked data, this heat balance just serves to compute it. All others measured data are taken without any modification.

$m_A\ [t/h]$	$T_{in}\ [°C]$	$T_{A,out}\ [°C]$	$T_{BC,in}\ [°C]$	$T_{BC,out}\ [°C]$
76,582	125,00	226,457	295,4453	167,59

$$\Rightarrow m_{BC} = 57{,}270\ t/h$$

Branch B :

$$\Delta H_{B,crude} = \Delta H_{LGO}$$

$$\Leftrightarrow m_B \int_{T_{in}}^{T_{B,out}} c_{p,crude} dT = m_{LGO,tot} \int_{T_{LGO,inter}}^{T_{LGO,in}} c_{p,LGO} dT + (m_{LGO,tot} - m_{LGO22}) \int_{T_{LGO,out}}^{T_{LGO,inter}} c_{p,LGO} dT$$

$$\Leftrightarrow m_B \left[T_{B,out} \left(k_{1,crude} \frac{T_{B,out}}{2} + k_{2,crude} \right) - T_{in} \left(k_1 \frac{T_{in}}{2} + k_2 \right) \right]$$
$$= m_{LGO,tot} \left[T_{LGO,in} \left(k_{1,LGO} \frac{T_{LGO,in}}{2} + k_{2,LGO} \right) - T_{LGO,out} \left(k_{1,LGO} \frac{T_{LGO,out}}{2} + k_{2,LGO} \right) \right]$$
$$- m_{LGO22} \left[T_{LGO,inter} \left(k_{1,LGO} \frac{T_{LGO,inter}}{2} + k_{2,LGO} \right) - T_{LGO,out} \left(k_{1,LGO} \frac{T_{LGO,out}}{2} + k_{2,LGO} \right) \right]$$

Since $m_{LGO,tot}$ was missing in the asked data, this heat balance just serves to compute it. All others measured data are taken without any modification. The temperature $T_{B,inter}$ of the crude oil between the two exchangers can then be estimated by the heat balance on the first heat exchanger.

$m_B[t/h]$	T_{in} [°C]	$T_{B,out}$ [°C]	$T_{LGO,in}$ [°C	$T_{LGO,inter}$ [°C]	$T_{LGO,out}$ [°C]	$m_{LGO22}[t/h]$
159,785	125,00	208,3047	267,820	235,285	179,117	39,930

$$\Rightarrow m_{LGO,tot} = 162{,}6105\ t/h$$

$$\Rightarrow T_{B,inter} = 172{,}202°C$$

Branch C :

$$\Delta H_{C,crude} = \Delta H_{HGO}$$

$$\Leftrightarrow m_C \int_{T_{in}}^{T_{C,out}} c_{p,crude} dT = m_{HGO} \int_{T_{HGO,out}}^{T_{HGO,in}} c_{p,HGO} dT$$

$$\Leftrightarrow m_C \left[T_{C,out} \left(k_{1,crude} \frac{T_{C,out}}{2} + k_{2,crude} \right) - T_{in} \left(k_1 \frac{T_{in}}{2} + k_2 \right) \right]$$

$$= m_{HGO} \left[T_{HGO,in} \left(k_{1,HGO} \frac{T_{HGO,in}}{2} + k_{2,HGO} \right) - T_{HGO,out} \left(k_{1,HGO} \frac{T_{HGO,out}}{2} + k_{2,HGO} \right) \right]$$

Since m_{HGO} was missing in the asked data, this heat balance just serves to compute it. All others measured data are taken without any modification.

$m_C\ [t/h]$	T_{in} [°C]	$T_{C,out}$ [°C]	$T_{HGO,in}$ [°C	$T_{HGO,out}$ [°C]
120,414	125,00	213,676	248,7734	141,254

$$\Rightarrow m_{HGO} = 97{,}075\ t/h$$

Branch D :

$$\Delta H_{D1,crude} = \Delta H_{MSR}$$

$$\Leftrightarrow m_D \int_{T_{in}}^{T_{D,inter}} c_{p,crude} dT = m_{MSR} \int_{T_{MSR,out}}^{T_{MSR,in}} c_{p,MSR} dT$$

$$\Leftrightarrow m_D \left[T_{D,inter} \left(k_{1,crude} \frac{T_{D,inter}}{2} + k_{2,crude} \right) - T_{in} \left(k_1 \frac{T_{in}}{2} + k_2 \right) \right]$$

$$= m_{MSR}\left[T_{MSR,in}\left(k_{1,MSR}\frac{T_{MSR,in}}{2}+k_{2,MSR}\right)-T_{MSR,out}\left(k_{1,MSR}\frac{T_{MSR,out}}{2}+k_{2,MSR}\right)\right]$$

$$\Delta H_{D2,crude} = \Delta H_{BSR}$$

$$\Leftrightarrow m_D\int_{T_{D,inter}}^{T_{D,out}} c_{p,crude}dT = m_{MSR}\int_{T_{BSR,out}}^{T_{BSR,in}} c_{p,BSR}dT$$

$$\Leftrightarrow m_D\left[T_{D,out}\left(k_{1,crude}\frac{T_{D,out}}{2}+k_{2,crude}\right)-T_{D,inter}\left(k_{1,crude}\frac{T_{D,inter}}{2}+k_{2,crude}\right)\right]$$

$$= m_{BSR}\left[T_{BSR,in}\left(k_{1,BSR}\frac{T_{BSR,in}}{2}+k_{2,BSR}\right)-T_{BSR,out}\left(k_{1,BSR}\frac{T_{BSR,out}}{2}+k_{2,BSR}\right)\right]$$

In these balances, we hopefully have all the data. But the equations do not match perfectly and reconciliation is needed.

$m_D\ [t/h]$	$T_{in}\ [°C]$	$T_{D,inter}\ [°C]$	$T_{MSR,in}\ [°C]$	$T_{MSR,out}\ [°C]$	$m_{MSR}\ [t/h]$
177,516	125,00	181,06	222,81	176,58	213,63

$T_{D,out}\ [°C]$	$T_{BSR,in}\ [°C]$	$T_{BSR,out}\ [°C]$	$m_{BSR}\ [t/h]$
207,00	268,617	243,906	174,090

For the given values, we observe that :

$$\Delta H_{D1} << \Delta H_{MSR}$$

$$\Delta H_{D2} < \Delta H_{BSR}$$

So we introduce two reconciliation factors $\varepsilon > 0$ and $\gamma > 0$ in order to enhance the overall heat transfer and redistribute as little as possible the heat exchange between the units :

$$m_{r,D} = m_D(1+2\varepsilon) \quad ; \quad T_{r,D,out} = T_{D,out}(1+\varepsilon)$$

$$T_{r,MSR,in} = T_{MSR,in}(1-\varepsilon) \quad ; \quad T_{r,MSR,out} = T_{MSR,out}(1+\varepsilon)$$

$$m_{r,MSR} = m_{MSR}(1-2\varepsilon) \quad ; \quad m_{r,BSR} = m_{BSR}(1-2\varepsilon)$$

$$T_{r,BSR,in} = T_{BSR,in}(1-\varepsilon) \quad ; \quad T_{r,BSR,out} = T_{BSR,out}(1+\varepsilon)$$

$$T_{r,D,inter} = T_{D,inter}(1+\gamma)$$

And we solve the previous heat balances with the new temperatures and flowrates in order to find:

$$\Rightarrow \varepsilon = 0{,}003296 \ ; \ \gamma = 0{,}01389$$

The corrected values are:

$m_{r,D}\ [t/h]$	$T_{in}\ [°C]$	$T_{r,D,inter}\ [°C]$	$T_{r,MSR,in}\ [°C]$	$T_{r,MSR,out}\ [°C]$	$m_{r,MSR}\ [t/h]$
178,686	125,00	181,06	222,078	177,164	212,225

$T_{r,D,out}\ [°C]$	$T_{r,BSR,in}\ [°C]$	$T_{r,BSR,out}\ [°C]$	$m_{r,BSR}\ [t/h]$
207,68	267,632	244,710	172,942

Branch E :

$$\Delta H_{E,crude} = \Delta H_{KERO}$$

$$\Leftrightarrow m_E \int_{T_{in}}^{T_{E,out}} c_{p,crude} dT = m_{KERO} \int_{T_{KERO,out}}^{T_{KERO,in}} c_{p,KERO} dT$$

$$\Leftrightarrow m_E \left[T_{E,out} \left(k_{1,crude} \frac{T_{E,out}}{2} + k_{2,crude} \right) - T_{in} \left(k_1 \frac{T_{in}}{2} + k_2 \right) \right]$$

$$= m_{KERO} \left[T_{KERO,in} \left(k_{1,BC} \frac{T_{KERO,in}}{2} + k_{2,BC} \right) - T_{KERO,out} \left(k_{1,BC} \frac{T_{KERO,out}}{2} + k_{2,KERO} \right) \right]$$

In this balance, we hopefully have all the data. But the equation does not match perfectly so reconciliation is needed.

$m_E[t/h]$	$T_{in}\ [°C]$	$T_{E,out}\ [°C]$	$T_{KERO,in}\ [°C]$	$T_{KERO,out}\ [°C]$	$m_{KERO}\ [t/h]$
126,092	125,00	200,070	241,836	180,551	142,441

For the given values, we observe that :

$$\Delta H_{E,crude} < \Delta H_{KERO}$$

So we introduce the reconciliation factors $\varepsilon > 0$ such that :

$$m_{r,E} = m_E(1 + 2\varepsilon)$$

$$T_{r,E,out} = T_{E,out}(1 + \varepsilon)$$

$$T_{r,KERO,in} = T_{KERO,in}(1 - \varepsilon)$$

$$T_{r,KERO,out} = T_{KERO,out}(1 + \varepsilon)$$

$$m_{r,KERO} = m_{KERO}(1 - 2\varepsilon)$$

And we solve the previous heat balances with the new temperatures and flowrates in order to find ε:

$$\Rightarrow \varepsilon = 0{,}00103$$

The corrected values are:

$m_{r,E}\ [t/h]$	$T_{in}\ [°C]$	$T_{r,E,out}\ [°C]$	$T_{r,KERO,in}\ [°C]$	$T_{r,KERO,out}\ [°C$	$m_{r,KERO}\ [t/h]$
126,351	125,00	200,276	241,587	180,7366	142,1482

Branch F : cfr. report.

Global balances on the crude oil :

Mass balance :

$$m_{tot} = m_A + m_B + m_C + m_{r,D} + m_{r,E} + m_{r,F}$$

Since m_{tot} was not part of the asked data, this mass balance is used to estimate it.

$$\Rightarrow m_{tot} = 915{,}4227\ t/h$$

Heat balance (cfr. 2.3.1. (*)) :

$$T_{tot} = \frac{-m_{tot}k_2 + \sqrt{{m_{tot}}^2{k_2}^2 + 2m_{tot}k_1 \sum_{streams} m_i T_i \left(k_1 \frac{T_i}{2} + k_2\right)}}{m_{tot}k_1}$$

In order to simplify the reconciliation procedure, T_{tot} is calculated by this expression.

$$T_{tot} = 207{,}6543°C$$

For information, the measured T_{tot} was 206,6836°C. The reconciliation forces it to a 0,47% adjustment.

B. PI controllers tuning (valve control with filters)

Open-loop step change in the valve position of branch E

At time t=5000s, z_{Ec} passes from 0.4428 to 0.4528

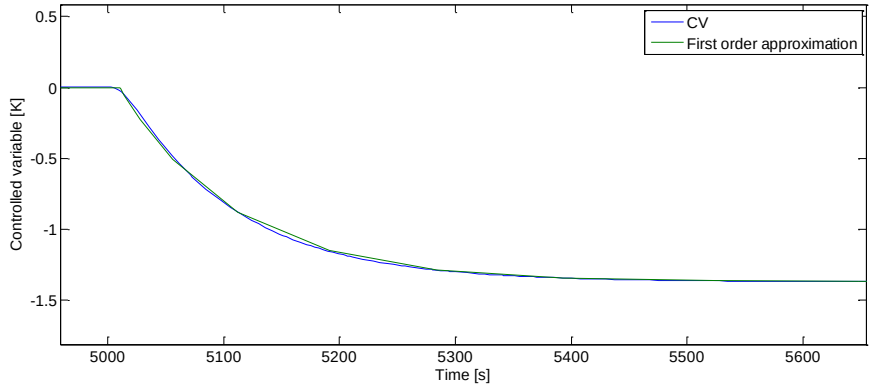

The step response is used to approximate a first order transfer function between the manipulated variable and the controlled variable including time delay:

$$g_E(s) = \frac{k_E}{(\tau_{1,E}s + 1)} e^{-\theta_E s}$$

With:

$$\begin{cases} k_E = \dfrac{\Delta c_E}{\Delta z_{Ec}} = \dfrac{-1.3705}{0.01} = -137.05 \\ \tau_{1,E} = 99.2s \\ \theta_E = 10s \end{cases}$$

According to the SIMC tuning rules and choosing $\tau_{c,E} = 240s$,

$$c(s)_{PI,E} = K_{c,E} \frac{(\tau_{I,E}s + 1)}{\tau_{I,E}s}$$

With :

$$\begin{cases} K_{c,E} = \dfrac{1}{k_E} \dfrac{\tau_{1,E}}{(\tau_{c,E} + \theta_E)} = -0{,}002895 \\ \tau_{I,E} = min\left(\tau_{1,E}, 4(\tau_{c,E} + \theta_E)\right) = \tau_{1,E} = 99.2s \end{cases}$$

Open-loop step change in the valve position of branch A

At time t=8000s, z_{Ac} passes from 0.3220 to 0.3320

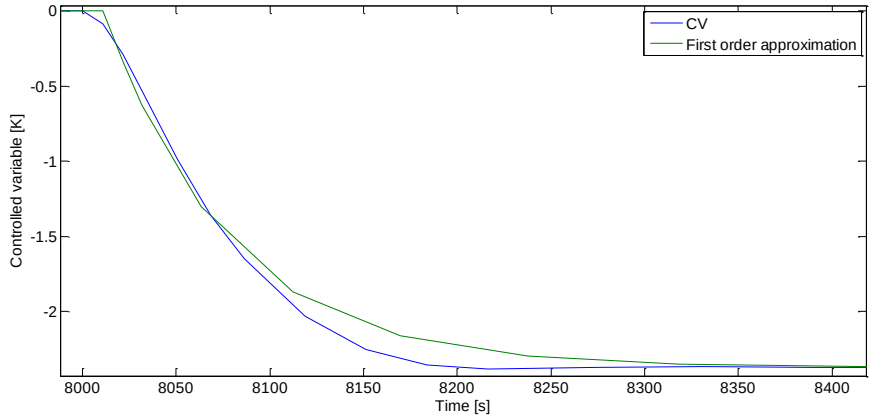

The step response is used to approximate a first order transfer function between the manipulated variable and the controlled variable including time delay:

$$g_A(s) = \frac{k_A}{(\tau_{1,A}s + 1)} e^{-\theta_A s}$$

With:

$$\begin{cases} k_A = \dfrac{\Delta c_A}{\Delta z_{Ac}} = \dfrac{-2.3711}{0.01} = -237.11 \\ \tau_{1,A} = 64.83s \\ \theta_A = 12s \end{cases}$$

According to the SIMC tuning rules and choosing $\tau_{c,A} = 240s$,

$$c(s)_{PI,A} = K_{c,A} \frac{(\tau_{I,A}s + 1)}{\tau_{I,A}s}$$

With :

$$\begin{cases} K_{c,A} = \dfrac{1}{k_A} \dfrac{\tau_{1,A}}{(\tau_{c,A} + \theta_A)} = -0{,}001085 \\ \tau_{I,A} = min\left(\tau_{1,A}, 4(\tau_{c,A} + \theta_A)\right) = \tau_{1,A} = 64.83s \end{cases}$$

Open-loop step change in the valve position of branch B

At time t=8000s, z_{Bc} passes from 0.5680 to 0.5780

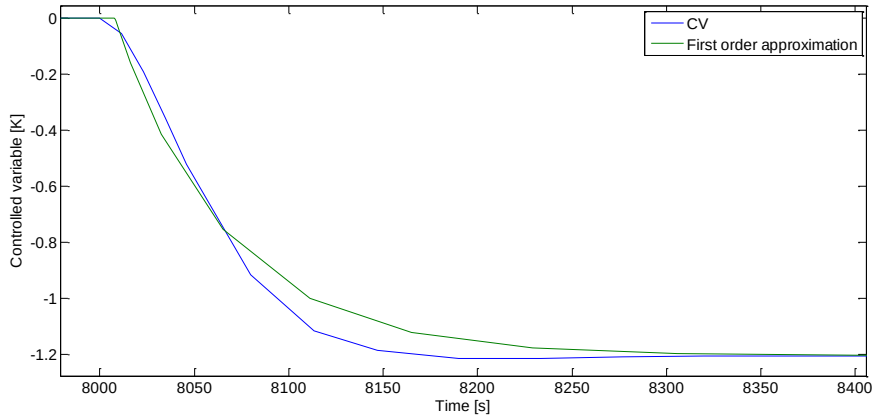

The step response is used to approximate a first order transfer function between the manipulated variable and the controlled variable including time delay:

$$g_B\,(s) = \frac{k_B}{(\tau_{1,B}s + 1)}\,e^{-\theta_B s}$$

With:

$$\begin{cases} k_B = \dfrac{\Delta c_B}{\Delta z_{Bc}} = \dfrac{-1.203}{0.01} = -120.3 \\ \tau_{1,B} = 58.33s \\ \theta_B = 8s \end{cases}$$

According to the SIMC tuning rules and choosing $\tau_{c,B} = 240s$,

$$c(s)_{PI,B} = K_{c,B}\,\frac{(\tau_{I,B}s + 1)}{\tau_{I,B}s}$$

With :

$$\begin{cases} K_{c,B} = \dfrac{1}{k_B}\dfrac{\tau_{1,B}}{(\tau_{c,B} + \theta_B)} = -0{,}001955 \\ \tau_{I,B} = min\left(\tau_{1,B}, 4\left(\tau_{c,B} + \theta_B\right)\right) = \tau_{1,B} = 58.33s \end{cases}$$

Open-loop step change in the valve position of branch C

At time t=8000s, z_{Cc} passes from 0.5240 to 0.5340

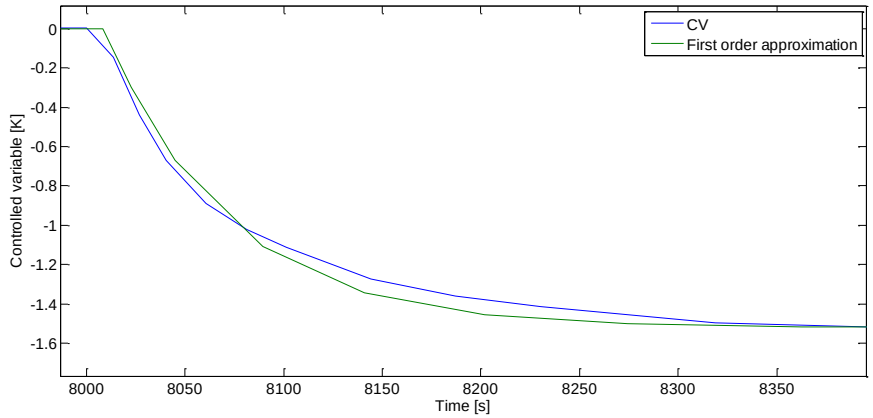

The step response is used to approximate a first order transfer function between the manipulated variable and the controlled variable including time delay:

$$g_C(s) = \frac{k_C}{(\tau_{1,C}s + 1)} e^{-\theta_C s}$$

With:

$$\begin{cases} k_C = \dfrac{\Delta c_C}{\Delta z_{Cc}} = \dfrac{-1.5217}{0.01} = -152.17 \\ \tau_{1,C} = 61.64s \\ \theta_C = 10s \end{cases}$$

According to the SIMC tuning rules and choosing $\tau_{c,C} = 120s$,

$$c(s)_{PI,C} = K_{c,C} \frac{(\tau_{I,C}s + 1)}{\tau_{I,C}s}$$

With :

$$\begin{cases} K_{c,C} = \dfrac{1}{k_B} \dfrac{\tau_{1,C}}{(\tau_{c,C} + \theta_C)} = -0{,}003116 \\ \tau_{I,B} = min\left(\tau_{1,B}, 4\left(\tau_{c,B} + \theta_B\right)\right) = \tau_{1,B} = 61.64s \end{cases}$$

Open-loop step change in the valve position of branch D

At time t=8000s, z_{Dc} passes from 0.8026 to 0.8126

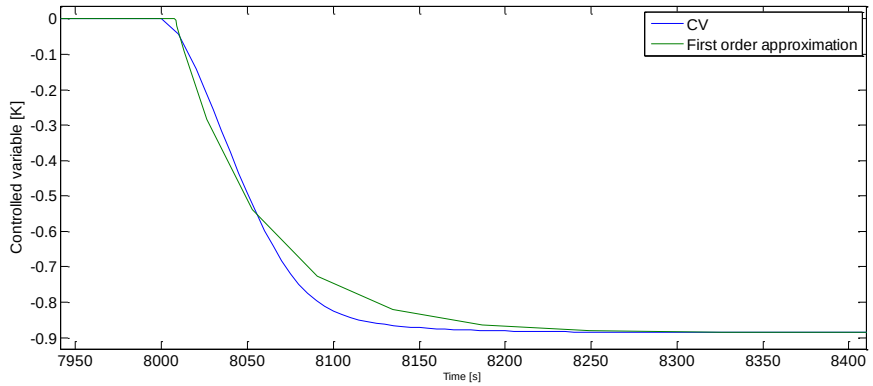

The step response is used to approximate a first order transfer function between the manipulated variable and the controlled variable including time delay:

$$g_D\,(s) = \frac{k_D}{(\tau_{1,D}s + 1)} e^{-\theta_D s}$$

With:

$$\begin{cases} k_D = \dfrac{\Delta c_D}{\Delta z_{Dc}} = \dfrac{-0.8852}{0.01} = -88.52 \\ \tau_{1,D} = 48.1s \\ \theta_D = 8s \end{cases}$$

According to the SIMC tuning rules and choosing $\tau_{c,D} = 120s$,

$$c(s)_{PI,D} = K_{c,D} \frac{(\tau_{I,D}s + 1)}{\tau_{I,D}s}$$

With :

$$\begin{cases} K_{c,D} = \dfrac{1}{k_D} \dfrac{\tau_{1,D}}{(\tau_{c,D} + \theta_D)} = -0{,}002119 \\ \tau_{I,D} = min\left(\tau_{1,D}, 4\left(\tau_{c,D} + \theta_D\right)\right) = \tau_{1,D} = 48.1s \end{cases}$$

C. MatLab© code

Main file – `run.m`

```
%% Load initial values
initial;
%% Choice of the control type and configuration
Case=1; %0:valve control, 1:flow control
PIControl=1; %0:off, 1:on
MPControl=0; %0:off, 1:on
Filters=0;   %0:off, 1:on

if MPControl ==1 %avoid errors, MPC not to be used with PIs or filters
    Filters=0;
    PIControl=0;
end

%Activation time for controllers
tPIControl=2000;
tMPControl=2000;

%% Controllers tuning
if Case==0
    load('MPC6010.mat'); %MPC
    if Filters==1        % PIs
        SIMCtuning;
    else
        SIMCtuningnf;
    end
else
    load('MPC6010flow.mat');
    if Filters==1;
        SIMCtuningflow;
    else
        SIMCtuningflownf;
    end
end

%% Filters time constants [seconds]
tm=5; %temperature sensor time constant

if Filters==1
   taT0=200;
   taF1in=20;
   taF2in=240;
   taEin=40;
   taAin=100;
   taBin=240;
   taCin=200;
   taD1in=160;
   taD2in=320;
    tfF=30;
    tfA=30;
    tfB=30;
    tfC=10;
    tfD=10;
    tfE=100;
else
   taT0=0;
   taF1in=0;
   taF2in=0;
   taEin=0;
   taAin=0;
   taBin=0;
   taCin=0;
   taD1in=0;
   taD2in=0;
    tfF=0;
    tfA=0;
    tfB=0;
    tfC=0;
    tfD=0;
    tfE=0;
end
```

```
%% Initial values for Self-optimising control
%Overwriting of the Mongstad initial values

if PIControl+MPControl == 1

zAin=0.321952537153837;
zBin=0.567990778724905;
zCin=0.523955679372974;
zDin=0.802799870251506;
zEin=0.442765317157139;
zin=[zAin zBin zCin zDin zEin];

ztotin=zAin+zBin+zCin+zDin+zEin+zFin;
mAin=0.088007924682618*m0;
mBin=0.155273650881162*m0;
mCin=0.143229693127898*m0;
mDin=0.219459994392951*m0;
mEin=0.121049941148732*m0;

end

%% Run Simulink

if Case == 0
    sim('Valvecontrol') %Simulink file for valve control
else
    sim('Flowcontrol') % Simulink file for flow control
end
```

initial.m

```
%%
%Load initial values, 23-10-2011 18h10 36''+reconciliation

%CRUDE OIL FEED
T0=125; %°C
m0A=76.582/3.6; %t/h -> kg/s
m0B=159.785/3.6;
m0C=120.414/3.6;
m0D=178.686/3.6;
m0E=126.351/3.6;
m0F=253.604/3.6;
m0=m0A+m0B+m0C+m0D+m0E+m0F;

%Heat capacities
capacities;

%Branch A
uAin=m0A/m0; %split fraction []
ThinA=295.4453; %Hot stream inlet temperature [°C]
cp_hA=k1A*ThinA+k2A; %Hot stream inlet heat capacity [J/kgK]
mhA=57.270/3.6;  %Hot stream flowrate [kg/s]

%Branch B
uBin=m0B/m0;
ThinB=267.82;
cp_hB=k1B*ThinB+k2B;
mhB=162.6105/3.6;
LGO22=39.92969/3.6;

%Branch C
uCin=m0C/m0;
ThinC=248.7734;
cp_hC=k1C*ThinC+k2C;
mhC=97.075/3.6;

% Branch D
uDin=m0D/m0;
ThinD1=222.078;
cp_hD1 =k1D1*ThinD1+k2D1;
mhD1=212.225/3.6;
```

```
ThinD2=267.632;
cp_hD2=k1D2*ThinD2+k2D2;
mhD2=172.942/3.6;

%Branch E
uEin=m0E/m0;
ThinE=241.587;
cp_hE=k1E*ThinE+k2E;
mhE=142.1482/3.6;

% Branch F
ThinF1=193.843;
cp_hF1=k1F1*ThinF1+k2F1;
mhF1=72.125/3.6;
ThinF2=244.379;
cp_hF2=k1F2*ThinF2+k2F2;
mhF2=(113.081+110.689)/3.6;

% Branch F - Sub-branches F2-F3
splith=110.689/(113.081+110.689); %Hot split fraction
splitc=119.91/253.604; %Cold split fraction

%%
%Initial valve positions computations

z0=[0.8 0.8 0.8 0.8 0.8];
uin=[uAin uBin uCin uDin uEin]; %We know the split fractions

zFin=1; %Olavalve - the valve position on the main branch (F) is fixed to 1

options = optimset('TolFun',1e-15);
z=fsolve(@(z) vav(z,uin,zFin),z0,options); %solver

zin=[z zFin]; %intial valve positions (result)

zF3in=1;
zF2in=(splitc/(1-splitc))*zF3in;

%%
%Initial values given to the filters

zeros = [0 0 0 0 0];
in3A=[125 295.4453 226.4550761762809];
in3B=[125 267.82 208.2976010282482];
in3C=[125 248.7734 213.6725976653782];
in5D=[125 222.078 267.632 181.0689995365419 207.6791409932723];
in3E=[125 241.587 200.2790677090032];
in5F=[125 193.843 244.379 137.5308748959151 202.2179313771867];
in3F2=[137.5308748959151 244.379 205.7564625690082];
in3F3=[137.5308748959151 244.379 199.0270239621444];
```

vav.m

```
function res=vav(z,uin,zFin)
for i=1:5
    res(i)=uin(i)-(z(i)/(sum(z)+zFin));
end
end
```

capacities.m

```
%capacities constants: cp=k1T+k2 [J/kgK]

%Crude oil
k1=1000*(2.0*2.1297e-003);
k2=1000*1.7895;

%Hot streams
k1A=1000*(2.0*1.9783e-003); %BC
k2A=1000*1.7771; %BC
```

```
k1B=1000*(2.0*2.0636e-003); %LGO
k2B=1000*1.7963; %LGO

k1C=1000*(2.0*1.9901e-003); %HGO
k2C=1000*1.7924; %HGO

k1D1=1000*(2.0*2.2292e-003); %MSR
k2D1=1000*1.7967; %MSR

k1D2=1000*(2.0*2.0483e-003); %BSR
k2D2=1000*1.7877; %BSR

k1E=1000*(2.0*2.2148e-003); %KERO
k2E=1000*1.7941; %KERO

k1F1=1000*(2.0*2.4663e-003); %HNA
k2F1=1000*1.7791; %HNA

k1F2=1000*(2.0*1.8189e-003); %RES
k2F2=1000*1.7798; %RES
```

SIMCtuning.m

```
%Branch E
kE=-137.05;
tetaE=10;
tau1E=109.2-tetaE;
taucE=240;
KcE=tau1E/(kE*(taucE+tetaE));
tauiE=tau1E;

%Branch A
kA=-237.11;
tetaA=12;
tau1A=76.83-tetaA;
taucA=240;
KcA=tau1A/(kA*(taucA+tetaA));
tauiA=tau1A;

%Branch B
kB=-120.3;
tetaB=8;
tau1B=66.33-tetaB;
taucB=240;
KcB=tau1B/(kB*(taucB+tetaB));
tauiB=tau1B;

%Branch C
kC=-152.17;
tetaC=10;
tau1C=71.64-tetaC;
taucC=120;
KcC=tau1C/(kC*(taucC+tetaC));
tauiC=tau1C;

%Branch D
kD=-88.52;
tetaD=8;
tau1D=56.1-tetaD;
taucD=240;
KcD=tau1D/(kD*(taucD+tetaD));
tauiD=tau1D;
```

SIMCtuningnf.m

```
%Branch E
kE=-137.05;
tetaE=5;
tau1E=19.25-tetaE;
taucE=60;
KcE=tau1E/(kE*(taucE+tetaE));
tauiE=tau1E;

%Branch A
kA=-237.11;
tetaA=5;
tau1A=42.9-tetaA;
taucA=60;
KcA=tau1A/(kA*(taucA+tetaA));
tauiA=tau1A;

%Branch B
kB=-120.3;
tetaB=5;
tau1B=33-tetaB;
taucB=60;
KcB=tau1B/(kB*(taucB+tetaB));
tauiB=tau1B;

%Branch C
kC=-152.17;
tetaC=5;
tau1C=44.2-tetaC;
taucC=60;
KcC=tau1C/(kC*(taucC+tetaC));
tauiC=tau1C;

%Branch D
kD=-88.52;
tetaD=5;
tau1D=40.25-tetaD;
taucD=240;
KcD=tau1D/(kD*(taucD+tetaD));
tauiD=tau1D;
```

SIMCtuningflow.m

```
%Branch E
kE=-2.9914;
tetaE=10;
tau1E=97-tetaE;
taucE=240;
KcE=tau1E/(kE*(taucE+tetaE));
tauiE=tau1E;

%Branch A
kA=-4.5573;
tetaA=8;
tau1A=76.9-tetaA;
taucA=240;
KcA=tau1A/(kA*(taucA+tetaA));
tauiA=tau1A;

%Branch B
kB=-2.7774;
tetaB=9;
tau1B=67.2-tetaB;
taucB=240;
KcB=tau1B/(kB*(taucB+tetaB));
tauiB=tau1B;
```

```
%Branch C
kC=-3.3026;
tetaC=6;
tau1C=73.9-tetaC;
taucC=120;
KcC=tau1C/(kC*(taucC+tetaC));
tauiC=tau1C;

%Branch D
kD=-2.3229;
tetaD=8;
tau1D=58.4-tetaD;
taucD=240;
KcD=tau1D/(kD*(taucD+tetaD));
tauiD=tau1D;
```

SIMCtuningflownf.m

```
%Branch E
kE=-137.05;
tetaE=5;
tau1E=19.25-tetaE;
taucE=60;
KcE=tau1E/(kE*(taucE+tetaE));
tauiE=tau1E;

%Branch A
kA=-237.11;
tetaA=5;
tau1A=42.9-tetaA;
taucA=60;
KcA=tau1A/(kA*(taucA+tetaA));
tauiA=tau1A;

%Branch B
kB=-120.3;
tetaB=5;
tau1B=33-tetaB;
taucB=60;
KcB=tau1B/(kB*(taucB+tetaB));
tauiB=tau1B;

%Branch C
kC=-152.17;
tetaC=5;
tau1C=44.2-tetaC;
taucC=60;
KcC=tau1C/(kC*(taucC+tetaC));
tauiC=tau1C;

%Branch D
kD=-88.52;
tetaD=5;
tau1D=40.25-tetaD;
taucD=240;
KcD=tau1D/(kD*(taucD+tetaD));
tauiD=tau1D;
```

Heat exchanger model – s-function

Heat exchanger	S-function m-file **[hexchXX.m]**	Indexch **[Y]**
A	hexch3.m	4
B1	hexch41.m	5
B2	hexch42.m	6
C1	hexch51.m	7
C2	hexch52.m	8
D1	hexch61.m	9
D2	hexch62.m	10
E	hexch2.m	3
F1	hexch11.m	1
F2	hexch12.m	2
F3	hexch13.m	11

hexchXX.m

```
function [sys,x0] = hexchXX(t,x,u,flag)
Indexch=Y;
N = 10;
%
%  Simulink interface, exchanger consisting of three series of lump systems :
%                      Hot side, Wall, Cold side
%
%            t    - time in [s].
%            X    - State, the first N states are hot temperatures,
%                          the second N states are wall temperatures,
%                          the last N states are cold temperatures.
% Inputs:
%            U(1) - Inlet hot temperature
%            U(2) - Inlet hot mass flow
%            U(3) - Inlet cold temperature
%            U(4) - Inlet cold mass flow

% Outputs:   When flag is 0 sys contains sizes and x0 contains initial condition.
%            When flag is 1, sys contains the state derivatives.
%            When flag is 3 sys contains outputs;
%            y(1)    - Oulet hot temperature
%            y(2)    - Oulet hot mass flow
%            y(3)    - Outlet cold temperature
%            y(4)    - Outlet cold mass flow

if abs(flag) == 1 % Return state derivatives.
  sys = mathisen(t,x,u,N,Indexch);

elseif abs(flag) == 3    % Return system outputs.

  sys(1,1) = x(N);       % Outlet hot temperature
  sys(2,1) = x(3*N);     % Outlet cold temperature

elseif flag == 0         % Initialise the system

  x0 = steadyvar(Indexch,N);
  sys = [3*N,0,2,4,0,0]; %number of continuous states, discrete states, outputs,
inputs
else
  sys = [];
end
end
```

mathisen.m

```
function xprime=mathisen(t,X,U,N,Indexch)

%Variables name substitution
Thot=X(1:N);
Twall=X(N+1:2*N);
Tcold=X(2*N+1:3*N);
Thin=U(1);
Mhin=U(2);
Tcin=U(3);
Mcin=U(4);

[Ai,Vh,Vc,V_w,rho_w,cp_w]=data(Indexch,N); %load heat exchanger data

%Computations of physical values in each fluid cell

cp_c   = 1000*(2.0*2.1297e-003)*Tcold + 1000*1.7895; %CRUDE OIL
rho_c  = 735.96;

if Indexch==1
    cp_h  = 1000*(2.0*2.4663e-003*Thot + 1.7791); %HNA
    rho_h = 663.196;
    h_c    = 1381; %W/(m^2K)
    h_h    = h_c;
elseif Indexch==2 | Indexch==11
    cp_h   = 1000*(2.0*1.8189e-003*Thot + 1.7798); %RES
    rho_h  = 832.86;
    if Indexch==2
    h_c    = 1462.5; %W/(m^2K)
    h_h    = h_c;
    else
    h_c    = 1257.5; %W/(m^2K)
    h_h    = h_c;
    end
elseif Indexch==3
    cp_h   = 1000*(2.0*2.2148e-003*Thot + 1.7941); %KERO
    rho_h  = 682.727;
    h_c    = 1976; %W/(m^2K)
    h_h    = h_c;
elseif Indexch==4
    cp_h   = 1000*(2.0*1.9783e-003*Thot + 1.7771); %BC
    rho_h  = 736.938; %BC like BSR
    h_c    = 1902; %W/(m^2K)
    h_h    = h_c;
elseif Indexch==5 |Indexch==6
    cp_h = 1000*(2.0*2.0636e-003*Thot + 1.7963); %LGO
    rho_h= 718.929;
    if Indexch==5
    h_c    = 1189; %W/(m^2K)
    h_h    = h_c;
    else
    h_c    = 713; %W/(m^2K)
    h_h    = h_c;
    end
elseif Indexch==7|Indexch==8
    cp_h   = 1000*(2.0*1.9901e-003*Thot + 1.7924); %HGO
    rho_h  = 788.892;
    h_c    = 1565; %W/(m^2K)
    h_h    = h_c;
elseif Indexch==9
    cp_h = 1000*(2.0*2.2292e-003*Thot + 1.7967); %MSR
    rho_h= 690.296;%MPA
    h_c    = 1250; %W/(m^2K)
    h_h    = h_c;
else
    cp_h  = 1000*(2.0*2.0483e-003*Thot + 1.7877); %BSR
    rho_h= 719.023; %BPA
    h_c    = 382.5; %W/(m^2K)
    h_h    = h_c;
end

w_h=Mhin*cp_h;
w_c=Mcin*cp_c;
```

```
% State equations

dThotdt(1)=(Thin-Thot(1)-((h_h*Ai)/(w_h(1)*N))*(Thot(1)-
Twall(N)))*((Mhin*N)/(rho_h*Vh));
dTwalldt(1)=(h_h*(Thot(N)-Twall(1))-h_c*(Twall(1)-
Tcold(1)))*(Ai/(rho_w*cp_w*V_w));
dTcolddt(1)=(Tcin-Tcold(1)-((h_c*Ai)/(w_c(1)*N))*(Tcold(1)-
Twall(1)))*((Mcin*N)/(rho_c*Vc));

for i=2:N
j=N-i+1;
dThotdt(i)=(Thot(i-1)-Thot(i)-((h_h*Ai)/(w_h(i)*N))*(Thot(i)-
Twall(j)))*((Mhin*N)/(rho_h*Vh));
end

for j=2:N
i=N-j+1;
dTwalldt(j)=(h_h*(Thot(i)-Twall(j))-h_c*(Twall(j)-
Tcold(j)))*(Ai/(rho_w*cp_w*V_w));
dTcolddt(j)=(Tcold(j-1)-Tcold(j)-((h_c*Ai)/(w_c(j)*N))*(Tcold(j)-
Twall(j)))*((Mcin*N)/(rho_c*Vc));
end

xprime=[dThotdt,dTwalldt,dTcolddt];
```

data.m

```
function [Ai,Vh,Vc,V_w,rho_w,cp_w]=data(Indexch,N)

%Areas data [m2]
A      =  [77,278,164,138,162,203,264,233,260,313,278];
Ai     =  A(Indexch);

%Volumes data [m3]
Vshell =  [0.67,2.5,1.2,1.7,1.287,1.718,2.38,2.049,1.86,2.61,2.53];
Vbundle=  [0.45,1.39,0.7,0.8,0.712,0.96,1.4,1.151,1.25,1.88,1.33];
Vcs    =
[Vbundle(1),Vbundle(2),Vbundle(3),Vshell(4),Vshell(5),Vbundle(6),Vbundle(7),Vbund
le(8),Vbundle(9),Vshell(10),Vbundle(11)]; %cold side - crude oil
Vhs    =
[Vshell(1),Vshell(2),Vshell(3),Vbundle(4),Vbundle(5),Vshell(6),Vshell(7),Vshell(8
),Vshell(9),Vbundle(10),Vshell(11)]; %hot side
Vc     =  Vcs(Indexch);
Vh     =  Vhs(Indexch);

% Wall = bundle
cp_w   = 460; %P, Wall heat capacity [J/kg*K]
rho_w  = 7800; %P, Wall density [kg/m3]
mass_w = [1580,5520,3060,3760,3080,4070,5480,4830,4910,6400,5610]; % Weight
bundle [kg]
V_w    = mass_w(Indexch)/(rho_w*N);  % Wall volumes [m3]
```

steadyvar.m

```
function [x0]=steadyvar(Indexch,N)

if N==10
    if Indexch==1
        x0 =
[188.821189347093,184.064371788945,179.563318018329,175.308633179628,171.29081248
9110,167.500294502864,163.927511482946,160.562936414220,157.397126327431,154.4207
61684806,140.172731397991,142.154641626783,144.264464582883,146.508736188978,148.
894114621792,151.427356930430,154.115292927563,156.964796452930,159.982754170073,
163.176032121504,125.924701111176,126.912156926135,127.965992751546,129.089960895
010,130.287934740721,131.563901371750,132.921952675497,134.366274887530,135.90113
6551200,137.530874895915];
```

```
    elseif Indexch==2
        x0 =
[236.645169196325,228.979210519106,221.380614583620,213.848839383696,206.38330963
3788,198.983416089576,191.648514843408,184.377926590477,177.170935861114,170.0267
90214042,157.069346005094,163.957862563544,170.904102585451,177.908794841917,184.
972632022200,192.096271600505,199.280336658768,206.525416670782,213.832068252481,
221.200815882667,144.111901796146,150.744789265973,157.430278580425,164.169074840
427,170.961847954824,177.809233567223,184.711833933841,191.670218757944,198.68492
5985856,205.756462569008];
    elseif Indexch==3
        x0 =
[236.373709983483,230.982947919496,225.404371406103,219.626676693288,213.63747114
0236,207.423123259489,200.968585365540,194.257182486298,187.270359391236,179.9873
75167395,156.991644174346,164.935106621032,172.549299704039,179.857723120800,186.
881362944870,193.639046937299,200.147738284952,206.422780261969,212.478101429496,
218.326388846243,133.995913181297,142.599853850828,150.841416921781,158.746860876
059,166.339602630251,173.640622734361,180.668799876615,187.441189117834,193.97325
4939495,200.279067709003];
    elseif Indexch==4
        x0 =
[280.105847433722,265.270155263516,250.942430745715,237.125749239346,223.82198694
6348,211.031764266429,198.754401507834,186.987888481732,175.728869220856,164.9726
42710383,149.132063850481,158.857418773925,169.038275704907,179.679070574804,190.
783037781288,202.352208176369,214.387421221824,226.888350549594,239.853541855826,
253.280461805001,133.291484990579,141.985968326993,151.088662928083,160.603739641
774,170.534311296148,180.882429406391,191.649093204303,202.834270353472,214.43692
8448136,226.455076176281];
    elseif Indexch==5
        x0 =
[229.238047599607,223.405389839306,217.617771012971,211.875806451550,206.18011234
3944,200.531305193487,194.930001245251,189.376815883875,183.872363001763,178.4172
54337545,153.974046795688,158.988798857398,164.049753115224,169.156353847588,174.
308042720652,179.504259408939,184.744442189478,190.028028509423,195.354455527254,
200.723160627711,129.530839253832,134.105234713033,138.722690346573,143.382706449
925,148.084780247816,152.828406473935,157.613077927406,162.438286005875,167.30352
1215201,172.208273655815];
    elseif Indexch==6
        x0 =
[264.692200523635,261.534750811916,258.346932040025,255.127997102887,251.87716905
9616,248.593639467202,245.276566593665,241.925073499929,238.538245978479,235.1151
30335586,205.559583175918,209.146689979542,212.693956598144,216.202467723492,219.
673261762548,223.107333507530,226.505636613024,229.869085896813,233.198559479426,
236.494900775942,176.004036016250,179.755133980605,183.462839696359,187.128368853
319,190.752884057893,194.337497955443,197.883276123161,201.391239753600,204.86236
8146937,208.297601028248];
    elseif Indexch==7
        x0 =
[182.272292850455,176.843076585376,171.615603404262,166.585564886212,161.74852084
1898,157.099915197607,152.635091998085,148.349311397130,144.237765510690,140.2955
94014675,134.247219694495,137.887419478860,141.684082346227,145.641708670084,149.
764751941108,154.057604478357,158.524582903218,163.169913483247,167.997717459778,
173.011996478471,128.198845374316,131.537073447029,135.018853295324,138.648325342
083,142.429588684609,146.366688114815,150.463600920224,154.724223562233,159.15235
8334180,163.751700106486];
    elseif Indexch==8
        x0 =
[241.856531929863,235.128785287557,228.588722295451,222.234732231908,216.06503511
2840,210.077686121872,204.270580760658,198.641460683738,193.187920175634,187.9074
13221824,177.987752554880,182.858447958401,187.889069413236,193.081998862273,198.
439490562996,203.963664534985,209.656500542987,215.519832659953,221.555344449053,
227.764564797621,168.068091887936,172.528975741168,177.136678142734,181.893416963
889,186.801295004120,191.862293957131,197.078268854066,202.450943024455,207.98190
3610549,213.672597665378];
    elseif Indexch==9
        x0 =
[218.366748198809,214.538364071445,210.586942906941,206.506116787787,202.28900309
0486,197.928145444251,193.415445759144,188.742085623184,183.898434972747,178.8739
45435695,155.230831495342,160.909458721864,166.378284382907,171.649914287006,176.
735827548507,181.646510395674,186.391570377922,190.979834353955,195.419432976257,
199.717873867675,131.587717554989,137.920482470982,144.014483142630,149.884382814
868,155.543509652762,161.004017700862,166.277023968057,171.372725800970,176.30050
1881070,181.068999536542];
```

```
    elseif Indexch==10
        x0 =
[265.140527603224,262.636329033046,260.119189310447,257.588887688189,255.04519743
6072,252.487885615914,249.916712845646,247.331433051856,244.731793210115,242.1175
33072322,212.960263773338,215.625872418588,218.275813675458,220.910374569084,223.
529833950492,226.134462812335,228.724524589289,231.300275443999,233.861964539406,
236.409834298248,183.802994474354,186.519951627062,189.220194299060,191.904036292
522,194.571782285069,197.223728188597,199.860161490388,202.481361577550,205.08760
0045767,207.679140993272];
    else
        x0 =
[236.484016663924,228.731279191491,221.120597378784,213.651707337774,206.32427103
2947,199.137875998381,192.092035239778,185.186187324936,178.419696665133,171.7918
53988770,157.470784094891,163.652452482809,169.962068428101,176.400252435500,182.
967557677246,189.664469641729,196.491405954709,203.448716371480,210.536682937366,
217.755520313034,143.149714201012,148.885208300486,154.737949531265,160.708469631
221,166.797239356111,173.004668250511,179.331104571644,185.776835364177,192.34208
6683241,199.027023962144];
        %Exchanger F3
    end

else

HXinitA  = [295.4453,167.5898,125,226.457];

HXinitB1 = [235.2852,179.1172,125,172.202];
HXinitB2 = [267.8203,235.2852,172.202,208.3047];

HXinitC1 = [176.75,141.2539,125,154.112];
HXinitC2 = [248.7734,176.75,154.112,213.6758];

HXinitD1 = [222.0782,177.164,125,183.5775];
HXinitD2 = [267.7319,244.7101,183.5775,207.6822];

HXinitE  = [241.587,180.7366,125,200.2762];

HXinitF1 = [193.8429,154.6104,125,137.535];
HXinitF2 = [244.3789,171.7525,137.535,202.2197];
HXinitF3 = [244.3789,171.7525,137.535,202.2197];


if Indexch==1
   exch=HXinitF1;
elseif Indexch==2
    exch=HXinitF2;
elseif Indexch==3
    exch=HXinitE;
elseif Indexch==4
    exch=HXinitA;
elseif Indexch==5
    exch=HXinitB1;
elseif Indexch==6
    exch=HXinitB2;
elseif Indexch==7
    exch=HXinitC1;
elseif Indexch==8
    exch=HXinitC2;
elseif Indexch==9
    exch=HXinitD1;
elseif Indexch==10
    exch=HXinitD2;
else
    exch=HXinitF3;
end

hotstep=(exch(2)-exch(1))/(N-1);
coldstep=(exch(4)-exch(3))/(N-1);
Thot0=exch(1):hotstep:exch(2);
Tcold0=exch(3):coldstep:exch(4);
Twall0=(Thot0+Tcold0)/2;
x0=[Thot0,Twall0,Tcold0];

end
```

optim.m

```
%% Initialisation
initial;
uuref=[0 0 0 0 0];
uF3=0;
uunew=uuref;
uu=uuref;

sim('al');
Tref=Ttot(end);
Tnew=Tref;
Told=0;

j=0; %j is used to identify the first pass of the loop
delta=0.01; %delta is used to enhance the precision from passes to passes

% Gradient computation
stepu=0.00000000001;
for i=1:5
    uu(i)=uunew(i)+stepu;
    sim('al');
    Tdelta(i)=Ttot(end);
    Tgrad(i)=(Tdelta(i)-Tnew)/stepu;
    uu(i)=uunew(i);
end

%% Loop
while max(abs(Tgrad))>0.1 %when <= 0.1, the optimum is found

%One pass is used to find the optimum in the gradient direction

linu(1,:)=uunew;
linT(1)=Tnew;


% If it is the first pass (j=0), the search scale is very large so we are sure to
go
% behind the maximum temperature in the gradient direction
if j==0
linstep=0.05/max(abs(Tgrad));
uu=uunew+Tgrad*linstep;
else
linstep=0.005/max(abs(Tgrad));
uu=uunew+Tgrad*linstep;
end

%Three points are always considered by the algorithm, the maximum is always
%between point 1 and point 3
sim('al');
linu(3,:)=uu;
linT(3)=Ttot(end);
linu(2,:)=(linu(1,:)+linu(3,:))/2;
uu=linu(2,:);
sim('al');
linT(2)=Ttot(end);
linstep=linstep/2; %the point 2 is initialised at equal distance from 1 to 3

%safety condition, if the search scale was not big enough
if linT(3)<linT(1)
    j=1;
else
    j=0;
end

%the distance is reduced between the points until a higher value is
%obtained on point 2
while linT(2)<linT(1)
    linT(3)=linT(2);
    linu(3,:)=linu(2,:);
    linstep=linstep/2;
    uu=linu(3,:)-Tgrad*linstep;
    sim('al');
    linT(2)=Ttot(end);
    linu(2,:)=uu;
end
```

```
% then, the point 1 or 3 are replaced by new inside points
% the highest temperature point always becomes the point 2

while linT(2)>max(linT(1),linT(3))+delta
[Tmin,index]=min(linT);
uu=(linu(index,:)+linu(2,:))/2;
sim('al');
if index==3
    if    Ttot(end)>linT(2)
          linT(1)=linT(2);
          linu(1,:)=linu(2,:);
          linT(2)=Ttot(end);
          linu(2,:)=uu;
    else  linT(3)=Ttot(end);
          linu(3,:)=uu;
    end
else
    if    Ttot(end)>linT(2)
          linT(3)=linT(2);
          linu(3,:)=linu(2,:);
          linT(2)=Ttot(end);
          linu(2,:)=uu;
    else  linT(1)=Ttot(end);
          linu(1,:)=uu;
    end
end
end

%update
Told=Tnew;
uunew=linu(2,:);
Tnew=linT(2);

uu=uunew;
sim('al');
% the eventual new optimal F* split is then computed
optimF2F3;

sim('al');
Tnew=Ttot(end);

% computation of the new local gradient
stepu=0.00000000001;
for i=1:5
    uu(i)=uunew(i)+stepu;
    sim('al');
    Tdelta(i)=Ttot(end);
    Tgrad(i)=(Tdelta(i)-Tnew)/stepu;
    uu(i)=uunew(i);
end

%Display the new point and gradient on workspace for supervision of the
%work being done by the algorithm
'New'
Tnew
uunew
Tgrad
delta=delta/2;
end

%% Display the result
'Finale'
uA=uAin+uunew(2)
pause
uB=uBin+uunew(3)
pause
uC=uCin+uunew(4)
pause
uD=uDin+uunew(5)
pause
uE=uEin+uunew(1)
pause
Toptim=Tnew
'End'
```

optimF2F3.m

```
%optimF2F3, same principle than the algorithm for the multivariable split
A,B,C,D,E,F

TF2b=ToutF2tot(end);
TnewF2=TF2b;
uF3b=uF3;

uF3a=uF3b-0.1;
uF3=uF3a;
sim('al');
TF2a=ToutF2tot(end);

uF3c=uF3b+0.1;
uF3=uF3c;
sim('al');
TF2c=ToutF2tot(end);

linTF2=[TF2a TF2b TF2c];
linuF2=[uF3a uF3b uF3c];

while linTF2(2)>max(linTF2(1),linTF2(3))+0.01
[TminF2,indexF2]=min(linTF2);
uF3=(linuF2(indexF2)+linuF2(2))/2;
sim('al');
if indexF2==3
    if    ToutF2tot(end)>linTF2(2)
          linTF2(1)=linTF2(2);
          linuF2(1)=linuF2(2);
          linTF2(2)=ToutF2tot(end);
          linuF2(2)=uF3;
    else  linTF2(3)=ToutF2tot(end);
          linuF2(3)=uF3;
    end
else
    if    ToutF2tot(end)>linTF2(2)
          linTF2(3)=linTF2(2);
          linuF2(3)=linuF2(2);
          linTF2(2)=ToutF2tot(end);
          linuF2(2)=uF3;
    else  linTF2(1)=ToutF2tot(end);
          linuF2(1)=uF3;
    end
end
end
%update
ToldF2=TnewF2;
uF3new=linuF2(2);
TnewF2=linTF2(2);
uF3=uF3new;
```